University of Garyounis

Faculty of Science- Department of Physics

The unified action of ionizing radiation on the induction of Hypoxanthineguanine Phosphor Ribosyltransferase (HPRT) mutations for mammalian cells

Maha M. El Gali

Supervised by

Dr. Ali S. Alkharam

Thesis submitted in partial fulfilment of the requirements

of the degree of Master of Science in Physics

Spring

2009-2010

University of Garyounis

Faculty of Science- Department of Physics

The unified action of ionizing radiation on the induction of Hypoxanthineguanine Phosphor Ribosyltransferase (HPRT) mutations for mammalian cells

Maha M. El Gali

Supervised by

Dr. Ali S. Alkharam

Thesis submitted in partial fulfilment of the requirements of the degree of Master of Science in Physics, 22-7-2010 at Department of Physics, Faculty of Science, University of Garyounis.

جامعة قار يونس

كلية العلوم - قسم الفيزياء

The unified action of ionizing radiation on the induction of Hypoxanthineguanine Phosphor Ribosyltransferase (HPRT) mutations for mammalian cells

مها منصور محمد الجالي

لجنة المناقشة:

1- د.على سالـــــــم الخرم	المشرف	.....
2- د.إبراهيم صالح اليسيري	الممتحن الداخلى	.....
3- د.عبدالحميد محمد يونس	الممتحن الخارجى	.....

د. علي يصكو دركوي

أمين قسم الفيزياء

د. أحمد محمد عبدالهادي مامي

أمين اللجنة الشعبية لكلية العلوم

A DEDICATION

I dedicate this piece of work to my brothers Muaath and Muataz, my sister Mai, my precious Fawzia, my brother-in-law Alaa and finally my sister-in-law Ghalia.

I am thankful to all of them for their ongoing support and enduring patience.

ACKNOLEDGEMENT

I am all grateful to my supervisor Dr. Ali S. Alkharam for his never-ending tutelage and inspiration.

I also extend my sincere gratitude to Dr. Ibrahim Hamamo, Dr. Naji Alamari , Dr. Daefalla M. Tawati, Mrs. Hend A. A. Houssein and all the teaching staff in the Department of Physics.

In addition, my thanks go out to all my colleagues at Benghazi Radiodiagnosis & Radiotherapy Center.

I propose a vote of thanks to all the people who helped me collate the data and information in this scientific project.

A special thank to:

- Pro. Jurgen Kiefer and Dr. C. Baumstark-Khan from Germany.
- Dr Alaa Eldarrat from the USA.
- Pro. Patrick O'Neil from the USA.
- My brother Muataz.

Table of Contents

1-Introduction 1

2. Interactions of Ionizing Radiation with Matter. 4

2.1. Ionization. 4

2.2. Charged Particles. 5

2.2.1. Types of Charged Particles Coulomb Interaction. 6

2.2.2. Maximum Energy Transfer in A single Collision. 6

2.2.2.a. Heavy Charged Particles. 7

2.2.2.b. Light Charged Particles. 7

2.2.3. Stopping Power 7

2.2.3.a. Heavy Charged Particles. 7

2.2.3.b. Light Charged Particles. 9

2.2.4. Mass Stopping Power. 9

2.2.5. Ranges. 10

2.2.5.a. Heavy Charged Particles. 10

2.2.5.b. Light Charged Particles. 10

2.2.6. Radiative Losses 11

2.2.7. Radiation Yield. 12

2.3. Photons. 13

2.4. Neutrons. 15

2.4.1. Neutrons Sources. 15

2.4.2. Neutrons Interactions with Matter. 15

3. Track Structure's Physical Parameters of Ionizing Radiation. 17

3.1. Unrestricted Linear Energy Transfer (LET) in Liquid Water. 17

3.2. Restricted Linear Energy Transfer L_{Δ}. 21

3.3. Katz's Parameter $(Z^{*}/\beta)^{2}$ 23

3.4. The Mean Energy (W). 28

3.5. Linear Primary Ionization (I). 30

3.6. The Mean Free Path (λ). 34

3.7. Ranges. 36

4. Radiation Effects on Mammalian Cells. 39

4.1. Mammalian Cell. 39

4.2. The Cell Cycle. 40

4.3. DNA Structure. 40

4.4. Chromosomes 42

4.5. Mechanism of Radiation Damage to DNA. 42

4.5.1. Direct Cell Damage. 42

4.5.2. Indirect Cell Damage. 43

4.6. Radiation Effects on DNA. 44

4.6.1. DNA Strands Breaks. 44

4.6.2. Chromosome Aberrations. 45

4.6.3. Somatic Effects. 46

4.6.4. Gene Mutations. 46

4.6.4.a. HPRT Gene. 46

4.6.4.b. HPRT Gene Importance. 47

4.6.4.c. Comparison of HPRT Gene Size and Structure. 47

5. Biological Parameters of Ionizing Radiation. 49

5.1. Models of Radiation Cell Killing. 49

5.1.1. Cell Survival Curves. 49

5.1.1.a. Calculations of Parameter α and β. 50

5.1.2. HPRT Mutations Curves. 51

5.1.2.a. Calculations of Parameter α and β. 52

5.2. The Cross Section. 52

5.2.1. The Geometrical Cross Section of HPRT Gene and Cells in Mammals. 52

5.2.2. The Effective (Biological) Cross Section. 52

5.3. Mutagenicity Factor. 53

6. Analysis of HPRT Mutations Biological and Physical Data. 54

6.1. Densely Ionizing Radiation. 54

6.1.1. Radiosensitivity Parameter $\alpha_m(Gy^{-1})$. 54

6.1.2. Mutation Cross Section $\sigma_m(\mu m^2)$. 60

6.1.3. Inactivation Cross Section $\sigma_i(\mu m^2)$. 65

6.1.4. The Mutagenicity Factor (σ_m/ σ_i). 66

6.2. Sparsely Ionizing Radiation. 68

6.3. Modeling the Biological Effects. 68

6.3.1. Densely Ionizing Radiation. 68

6.3.2. Sparsely Ionizing Radiation. 69

6.4. Comparison between Densely and Sparsely Ionizing Radiation Mutation Actions 70

-Conclusion. 72

-Appendix. 73

-References. 86

Glossary

C3H10T1/2	Mouse embryo-derived cells
CHO	Chinese Hamster Ovary
DNA	Deoxyribonucleic Acid
DSB	Double Strand Break
HPRT (HGPRT)	Hypoxanthine-guanine phosphoribosyl transferase
HSF	Human Skin Fibroblasts
ICRP	International Commission on Radiological Protection
ICRU	International Commission on Radiation Units & Measurements
kbp	Kilo Base Pair
L_{100} OR L_{Δ}	Restricted Linear Energy Transfer
LET or L_{∞}	Unrestricted Linear Energy Transfer
NCRP	National Council on Radiation Protection & Measurements
RBE	Relative Biological Effectiveness
SSB	Single Strand Break
TK6	Human Lymphoblasts
V79	Chinese Hamster Lung Fibroblast
$Z^{*}(Z_{eff})$	The Effective Charge Number

ABSTRACT

Mutation induction at the HPRT ((Hypoxanthine-guanine phosphoribosyl- transferase) locus, which is located in X-chromosome, in different cell lines for mammals by exposure to ionizing radiation were studied in this research. The radiobiological database consist of measurements were done in different laboratories all over the world.

In order to select a unifying parameter to express the HPRT mutation, it was necessary to demonstrate the trend of the biological effectiveness against several physical parameters.

The mean free path for linear primary ionization λ, found to be a meaningful physical parameter that describes the biological effects. The biological effectiveness expressed as effective cross section, is modeled against this physical parameter, and seems to be closest to the equation below;

$$s(l) = \frac{s_0}{1 + \left(\frac{l}{l_0}\right)^m}$$

Where $\begin{cases} m=1.4,\ \sigma_0 = 0.0009\ \mu m^2,\ \lambda_0 = 4nm & \text{densely ionizing radiation} \\ m=1.4,\ \sigma_0 = 0.00004\ \mu m^2,\ \lambda_0 = 4nm & \text{sparsely ionizing radiation} \end{cases}$

For densely ionizing radiation, the maximum mutation cross section, which represented in the saturation region, was nearly equal to the average of the geometrical size of the gene in mammals ($1.06\times10^{-3}\ \mu m^2$), $\sigma_0 / \sigma_g = (1/1.17)$.

While it was about (1/26.3) of this average in sparsely ionizing radiation, that means the damage caused by densely ionizing radiation was twenty times greater than that of sparsely ionizing radiation. It can be explained due to the difference of their track structures and energy deposition.

The mutagenicity factor (σ_m/ σ_i) and inactivation cross section $\sigma_i(\mu m^2)$ were briefly studied. It is obvious that the DSB causes cell killing and mutations. Finally, for radiation protection purposes, the DSB could be the most important key to set the dose limits for radiation exposure in radiation fields whether on earth or space.

الملخـــــــــــــــص

في هذا البحث تمت دراسة ظاهرة التشوهات في جين HPRT (الموجود ضمن الكروموسوم x) في خلايا مختلفة من الثدييات الناتجة عن التعرض للإشعاع المؤين. قاعدة البيانات البيولوجية المستخدمة هنا تحتوي على قيم تم قياسها في معامل مختلفة.

لاختيار المتغير الموحد لتفسير تشوهاتHPRT كان من الضروري دراسة التأثير البيولوجي كدالة للعديد من المغيرات الفيزيائية, وجد أن متوسط المسار الحر للتأين الابتدائي الخطي λ أفضل متغير لوصف التأثير البيولوجي.

التأثير البيولوجي يمكن التعبير عنه بدلالة المقطع العرضي الفعال σ كدالة لمتوسط المسار الحر للتأين الابتدائي الخطي λ و تم الحصول على المعادلة أدنه:

$$s(l) = \frac{s_0}{1 + \left(\frac{l}{l_0}\right)^m}$$

للإشعاع المؤين الكثيف: $m=1.4,\ \sigma_0 = 0.0009\ \mu m^2,\ \lambda_0 = 4nm$

للإشعاع المؤين الخفيف: $m=1.4,\ \sigma_0 = 0.00004\ \mu m^2,\ \lambda_0 = 4nm$

للإشعاع المؤين الكثيف القيمة القصوى للمقطع العرضي للتشوهات مقاربة لقيمة متوسط المقطع الهندسي ($1.06\times10^{-3}\ \mu m^2$) للجين في الثدييات (1/1.17) $= \sigma_0 / \sigma_g$, بينما كانت حوالي (1/26.3) من متوسط المقطع الهندسي للإشعاع المؤين الخفيف.

و هذا يعني أن الضرر الناتج عن الإشعاع المؤين الكثيف يكافئ عشرين ضعف من تأثير الإشعاع المؤين الخفيف و قد يكون بسبب الفرق في المسارات و إيداع الطاقة لإشعاع المؤين الكثيف و الخفيف.

من خلال دراسة التأثير البيولوجي يتضح أن القطع الثنائي للحمض النووي هو المسبب لتشوهات و موت الخلية. و يعتبر المفتاح لوضع المعايير للوقاية الإشعاعية في الحقول الإشعاع سواء على الأرض أو الفضاء.

Chapter 1

INTRODUCTION

Over the last few decades there has been a skyrocketing interest in the field of study concerning the biological ramifications of the radiation. Radiation biophysics deals with the molecular mechanisms of the biological effects of ionizing (photons, neutrons and charged particles) and non-ionizing (ultraviolet, visible light, infrared and ultrasound) radiation. Associating with radiobiology and radiation chemistry for better understanding for the interactions of radiations with the biological matters.

The scientific society has raised the concern of the radiation hazards after the occurrence of several nuclear calamities like Hiroshima and Nagasaki, and Chernobyl. In addition, space travelling, which began in the 20^{th} century, has imposed the necessity of conducting more scientific studies in this field to come to know the detrimental effect of radiation upon astronauts.

Based on these studies and researches, international foundations like **ICRP** (International Commission on Radiological Protection), **NCRP** (National Council on Radiation Protection & Measurements) and **ICRU** *(* International Commission on Radiation Units & Measurements*)* have determined the limitations of radiation exposure for workers in the field and the public on an equal footing. The main purpose of the establishment of such limitations is to reach the level of radiation protection and utilize it into radiotherapy as well as other practices.

The mammalian living cell is considered to be the pivot on which the studies are based, for epidemiological purposes. The biological data of the radiation effect is obtained through the survival of nuclear accidents, or by exposing cells inside the body **(in vivo)**, or outside it **(in vitro)**; the latter is considered to be more commonly used.

The harmful effects of radiation could be classified into two general categories; stochastic and deterministic (tissue reaction). The Relative Biological Effectiveness **(RBE)** is the scale of radiation damage, which commonly used in radiobiology and it depends on the linear part of X-ray curve of a specific damage.

Mammalian cells contain about 80% water; this fact helps researches like D. E. Watt and others to extensively study the track structure of ionizing radiation in liquid water and its physical parameters. The unrestricted linear energy transfer **LET** is one of the most outstanding parameters to describe the biological damages, in 1992; Harder used the restricted linear energy transfer $\mathbf{L_{\Delta}}$ as a radiation quality parameter. One better known parameter is Katz's parameter $\mathbf{(Z^{*}/\beta)^{2}}$ which Katz used to set out his cellular track model and regarding the effect of the secondary electrons **(δ rays)**.

We are still far away from understanding the effects of radiation in a quantitative predictable way, therefore; we need to study the relationship between the physical parameters and the endpoints like cell killing, chromosome aberration, mutation induction and neoplastic transformation. Recently, a lot of studies have based on the action of densely radiation and the track structure has been extensively studied, one by which Monte Carlo calculation, to predict DNA damage.

Mutations play an important role in carcinogenesis either by activating silent oncogene, or by eliminating the activity of tumor suppressor gene. One of these mutations is the **HPRT** (Hypoxanthine-guanine phosphoribosyltransferase locus, which is located in the q-arm of the X-chromosome) which forms the main concern of this research. The system of HPRT gene mutation is able to detect different types of mutations and to differentiate the mutagenic action of different types of DNA damage.

There are many scholars who have studied the relationship between the biological parameter of the HPRT and the physical parameters. Recently, (Kiefer, J., 2001) has set out a model which gave a good approximation of the RBE mutation and is considered to be better than the one which was designed by the ICRP foundation. One of the disadvantages of using the RBE factor is the double values before and after the peak.

In 1995 (Stoll, U. et al, 1995) mentioned that the LET ignores the track's width, L_{Δ} takes into account only the inner part of the track and Katz's parameter $(Z^{*}/\beta)^{2}$ describes essentially only the number of δ-rays per unit pathlength. Now, it is important to find out a new parameter related to the distances in the biological matters and the track structure of the radiation, especially densely ionizing radiation, as it forms the main concern in the recent studies.

AIMS AND OBJECTIVES

- **AIMS**

1. Determination of dose limits for public and occupational workers.
2. Study the low doses harmful effects.
3. Estimating the exposure from natural sources and doses delivery in diagnostic and therapeutic medicine.

- **OBJECTIVES**

1. **Establishing a database:**

This is done by collecting data from various researches in which different mammalian cell lines have been exposed to different types of radiation.

2. **Data analysis:**

In this phase the biological damage is analyzed as a function in several physical parameters.

3. **Modeling the radiation effect:**

After the execution of the previous two phases, we ought to design the modeling of the biological damage by using one of the physical parameters to explain the possibility of this damage to occur.

Chapter 2

Interactions of Ionizing Radiation with Matter

Ionizing radiation is a part of electromagnetic radiation spectrum, which occurs in nature (primary and secondary cosmic ray, decay of radionuclides) and generated by artificial sources, (atomic interaction of accelerated particles). Both ionizing and non-ionizing radiation have biological effects on the cell and the organism. Table (2.1) shows the electromagnetic radiation spectrum.

Table (2.1) Electromagnetic radiation spectrum, from (Kudryashov, Y. B., 2008).

Radiation		**Wavelength range, m**	**Sources**
Type	**Kind**		
Ionizing	γ- radiation	10^{-10}-10^{-15}	Sources of cosmic rays, atomic interaction of accelerated particles; decay of radionuclides, nuclear reactions.
	Roentgen radiation	10^{-8}-10^{-11}	
Optical (Light)	Ultraviolet	$4x10^{-7}$-10^{-8}	Sun and moon, stars and nebulas, other cosmic sources, terrestrial objects, excited molecules and atoms, any heated body.
	Visible	$7x10^{-7}$-$4x10^{-7}$	
	Infrared	10^{-4}-$7x10^{-7}$	
Radio-frequency	Decimillimeter	10^{-3}-10^{-4}	Sun and moon, planets, stars and other cosmic objects, lightning discharges, aurora borealis, any electric influence, living organisms, etc.
	High frequency	10^{2}-10^{-3}	
	Medium	10^{3}-10^{2}	
	Low frequency	10^{8}-10^{3}	

2.1.Ionization:

The process by which a neutral atom acquires a positive or negative charge is known as ionization. If, on the other hand, the energy lost by the incident particle is not

sufficient to eject an electron from the atom but is used to raise the electrons to higher energy levels, the process is termed excitation.

Ionizing radiations produce biological effects because the energy released is large enough to break chemical bonds and initiate chain of events that lead ultimately to a biological effect.

Ionizing radiation is classified into two types; direct ionizing radiation and indirect ionizing radiation.

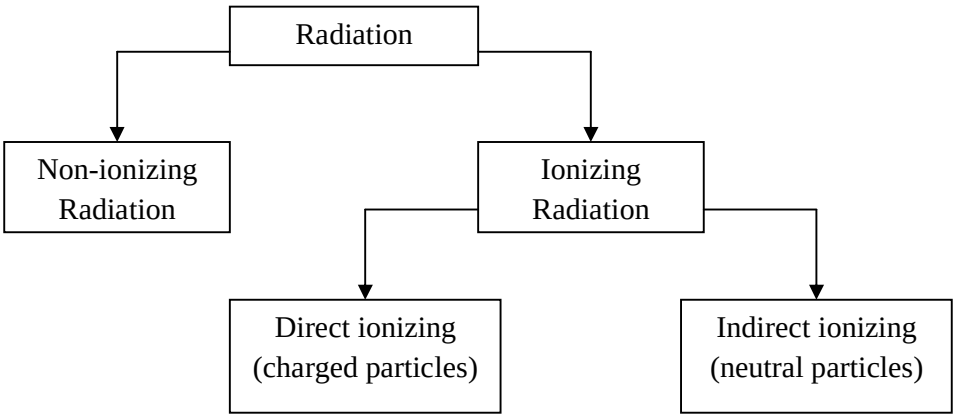

Fig. (2.1) Classification of radiation.

2.2 Charged Particles

Charged particles such as electrons, protons, and α particle are known as directly ionizing radiation provided they have sufficient kinetic energy to produce ionization by collision as they penetrate matter. The energy of the incident particle is lost in a large number of small increments along the ionization track in the medium, with an occasional interaction in which the ejected electron receives sufficient energy to produce a secondary track of its own, known as a δ rays.

2.2.1. Types of Charged Particles Coulomb Interactions:

A charged particle along its path in each interaction may be experience elastic or inelastic scattering and it may lose some of its kinetic energy and transfer it to the medium (collision loss) or to photons (radiative loss), (Podgoršak, E. B., 2006).

Charged particles interactions with the nuclei and its orbital electrons depend on the size of the classical parameter b (impact parameter) compared to the classical atomic radius a, (Attix, F. H., 1986). The three main types are illustrated in Fig (2.2).

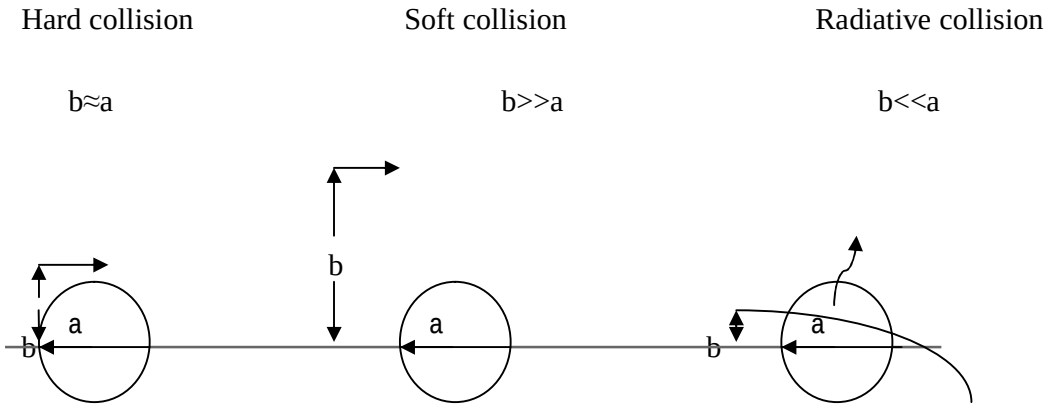

Fig. (2.2) Types of collisions of charged particles, (From Podgoršak, E.B., 2006).

In hard and soft collisions, a charged particle interacts with orbital electron. Both heavy and light charged particle experience hard and soft collisions. On the other hand, radiative collision (Bremsstrahlung Production) occurs only for light charged particles.

2.2.2. Maximum Energy Transfer in A single Collision (Q_{max}):

The maximum energy that a charged particle can lose in colliding with an atomic electron.

2.2.2. a. Heavy Charged Particles:

The particle moves rapidly compared with electron and that energy transfer is large compared with the binding energy of the electron in its atom. So the electron can be considered to be initially free and at rest that means the collision is elastic.

$$Q_{\max} = \frac{4mM}{(M+m)^2} E \qquad (2.1)$$

Where E is the initial kinetic energy of the incident particle.

2.2.2. b. Light Charged Particles:

The electrical forces act over long distances, the collision between the electrons can actually occur without coming into contact.

Where M=m, then

$$Q_{max} = E \qquad (2.2)$$

A particle “colliding” with a particle of identical mass then large scattering angles are possible.

2.2.3. Stopping power:

2.2.3. a. Heavy Charged Particles:

The average linear rate of energy loss of a heavy charged particle in a medium(-dE/dx in MeV/cm) has fundamental importance in radiation physics, dosimetry and radiation biology. It is also referred to as linear energy transfer (LET). Stopping power and LET are closely associated with the dose and with the biological effectiveness of different kinds of radiation.

The non-relativistic quantum-mechanical expression was derived by Hans Beth and Felix Bloch, (Beth-Bloch stopping power):

$$-\frac{dE}{dx} = \frac{4pk_0 Z^2 e^4 n}{mc^2 b^2}\left[\ln\frac{2mc^2}{I}\right] \quad (2.3)$$

Bethe derived the following expression for the stopping power of a uniform medium for a heavy charged particle (Beth's relativistic quantum-mechanical expression):

$$-\frac{dE}{dx} = \frac{4pk_0 Z^2 e^4 n}{mc^2 b^2}\left[\ln\frac{2mc^2 b^2}{I(1-b^2)} - b^2\right] \quad (2.4)$$

The term ($-2\beta^2$), is derived in quantum treatment of energy loss by collisions a heavy, spin 0 incident particle, as spin plays an important role when the transferred energy is almost equal to the incoming energy.

Beside, there are other terms such as shell correction $\left(\frac{C}{Z}\right)$ and polarization correction (δ). The shell correction term is due to nonparticipation of inner shell (K, L,….) electrons in collision loss process, and as the range of distant collision is extending the atoms close to the path of the particle will produce a polarization, (From Leroy, C. and Rancoita, P-G., 2004). The third formula includes the K-shell correction $\left(\frac{C_K}{Z}\right)$ and polarization correction (δ),

$$-\frac{dE}{dx} = \frac{4pk_0 Z^2 e^4 n}{mc^2 b^2}\left[\ln\frac{2mc^2 b^2}{I(1-b^2)} - b^2 - \frac{C_K}{Z} - d\right] \quad (2.5)$$

(Turner, J., 2007 & Attix, F. H. , 1986 & Podgoršak, E. B., 2006 and Krane, K. S., 1988).

Where,

Z is atomic number of the heavy charged particle,

β is the relative speed V/c,

c is speed of light in vacuum,

k_0 = 8.99 x 109 N m^2 C^{-2},

e is the magnitude of the electron charge,

n is the number of electrons per unit volume in the medium,

m is the electron rest mass,

I is the mean excitation potential, the first approximation is given by:

$I \approx 11.5 x Z x 10^{-6}$MeV, or by $I \approx 9.1 x Z\ (1+1.9 x Z^{-2/3}) 10^{-6}$ MeV.

(From Leroy, C. and Rancoita, P-G., 2004)

2.2.3. b. Light Charged Particles:

The linear rate of energy loss due to excitations and ionization (collisional energy loss). The collisional stopping power for electrons and positrons can be written:

$$-\left(\frac{dE}{dx}\right) = \frac{2pk_0 Z^2 e^4 n}{mc^2 b^2}\left[\ln\left(\frac{t^2(t+2)}{2\left(I/m_0 c^2\right)^2}\right) + F^{\pm}(b) - d - \frac{2C}{Z}\right] \qquad (2.6)$$

$$F^{-}(b) = 1 - b^2 + \frac{1}{(1+t)^2}\left[\frac{t^2}{8} - (1+2t)\ln 2\right] \qquad (2.7)$$

is used for electrons and

$$F^{+}(b) = 2\ln 2 - \frac{b^2}{12}\left[23 + \frac{14}{t+2} + \frac{10}{(t+2)^2} + \frac{4}{(t+2)^3}\right] \qquad (2.8)$$

For positrons, τ is the electron or positron kinetic energy normalized to m_0c^2, from (Attix, F. H. , 1986).

2.2.4. Mass Stopping Power:

It is obtained by dividing the stopping power by density ρ. The mass stopping power is a useful quantity because it expresses the rate of energy loss of the charged particle per g cm^{-2} of the medium traversed.

2.2.5. Ranges

The range of a charged particle is the distance it travels before coming to rest “R”.

$$R(T) = \int_0^T \left(\frac{-dE}{dx} \right)^{-1} dE \tag{2.9}$$

,where T is the kinetic energy of the particle. CSDA (continuous-slowing-down approximation range).

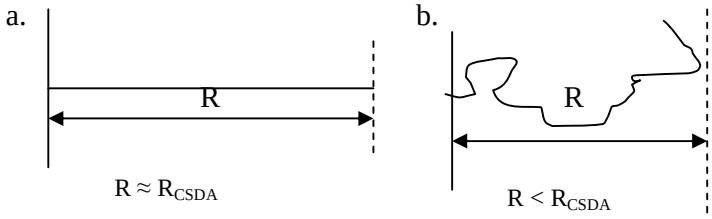

Fig. (2.4) Charged particles penetration into a medium. a. Heavy charged particle; b. Light charged particle.

2.2.5. a. Heavy Charged Particles:

For two heavy charged particles at the same initial speed β

$$\frac{R_1(b)}{R_2(b)} = \frac{Z_2^2 M_1}{Z_1^2 M_2} \tag{2.10}$$

$R(b) = \frac{M}{Z^2} R_P(b)$, Where $R_p(\beta)$ is the proton range, (Turner, J., 2007 & Krane, K. S., 1988).

2.2.5. b. Light Charged Particles:

In low-Z materials, electrons range is determined from an empirical equation, R in $g.cm^{-2}$ and kinetic energy T in MeV,

1- $R = 0.412T^{(1.27-0.0954\ln T)}$, 0.01 MeV≤T≤2.5 MeV. (2.11)

2- R= 0.530T-0.106 , T>2.5 MeV. (2.12)

From (Turner, J., 2007).

2.2.6. Radiative Losses

Bremsstranhlung radiation is electromagnetic, while the particle passing a change in acceleration occurs. The small mass of the light charged particle leads this radiation to be significant. If the electron passes close to nucleus, the deflection is very large and the emitted photon is very energetic.

The total stopping power for light charged particle is the sum of both collisional and bremsstrahlung stopping power, (Attix, F. H., 1986 & Turner, J., 2007):

$$\left(-\frac{dE}{dx}\right)^{\pm}_{tot} = \left(-\frac{dE}{dx}\right)^{\pm}_{col} + \left(-\frac{dE}{dx}\right)^{\pm}_{rad} \tag{2.13}$$

Within a broad range of kinetic energies below 10MeV collision (ionizational) losses are dominant

$$\left(\frac{dE}{dx}\right)_{col} > \left(\frac{dE}{dx}\right)_{rad}$$

At high kinetic energies, at a critical kinetic energy (E_{crit}), the two stopping powers are equal. For a given absorber Z, E_{crit} can be estimated from:

$$E_{crit} \approx \frac{800}{Z} MeV \tag{2.14}$$

$$\frac{\left(-\frac{dE}{dx}\right)_{rad}}{\left(-\frac{dE}{dx}\right)_{col}} \cong \frac{ZE}{800} \tag{2.15}$$

(Turner, J., 2007 & Krane, K. S., 1988)

2.2.7. Radiation Yield

Radiation yield of a charged particle of initial kinetic energy T is the total fraction of that energy that is emitted as electromagnetic radiation while the particle slows and comes down. Radiation yield increases with electron energy and atomics number, for heavy charged particles Y≈0, (Attix, F. H., 1986)

$$Y = \frac{6 * 10^{-4} ZT}{1 + 6 * 10^{-4} ZT} \tag{2.16}$$

T is the initial kinetic energy of electrons, Z the absorber atomic number, (Turner, J., 2007).

2.3. Photons:

Photons (such as x-ray and gamma ray) may interact either with orbital electrons or with the nucleus of atoms. They go under sequences of absorption and scattering depending on their energies and number of electrons in the medium, (Curry, T.S. et al, 1990), there are five types of photons interactions with matter:

1. Compton effect.

2. Photoelectric effect.

3. Pair production.

4. Rayleigh (coherent) scattering.

5. Photonuclear interactions.

The first three are the most important in medical applications; they are illustrated in figure (2.5).In table (2.2),the comparison between four kinds of photons' interactions.

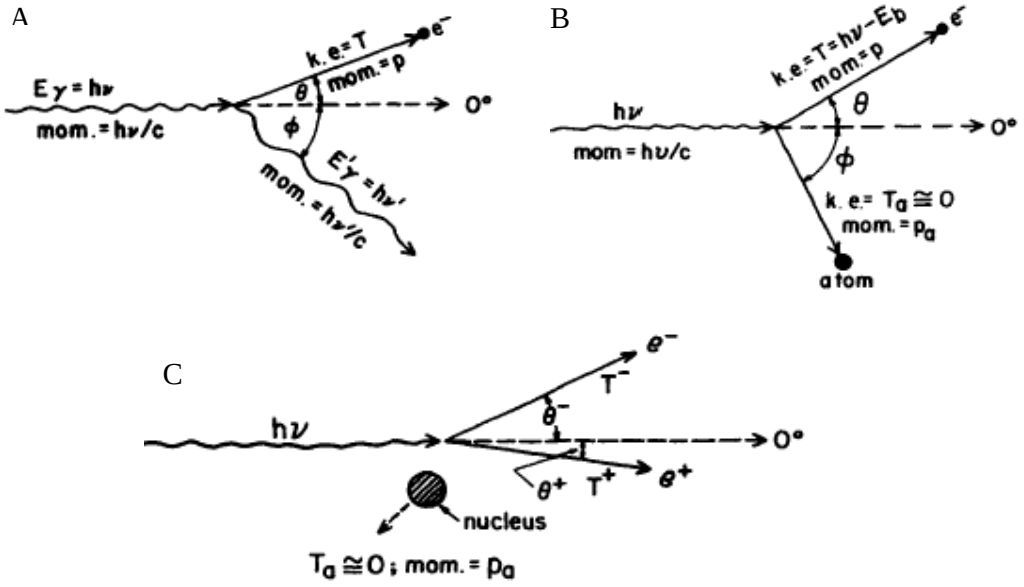

Fig. (2.5) A. Compton effect, B. Photoelectric effect, C. Pair production.

2.4. Neutrons

Neutrons, as they are neutral, are incapable of the typical Coulombic interactions in comparison with charged particles. Neutrons interact with the medium through two steps:

1-Energy transfer to heavy charged particles.

2-Energy deposition through Coulomb interaction of the charged particles with atoms, (Podgoršak, E. B., 2006)

2.4.1. Neutrons Sources

The most available neutron sources are nuclear fission reactors, accelerators, and radioactive sources.

2.4.2. Neutrons Interactions with Matter:

Neutron's interaction depends on two parameters, (IAEA, 1995):

1- Neutron energy.

2- Relative abundances of the elements in irradiated object.

According to neutron kinetic energy, neutrons are classified into seven categories (Table. 2.3).

Table (2.3) Neutrons classification, from (Podgoršak, E. B., 2006).

Type	Energy
Ultracold neutrons	$E<2x10^{-7}eV$
Very cold neutrons	$2x10^{-7}\ eV\leq E\leq 5x10^{-5}eV$
Cold neutrons	$5x10^{-5}eV \leq E\leq 0.025eV$
Thermal neutrons	$E\approx 0.025eV$
Epithermal neutrons	$1eV<E<1KeV$
Intermediate neutrons	$1KeV<E<0.1MeV$
Fast neutrons	$E>0.1MeV$

Neutrons interact in six ways, (IAEA, 1995 & Alpen, E. L., 1998):

1- **Elastic Scattering** is the most important in biological substances, produces recoil ions, E_n>14MeV.

$$E_t = E_n \frac{4M_a M_n}{(M_a + M_n)^2} \cos^2 q \qquad (2.17)$$

Where E_t is energy transfer, E_n is Initial neutron energy, M_a is target mass, M_n is neutron mass, θ is recoil angel.

2- **Inelastic Scattering** This interaction is important in neutron dosimetry and leads to excitation of the struck nucleus and a slower neutron, (gamma emission is included). An example for this kind of interaction, $^{14}N(n,n')^{14}N : E_\gamma = 10MeV$.

3- **Nonelastic Scattering** ejects another particle out of the hit nucleus. [$^{12}C(n,\alpha)^{9}Be : E_\alpha = 1.75MeV$].

4- **Neutron Capture** The interaction is important for slow neutrons and leads to their disappearance, E_n=0.025eV. [$^{14}N(n,p)\ ^{14}C : E_p = 0.58MeV$, $^{1}H(n,\gamma)\ ^{2}H : E_\gamma$ = 2.2MeV].

5- **Spallation** The process in which neutron breaks up the hit target nucleus and ejects significant pieces of it, E_n >10MeV and emits deexcitation gamma ray.

6- **Fission** induces in ^{235}U, ^{239}Pu and ^{233}U by absorption of a thermal neutron, $E_n \approx 1MeV$, from (Turner, J., 2007).

$$^{1}n_0 + ^{235}U_{92} \rightarrow ^{147}La_{57} + ^{87}Br_{35} + 2^{1}n_0$$

Chapter 3

Track Structure's Physical Parameters of Ionizing Radiation

Fundamental dosimetry and modeling of different types of biological damage in mammals can be described by studying their relation with several physical parameters in biological matter. Tables of calculation for these parameters in liquid water have been presented in (Watt, D. E., 1996) and their explanations.

In order to understand the track structure of ionizing radiation, especially heavy charged particles, parameters such as LET, L_{100}, $(Z^*/\beta)^2$, W, I, λ and R as functions of E for 21 ions will be considered.

3.1. Linear Energy Transfer (LET) in Liquid Water:

The linear energy transfer is the deposited energy by a charged particle in traversing a distance dx, which can be referred as L_∞ , (ICRU, 1998):

$$L_\infty = LET = \frac{dE}{dx} \tag{3.1}$$

The unrestricted linear energy transfer due to collisions with electrons, known as linear electronic collision stopping powers L_∞, which depends on projectile speed (ICRU, 2005). Many researchers describe biological damage in term of LET (L_∞), (Scolz, M. and Kraft, G., 1996).

For low particle energies, at and below the maximum stopping power, empirical relations is used to determine the energy E_{pk}(the projectile's energy at the maximum stopping power) , For all heavy particles other than protons (Watt, D. E., 1996) where,

$$\begin{cases} E_{pk} = 84.A_i.\, z_i^{*0.83} & \text{For } Z=2 \\ E_{pk} = 84.\, A_i.\, z_i^{*1.11} & \text{For } Z>2 \end{cases} \quad (3.2)$$

A_i is the mass number and z_i^* the effective charge number of the projectile.

Where 84 keV is the energy at the maximum LET for protons in water, Z^*

Energies below and above the maximum LET, their LETs obtained from scaled equation (3.3) and (3.4), respectively.

$$\frac{L_i}{L_{\max,i}} = \left(\frac{E_i}{E_{pk,i}}\right)^p . \left[2 - \left(\frac{E_i}{E_{pk,i}}\right)^p\right] \quad (3.3)$$

$$\frac{L_i}{L_{\max,i}} = \left(\frac{E_i}{E_{pk,i}}\right)^q . \left[1 - q.\ln\left(\frac{E_i}{E_{pk,i}}\right)\right] \quad (3.4)$$

Where p= 0.565, q= 1.0944 for liquid water.

Figures (3.1) to (3.4) illustrate the relationship between unrestricted linear energy transfer and energy in liquid water.

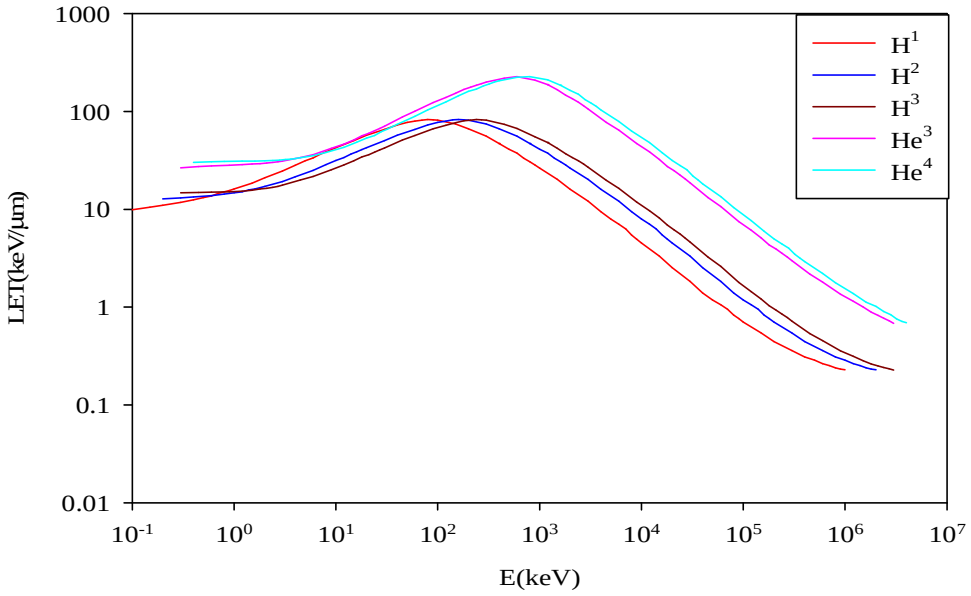

Fig. (3.1) The unrestricted linear energy transfer of H^1, H^2, H^3, He^3 and He^4 particles (vs) energy in liquid water.

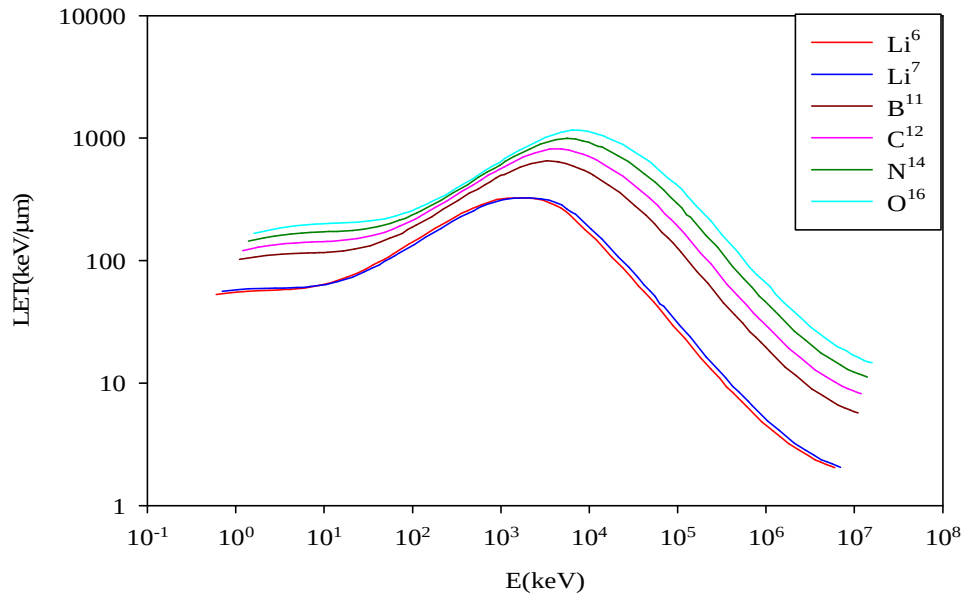

Fig. (3.2) The unrestricted linear energy transfer of Li^6, Li^7, B^{11}, C^{12}, N^{14}, O^{16} particles (vs) energy in liquid water.

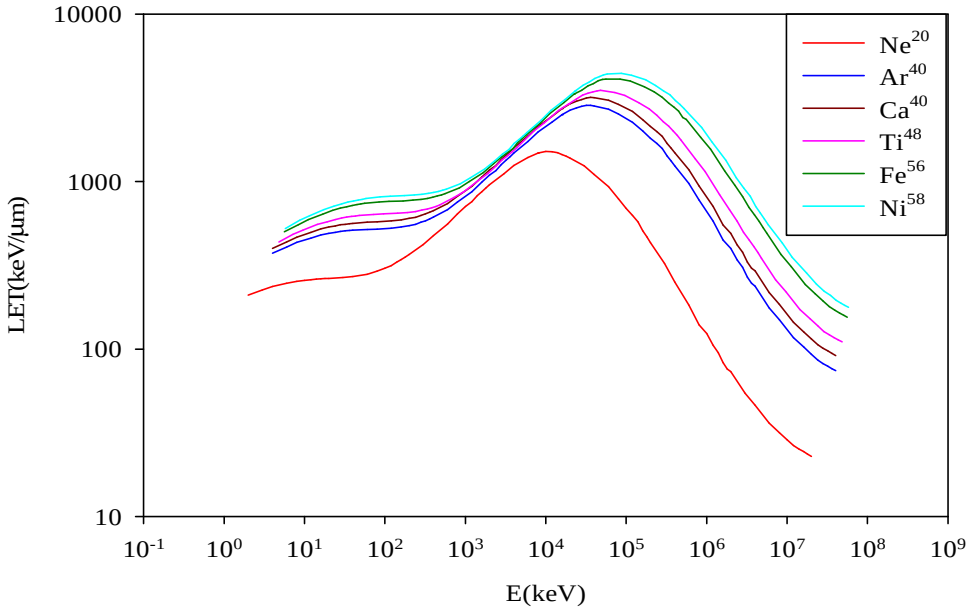

Fig. (3.3) The unrestricted linear energy transfer of Ne^{20}, Ar^{40}, Ca^{40}, Ti^{48}, Fe^{56}, Ni^{58} particles (vs) energy in liquid water..

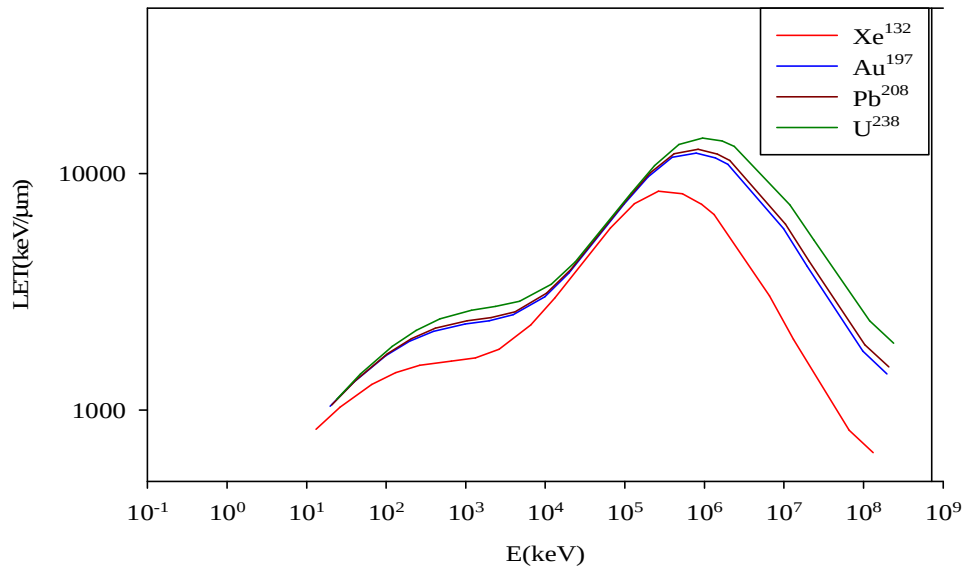

Fig. (3.4) The unrestricted linear energy transfer of Xe^{132}, Au^{197}, Pb^{208}, U^{238} particles (vs) energy in liquid water.

3.2. Restricted Linear Energy Transfer (L_D):

Restricted linear energy electronic stopping power, L_Δ, is the energy lost by a charged particle dE_Δ due to electronic collision in traversing a distance dx , where the sum of the kinetic energies of all the electrons released with kinetic energies greater than Δ, are subtracted. It is related to LET_∞ by

$$L_\Delta = L_\infty - \frac{dE_{K_e,\Delta}}{dx} \tag{3.5}$$

L_{100} is understood to be the linear energy transfer for an energy cutoff of 100 eV, (ICRU, 1998).

Harder (Harder, D. et al, 1994) used L_Δ as a radiation quality parameter to describe the damage of ionizing radiation, where the cutoff energy eliminates the damage of δ-rays outside the interested biological site. Figures (3.5) to (3.8) illustrate the relationship between restricted linear energy transfer and energy in liquid water.

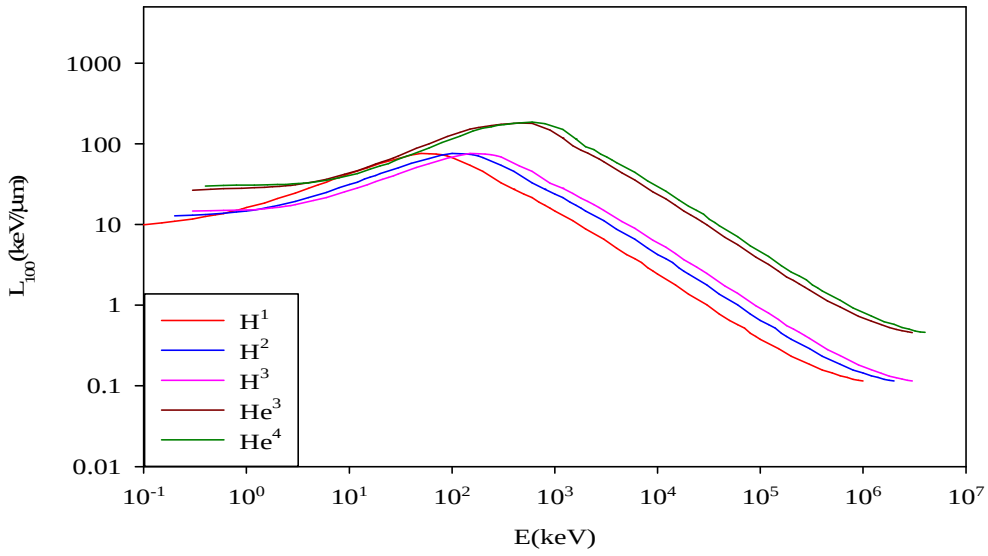

Fig. (3.5) The restricted linear energy transfer of H^1, H^2, H^3, He^3 and He^4 particles (vs) energy in liquid water.

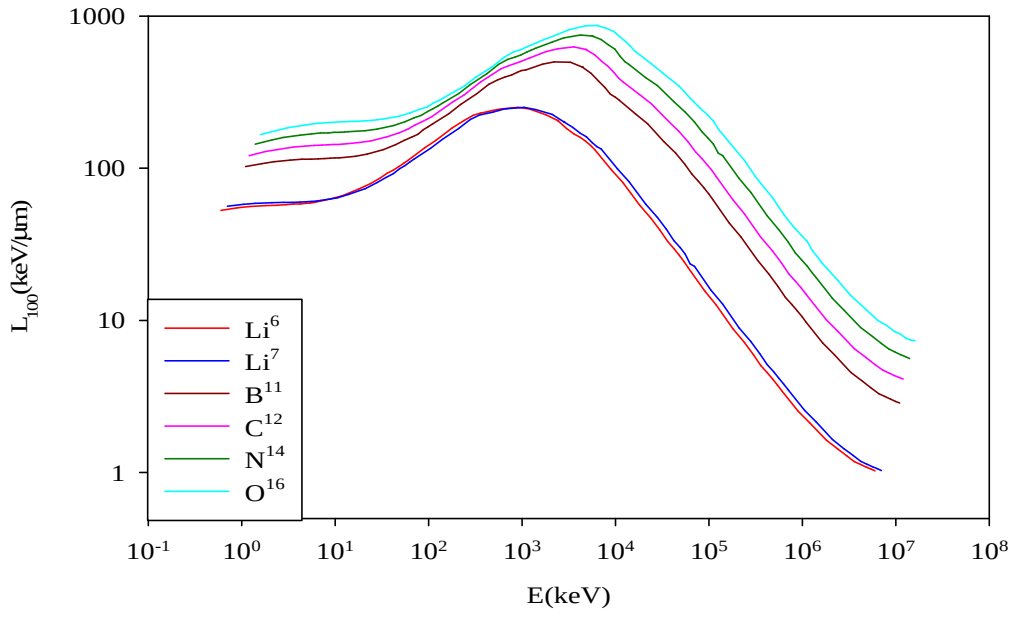

Fig. (3.6) The restricted linear energy transfer of Li^6, Li^7, B^{11}, C^{12}, N^{14}, O^{16} particles (vs) energy in liquid water.

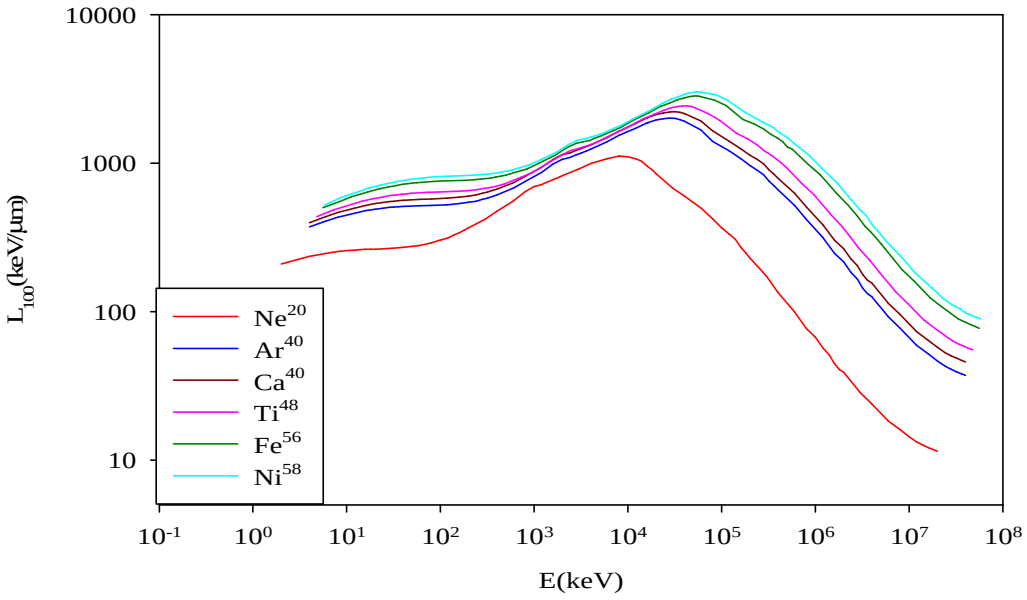

Fig. (3.7) The restricted linear energy transfer of Ne^{20}, Ar^{40}, Ca^{40}, Ti^{48}, Fe^{56}, Ni^{58} particles (vs) energy in liquid water.

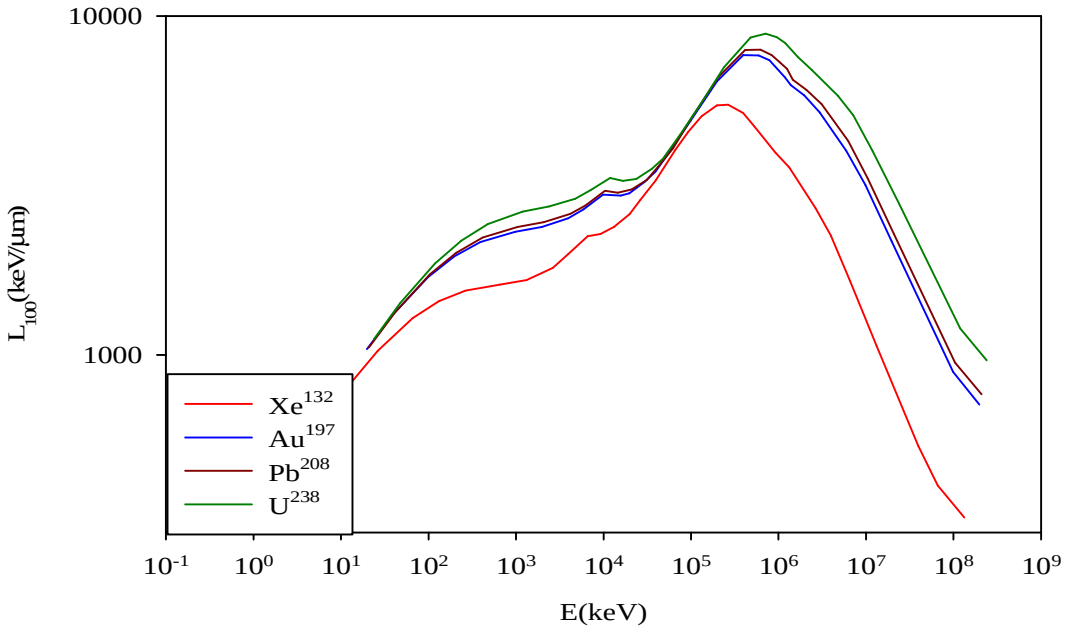

Fig. (3.8) The restricted linear energy transfer of Xe^{132}, Au^{197}, Pb^{208}, U^{238} particles (vs) energy in liquid water.

3.3. Katz 's Parameter $(Z^*/\beta)^2$:

The cellular track model of Katz describes biological damage from energetic ions to the secondary electrons (δ rays) produced along the ion path which scales as $(Z^*/\beta)^2$, (Cucinotta, F. A. et al, 1995).

For heavy ion stopping power, there is difference between a particle and its antiparticle, (ICRU, 2005), and was given by the following an expression (Butts, J. J. and Katz, R., 1967),

$$Z^*=Z[1-e^{-(125\beta Z^{-2/3})}] \qquad (3.6)$$

Z^* is the effective charge of the ion at speed βc.

Figures (3.9) to (3.16) illustrate the relationship between effective charge, Katz's parameter and energy in liquid water.

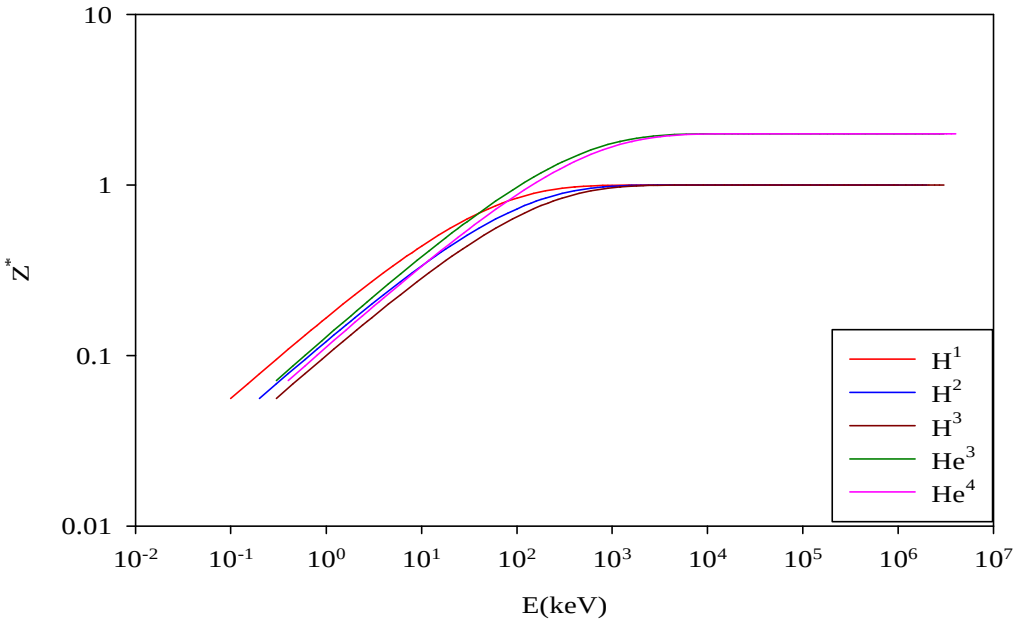

Fig. (3.9) The effective charge of H^1, H^2, H^3, He^3 and He^4 particles (vs) energy in liquid water.

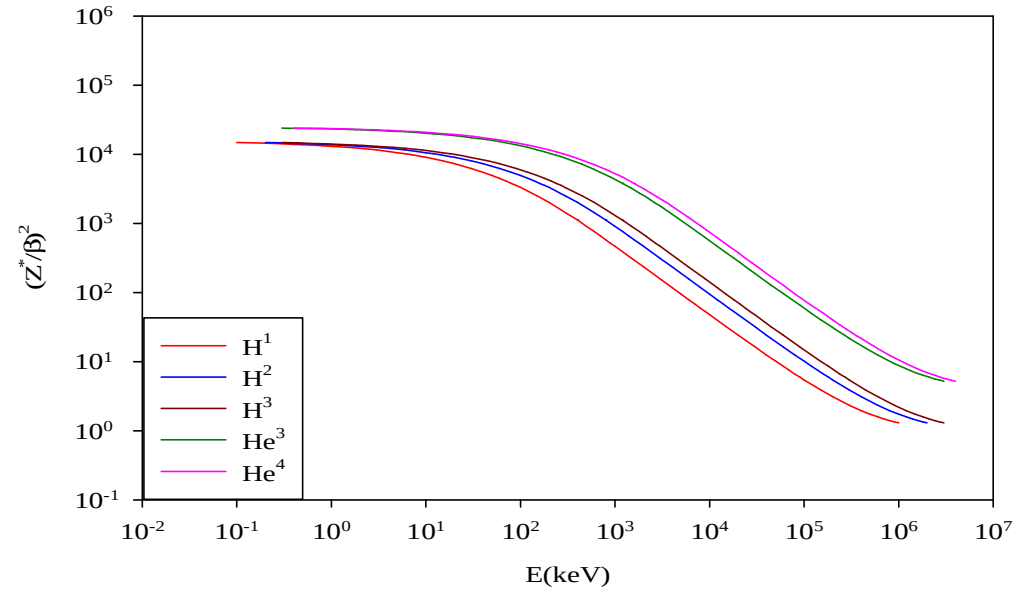

Fig. (3.10) Katz's Parameter of H^1, H^2, H^3, He^3 and He^4 particles (vs) energy in liquid water.

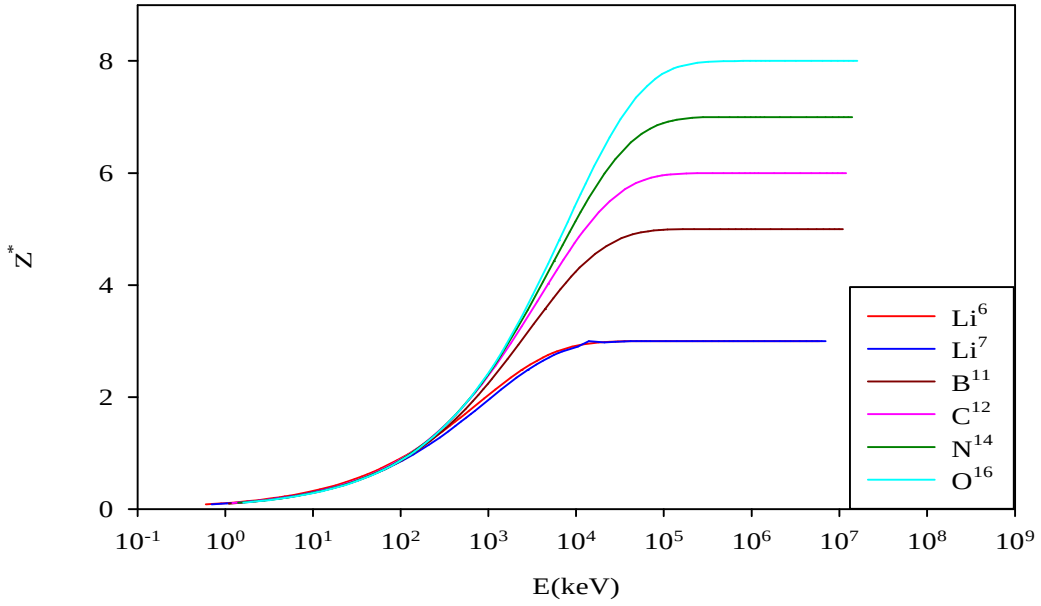

Fig. (3.11) The effective charge of Li^6, Li^7, B^{11}, C^{12}, N^{14}, O^{16} particles (vs) energy in liquid water.

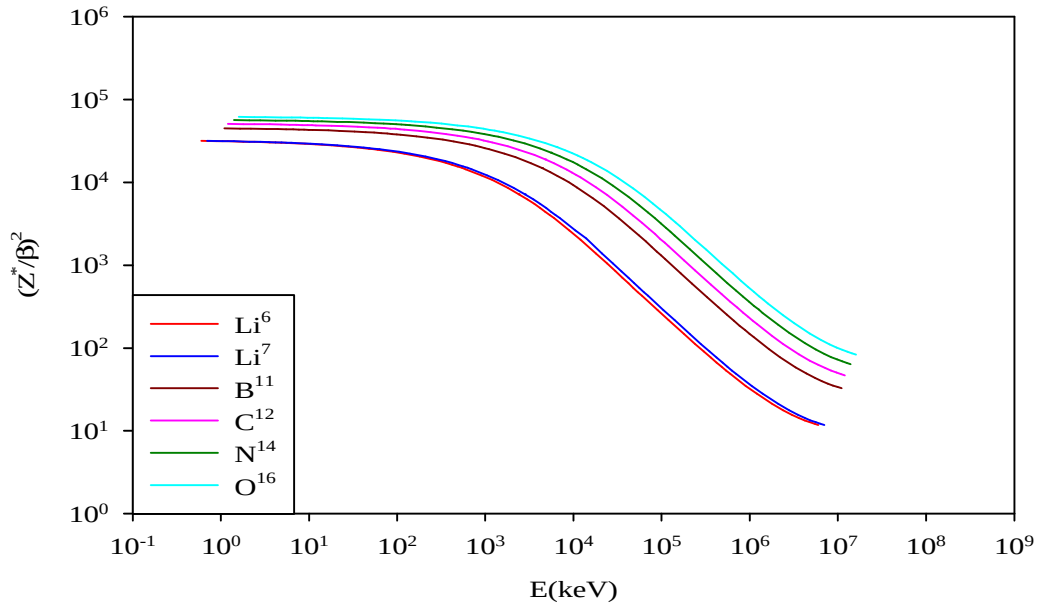

Fig. (3.12) Katz's Parameter of Li^6, Li^7, B^{11}, C^{12}, N^{14}, O^{16} particles (vs) energy in liquid water.

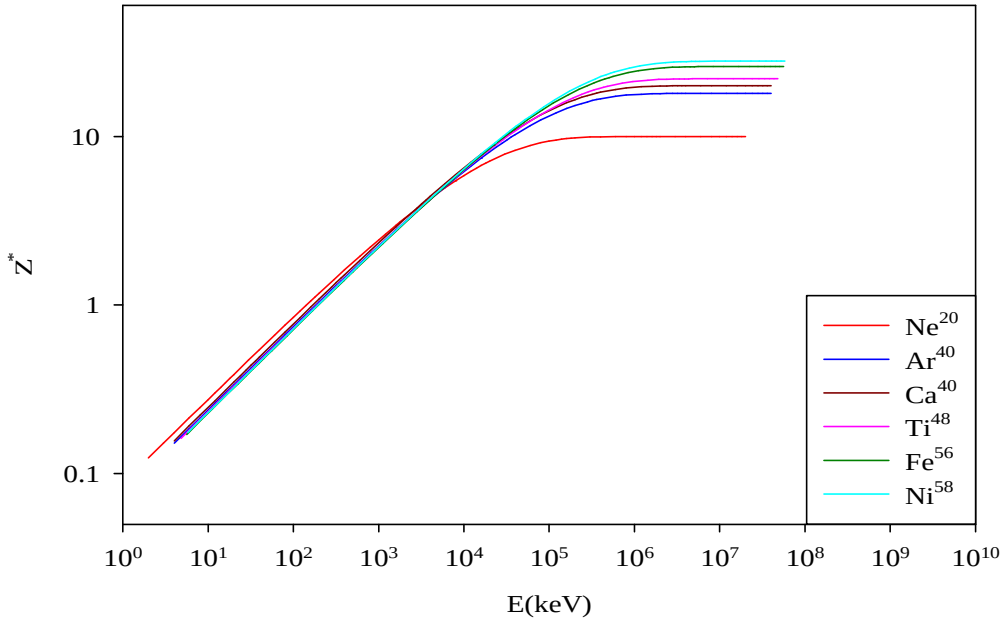

Fig. (3.13) The effective charge of Ne^{20}, Ar^{40}, Ca^{40}, Ti^{48}, Fe^{56}, Ni^{58} particles (vs) energy in liquid water.

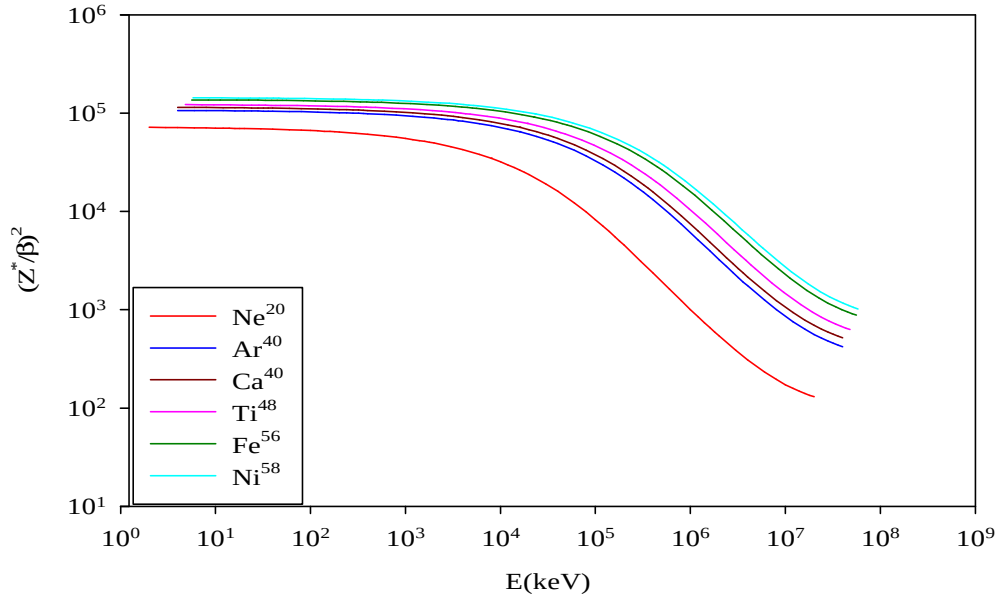

Fig. (3.14) Katz's Parameter of Ne^{20}, Ar^{40}, Ca^{40}, Ti^{48}, Fe^{56}, Ni^{58} particles (vs) energy in liquid water.

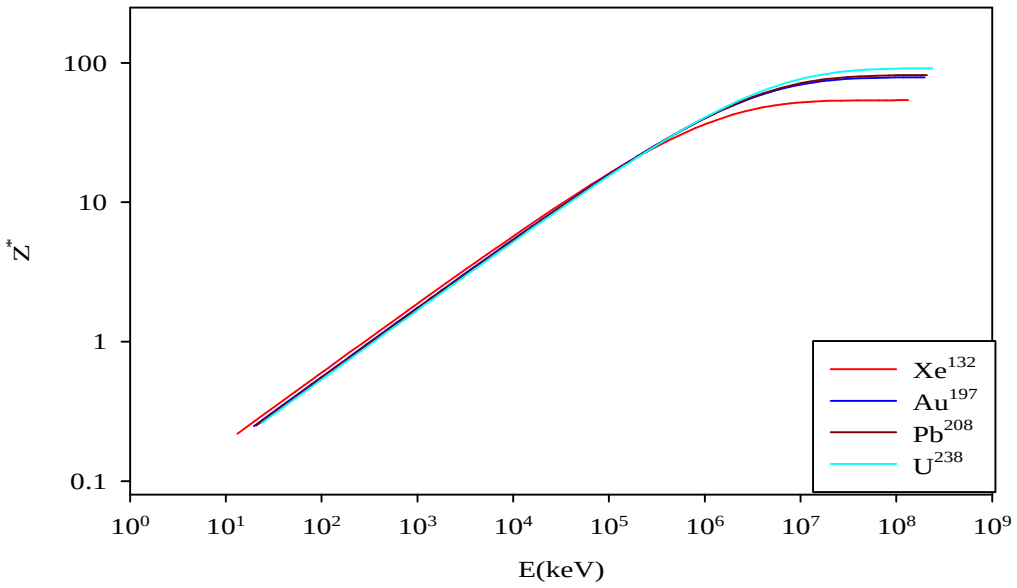

Fig. (3.15) The effective charge of Xe^{132}, Au^{197}, Pb^{208}, U^{238} particles (vs) energy in liquid water.

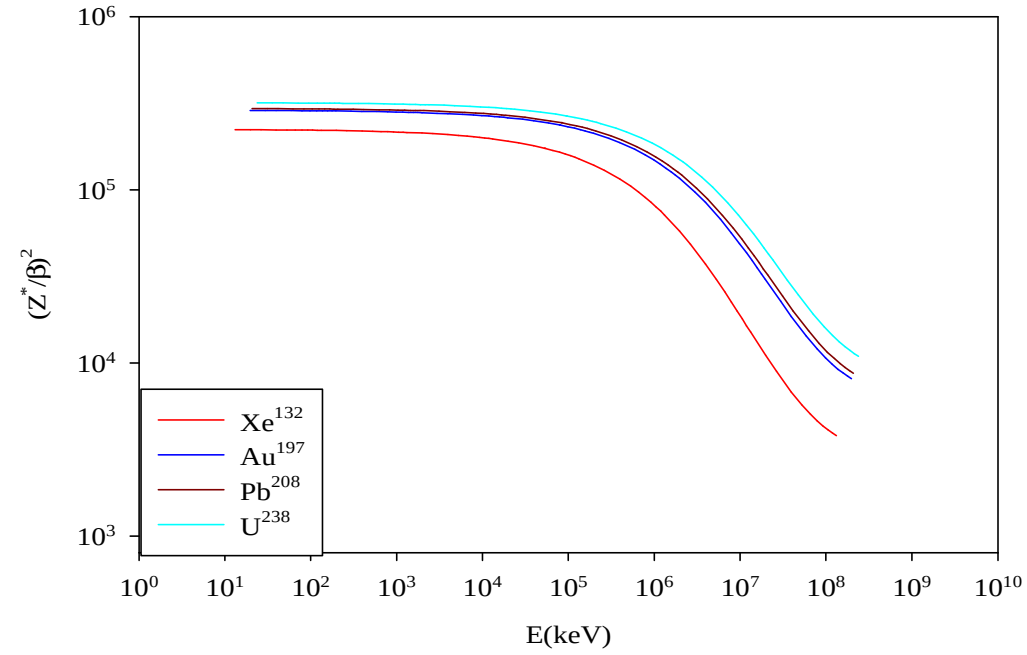

Fig. (3.16) Katz's Parameter of Xe^{132}, Au^{197}, Pb^{208}, U^{238} particles (vs) energy in liquid water.

3.4. The Mean Energy W:

The mean energy expanded in a gas per ion pair formed, (ICRU, 1998)

$$W = \frac{E}{N} \tag{3.7}$$

E is the initial kinetic energy of charged particles.

N is mean number of ion pairs formed by E.

For liquid water, (Watt, D. E., 1996):

$$\frac{W_i}{W_0} = Z_{eff_i}^{0.1} \cdot \left[1 + 0.4058 \Big/ \left(\frac{Ei}{Ai.Z_{eff_i}^{1.3333}} \right)^{0.4194} \right] \tag{3.8}$$

Where $W_0 = 25.Z_{eff_i}^{0.1}$

Figures (3.17) to (3.20) illustrate the relationship between mean energy and energy in liquid water.

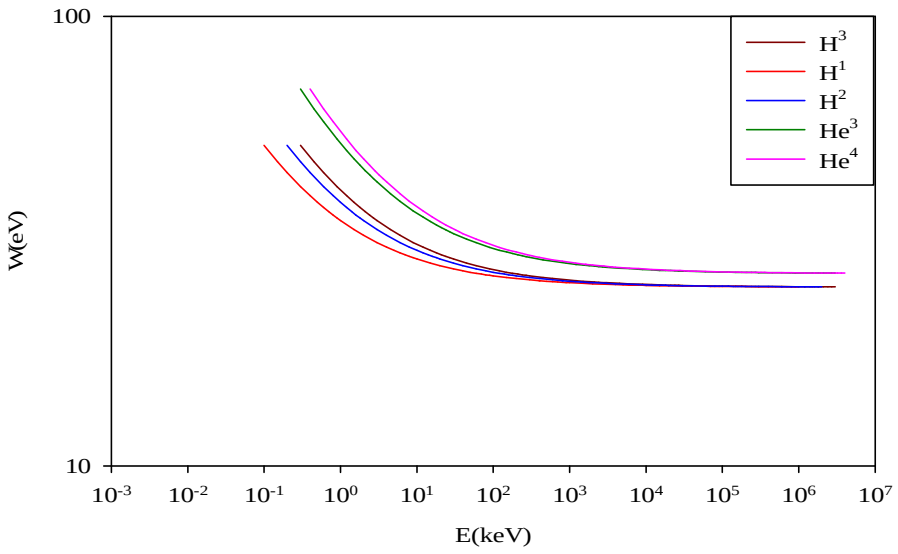

Fig. (3.17) The mean energy of H^1, H^2, H^3, He^3 and He^4 particles (vs) energy in liquid water.

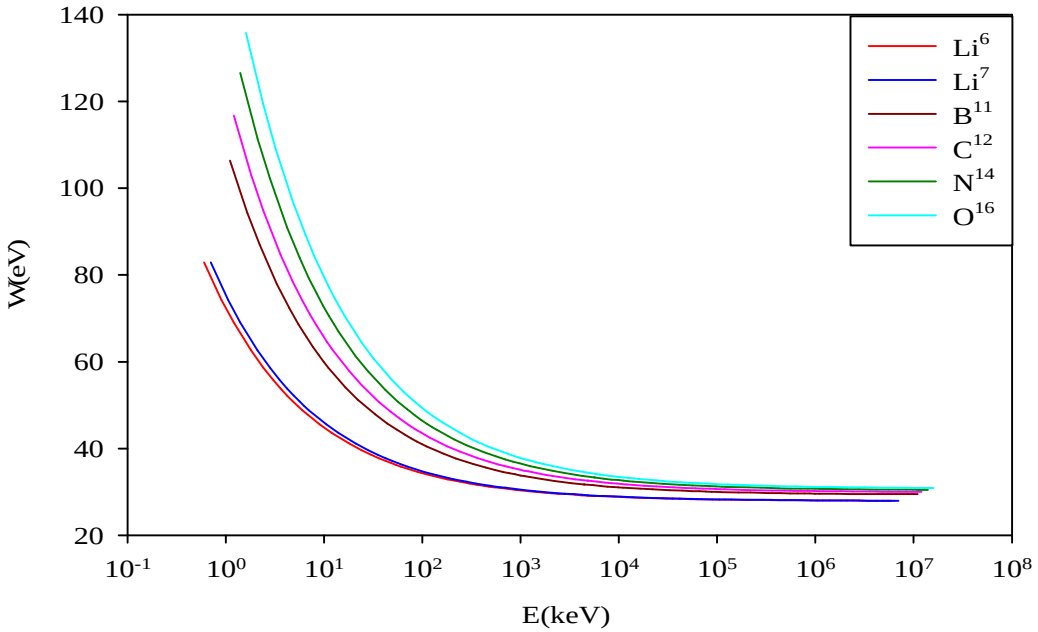

Fig. (3.18) The mean energy of Li^{6}, Li^{7}, B^{11}, C^{12}, N^{14}, O^{16} particles (vs) energy in liquid water.

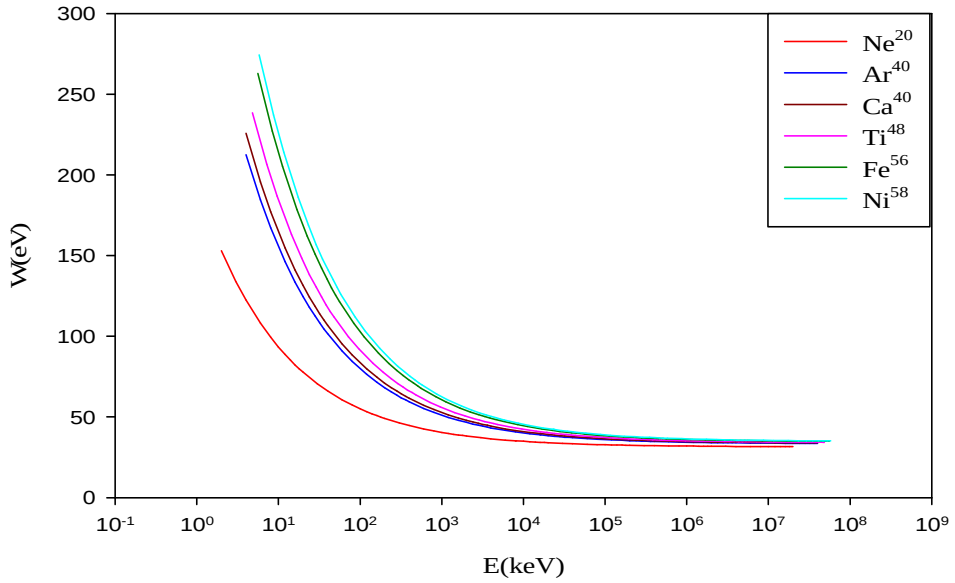

Fig. (3.19) The mean energy of Ne^{20}, Ar^{40}, Ca^{40}, Ti^{48}, Fe^{56}, Ni^{58} particles (vs) energy in liquid water.

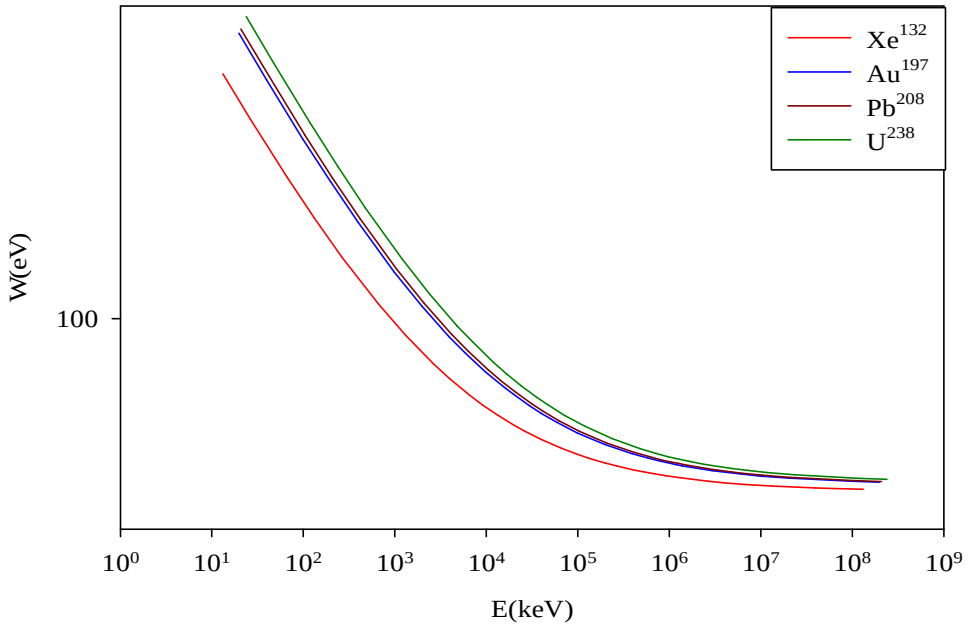

Fig. (3.20) The mean energy of Xe^{132}, Au^{197}, Pb^{208}, U^{238} particles (vs) energy in liquid water.

3.5. Linear Primary Ionization (I):

Linear primary ionization physically represents the primary ionization per unit path, for fast particles is given as (Watt, D. E., 1996),

$$I\left(nm^{-1}\right) = 0.01536.\frac{Z}{A}.\left(\frac{Z^*}{b}\right)^2.\left(\frac{1}{IP} - \frac{1}{T_{\max}}\right) \tag{3.9}$$

Where:

IP is the ionization potential IP of water (in eV) and equal 12.6eV, (Kudryashov, Y. B., 2008), T_{max} is the maximum delta-ray energy, which is given by (Watt, D. E., 1996),

$$T_{\max} = \frac{1022.t\left(t+2\right)}{\left[1+2\left(t+1\right).\left(\frac{m}{M_i}\right)+\left(\frac{m}{M_i}\right)^2\right]} \tag{3.10}$$

τ is the ratio of the kinetic energy E_i of the projectile to its rest mass energy.

m is the rest mass of an electron.

M_i is the mass of the ion.

Over the whole energy range, I can be approximated to be, (Watt, D. E., 1996):

$$I\left(nm^{-1}\right)=\frac{L}{\left(T_{av}+W_i\right)} \tag{3.11}$$

Where L is the LET, W_i is the mean energy, T_{av} is the average δ-rays energy

$$\frac{T_{av}}{T_{\max}}=\frac{\frac{2}{3}.\left(1-\frac{1}{y}\right).\left(1-f^{3/2}\right)+\ln(y)-\left(1-\frac{1}{y}\right)}{2.y.\left(1-\frac{1}{y}\right).\left(1-f^{1/2}\right)+(y-1)-\ln(y)} \tag{3.12}$$

$$y=\frac{T_{\max}}{T_p} \qquad \text{and} \qquad f=\frac{T_{th}}{T_p}$$

T_{th} (the threshold energy)= 30 eV.

T_p (the electron energy at the maximum stopping power)= 100 eV.

Figures (3.21) to (3.24) illustrate the relationship between linear primary ionization and energy in liquid water.

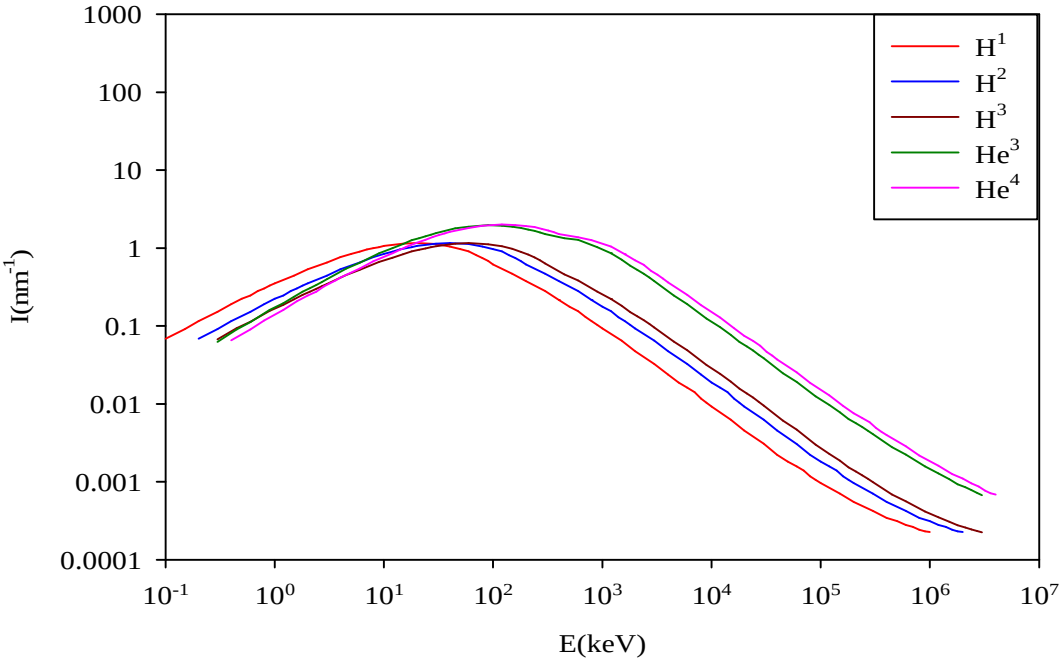

Fig. (3.21) Linear Primary Ionization of H^1, H^2, H^3, He^3 and He^4 particles (vs) energy in liquid water.

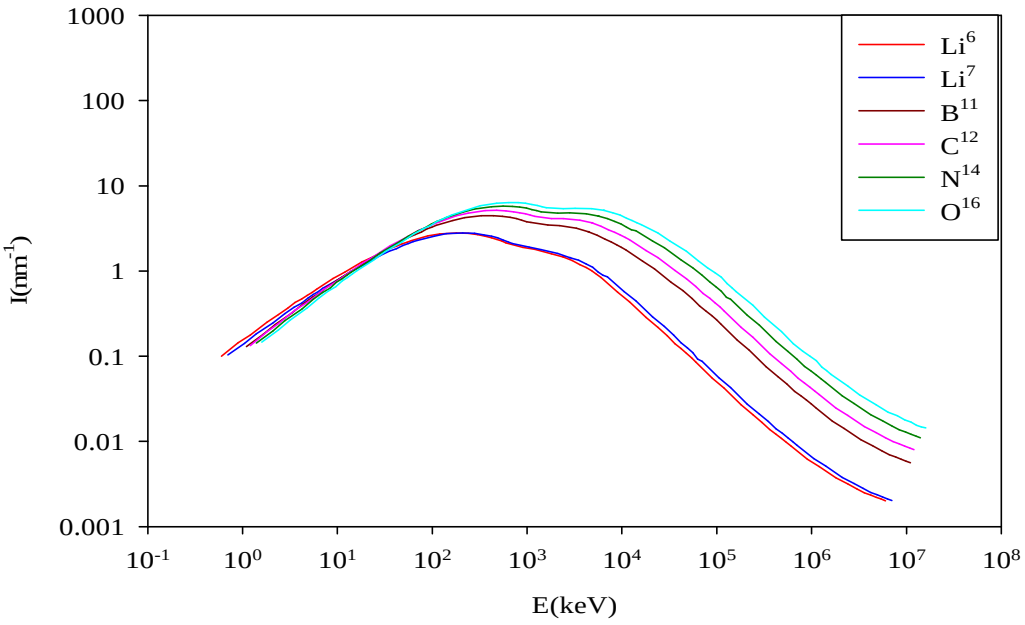

Fig. (3.22) Linear Primary Ionization of Li^6, Li^7, B^{11}, C^{12}, N^{14}, O^{16} particles (vs) energy in liquid water.

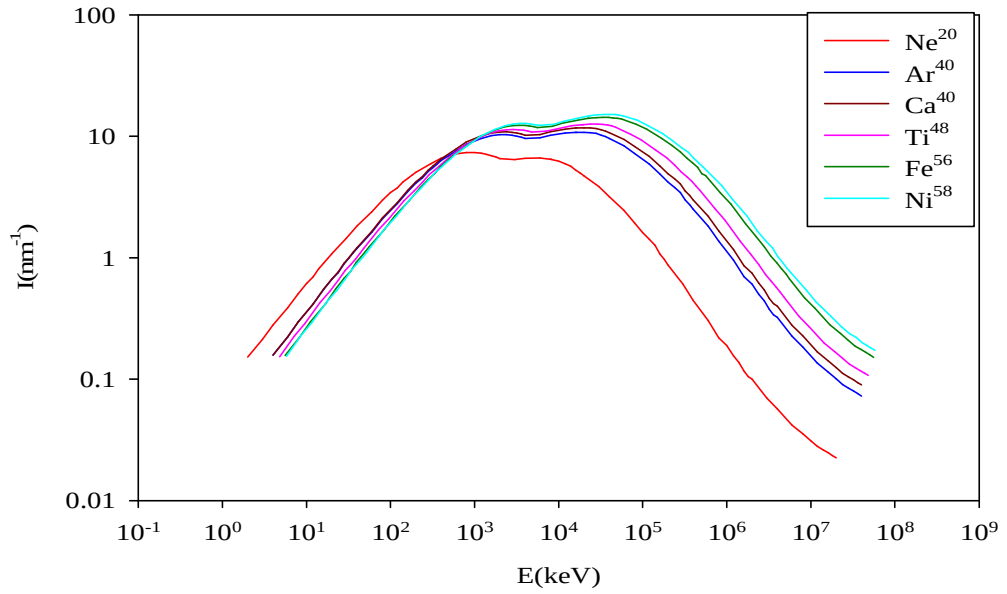

Fig. (3.23) Linear Primary Ionization of Ne^{20}, Ar^{40}, Ca^{40}, Ti^{48}, Fe^{56}, Ni^{58} particles (vs) energy in liquid water.

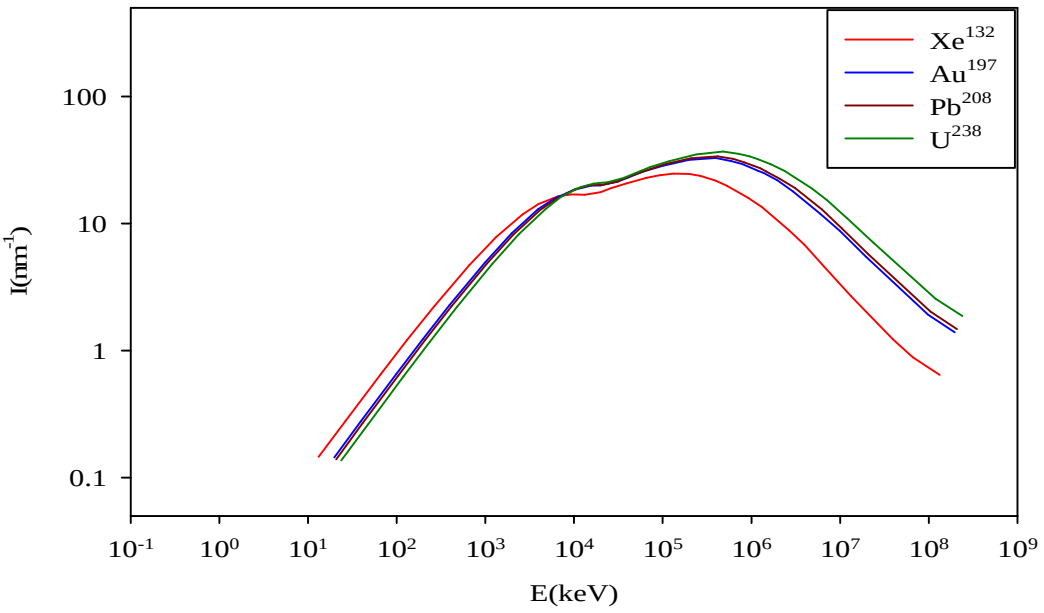

Fig. (3.24) Linear Primary Ionization of Xe^{132}, Au^{197}, Pb^{208}, U^{238} particles (vs) energy in liquid water.

3.6. The Mean Free Path for Linear Primary Ionization λ:

The average distance between depositing energy events along the main track of a charged particle, can be referred to as “mfp”. And simply equals the reciprocal of I, (Watt, D. E., 1996);

$$l\left(nm\right)=\frac{1}{I} \tag{3.13}$$

Figures (3.25) to (3.28) illustrate the relationship between the mean free path and energy in liquid water.

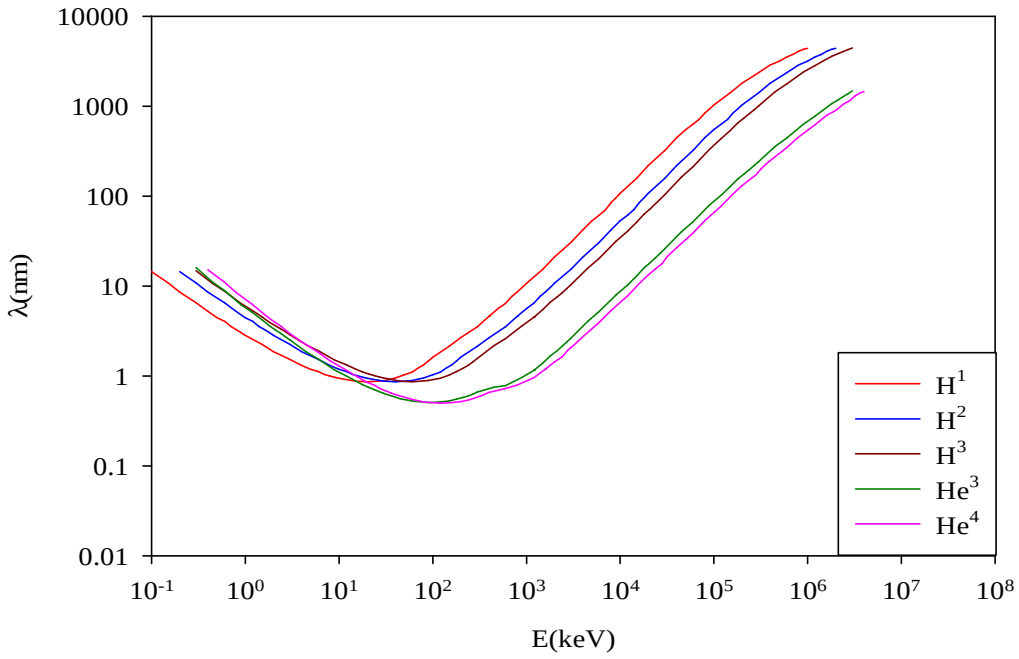

Fig. (3.25) The Mean Free Path of H^1, H^2, H^3, He^3 and He^4 particles (vs) energy in liquid water.

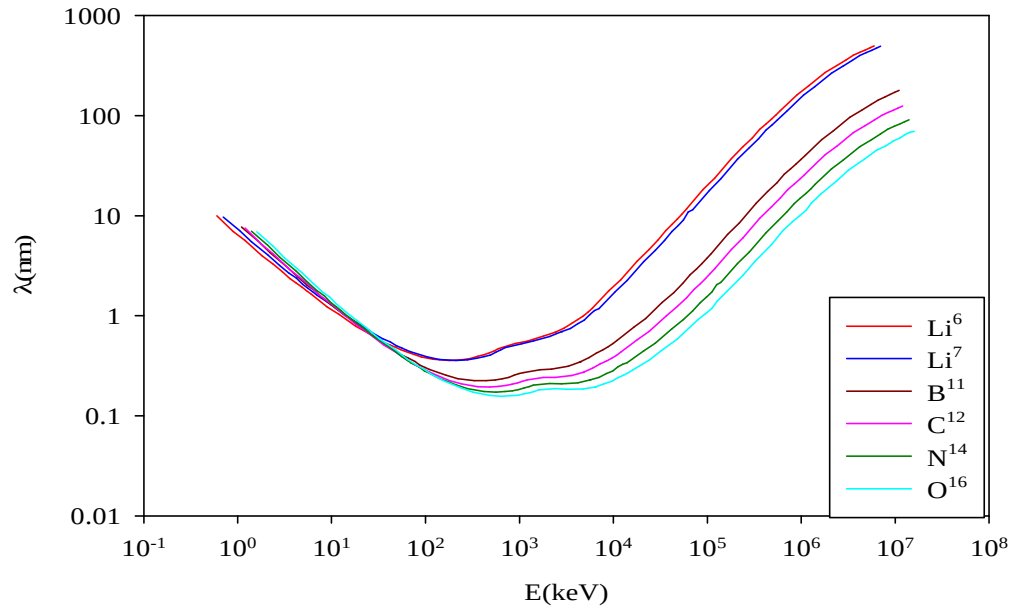

Fig. (3.26) The Mean Free Path of Li^{6}, Li^{7}, B^{11}, C^{12}, N^{14}, O^{16} particles (vs) energy in liquid water.

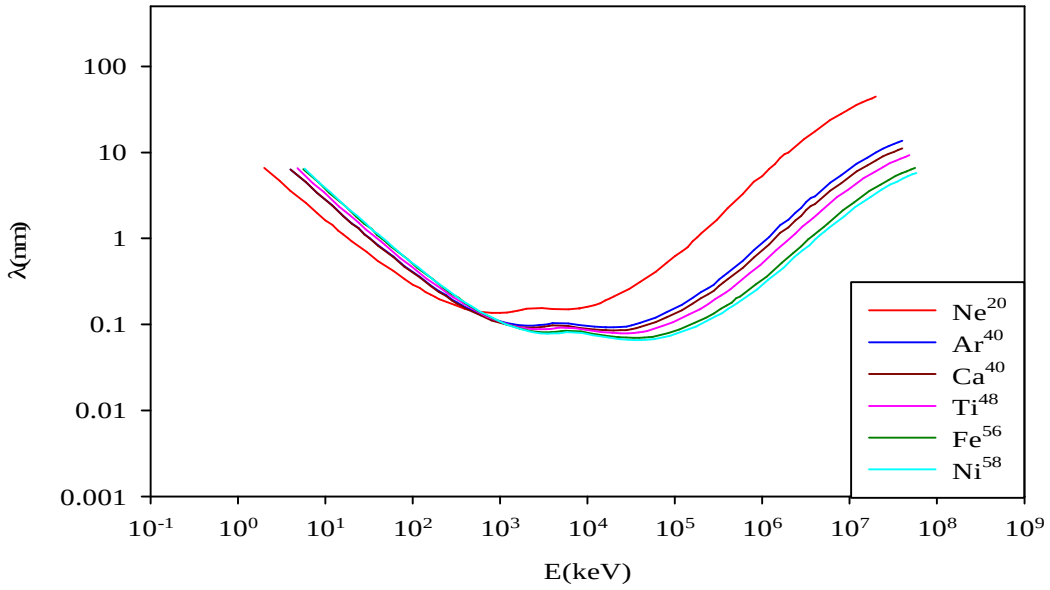

Fig. (3.27) The Mean Free Path of Ne^{20}, Ar^{40}, Ca^{40}, Ti^{48}, Fe^{56}, Ni^{58} particles (vs) energy in liquid water.

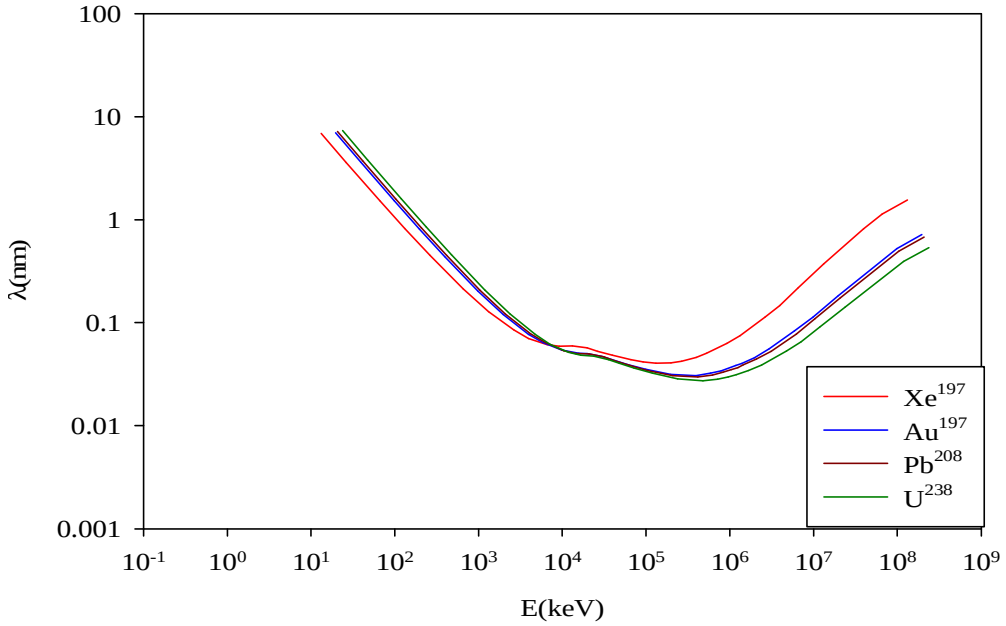

Fig. (3.28) The Mean Free Path of Xe^{132}, Au^{197}, Pb^{208}, U^{238} particles (vs) energy in liquid water.

3.7. Ranges:

The range or range along the path or CSDA (continuous-slowing-down approximation range), (ICRU, 2005) is given by,

$$R = \int_0^{E_0} \frac{dE}{n.S(E)} \qquad (3.14)$$

Where

n is number of target atoms per volume.

S(E) is the stopping cross section.

The range is added by straggling term ($0.6(E_{th}/A)$) μm, and the threshold energy E_{th}=15 eV, (Watt, D. E., 1996).

Figures (3.29) to (3.32) illustrate the relationship between ranges transfer and energy in liquid water.

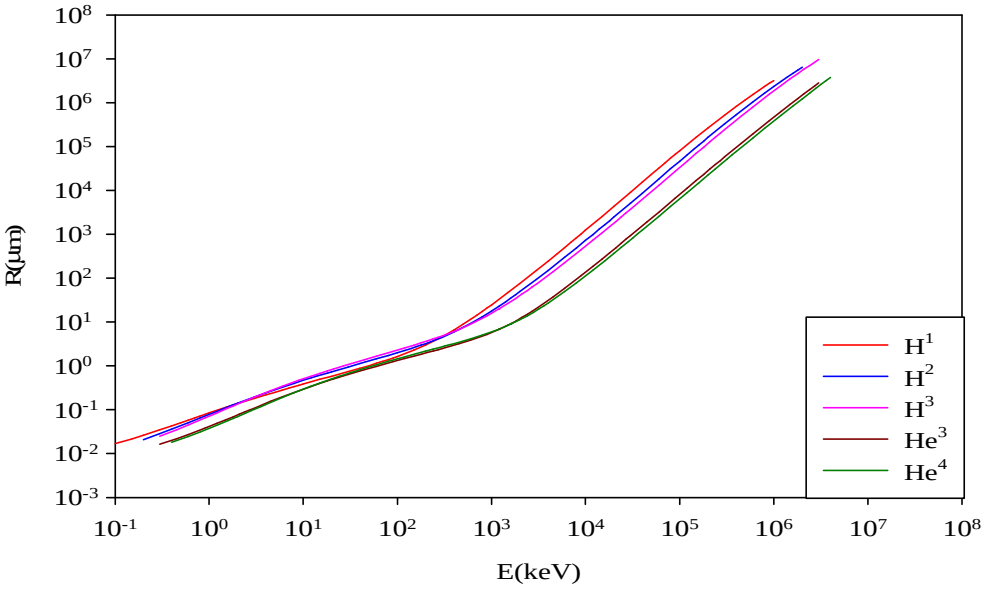

Fig. (3.29) The ranges of H^1, H^2, H^3, He^3 and He^4 particles (vs) energy in liquid water.

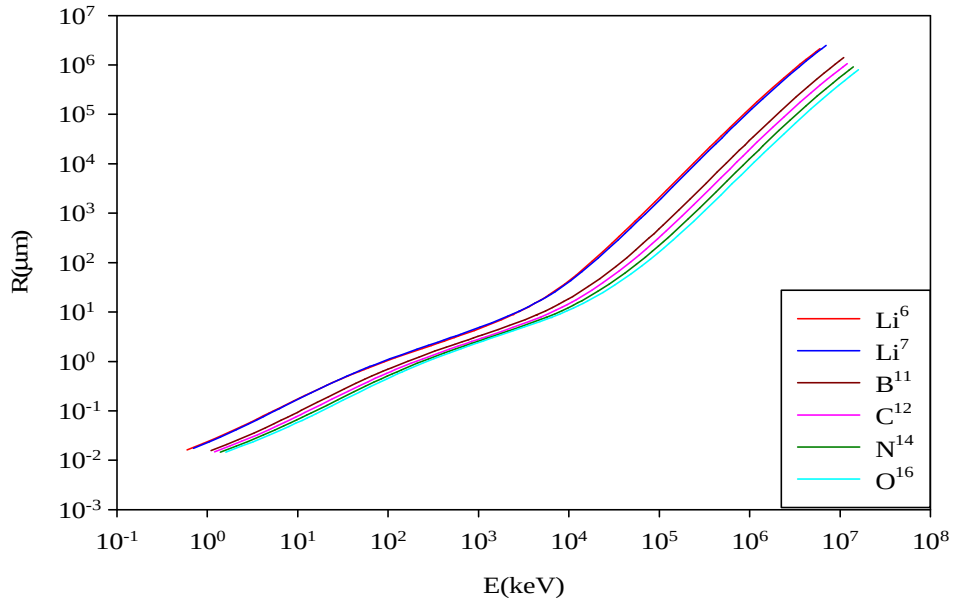

Fig. (3.30) The ranges of Li^6, Li^7, B^{11}, C^{12}, N^{14}, O^{16} particles (vs) energy in liquid water.

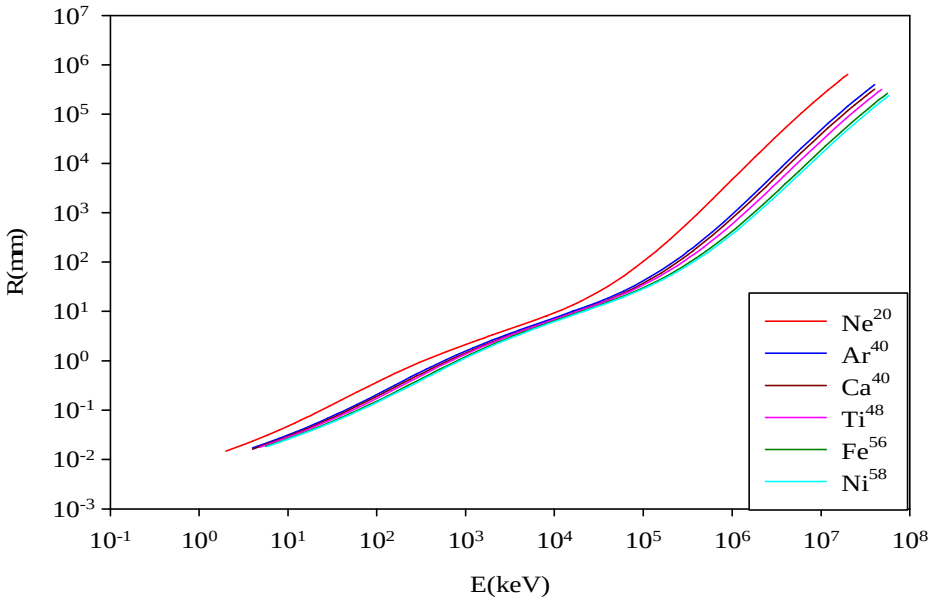

Fig. (3.31) The ranges of Ne^{20}, Ar^{40}, Ca^{40}, Ti^{48}, Fe^{56}, Ni^{58} particles (vs) energy in liquid water.

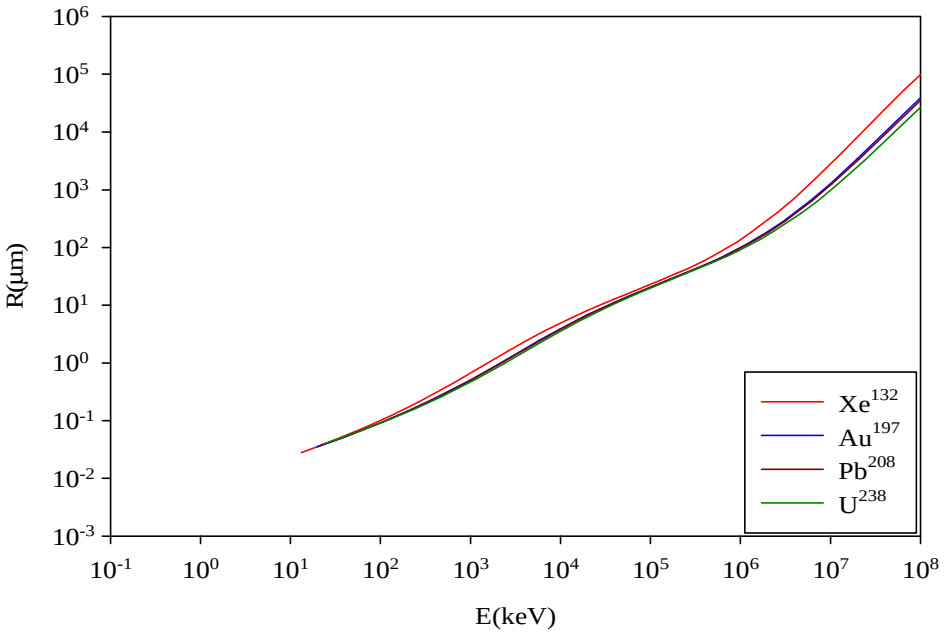

Fig. (3.32) The ranges of Xe^{132}, Au^{197}, Pb^{208}, U^{238} particles (vs) energy in liquid water.

Chapter 4

Radiation Effects on Mammalian Cells

In order to understand the damage induced when ionizing radiation crosses the living cell, a brief knowledge of the structure of mammalian cells including chromosome and DNA is needed. The damage can be associated with any entity inside the cell, including chromosomal aberrations, genetic mutations and DNA strand breaks.

4.1. Mammalian Cell

Mammals including human are made up of very small cells called mammalian cells. All mammalian cells have a nucleus (the average diameter of the nucleus is approximately 6μm)) containing DNA, and cytoplasm. The nucleus is surrounded by a nuclear membrane. Nucleoli contain ribosomal RNA. Cytoplasm consists of; Mitochondria (energy production), Ribosome (RNA and protein), Lysosomes (contain enzymes responsible for dissolution of foreign particles, the death of the cell, the breakdown of cell structures), Centrioles(have role in cell division).

Types of mammalian cells are; epithelial tissues, connective cells, muscular tissue, nervous tissue, blood cells. Mammalian cells usually contain about 80% water, which makes cells very sensitive to radiation.

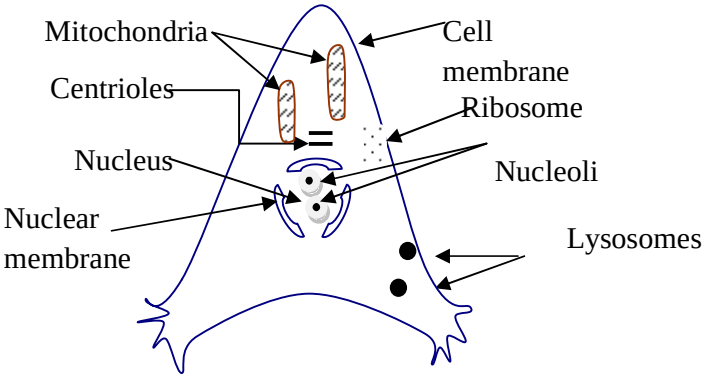

Fig. (4.1) Mammalian cell diagram (Reproduced from Nias, A. H. W., 1998)

4.2. The Cell Cycle:

The cell cycle can be described in four phases:

1- Mitosis or cell division, before division the mother cell doubles its DNA and the two daughter cells receive all the genetic in formation. During cell division, the chromatin condensed into chromosomes and nucleoli disappeared.

2- G_1phase, the time between the end of M phase and beginning of S phase.

3- S phase is the time during DNA duplication (Intermediate DNA between G_1, G_2).

4- G_2 phase, the time between S and the next mitosis (DNA content is double that of in G_1), (Tubiana, M., 1990).

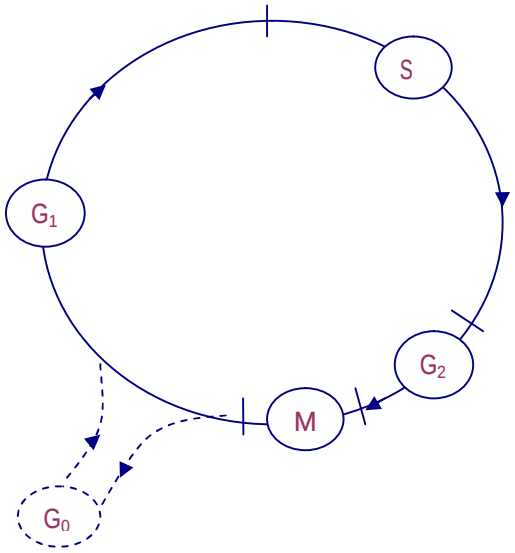

Fig. (4.2) Cell Cycle

4.3. DNA Structure

Deoxyribonucleic acid (DNA) is a large molecule contains two strands, each made up of a sequence of nucleotides. The two strands of double-helix are held together by hydrogen bonding between the bases, (Thymine T and adenine A, guanine G and cytosine C), (Steel,G. Gordon, 1997). The nucleotides are joined together by

phosphodiester bonds linking the molecules of sugar to phosphoric acid, (Tubiana, M., 1990).

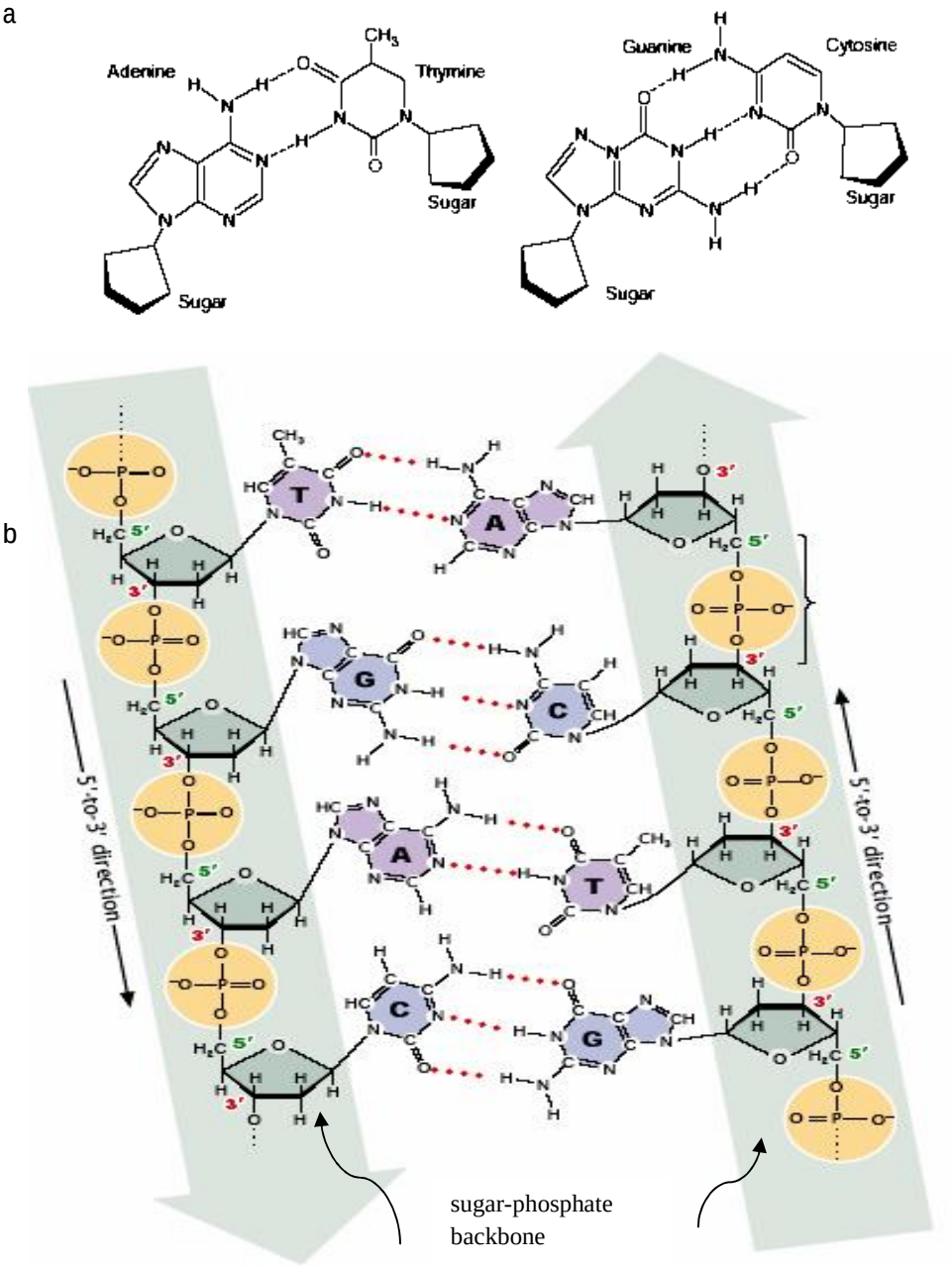

Fig. (4.3) The chemical structure of DNA (Ahluwalia, K. B., 2009). **a.** The pairing of the four nitrogenous bases of DNA: Adenine (A) pairs with Thymine (T),Guanine (G) pairs with Cytosine (C) **b.** The four bases form the genetic code. The sequence of the bases along the sugar-phosphate backbone encodes the genetic information.

4.4. Chromosome:

Most of mammalian cells have a diploid complement of 40 or more chromosomes, (Hall, E., 1994). The DNA doubled helix is wrapped around histone beads and forms nucleosomes which pile up to form the fiber. These are folded and rolled up in irregular spirals to form the chromosomes, (Tubiana, M., 1990).

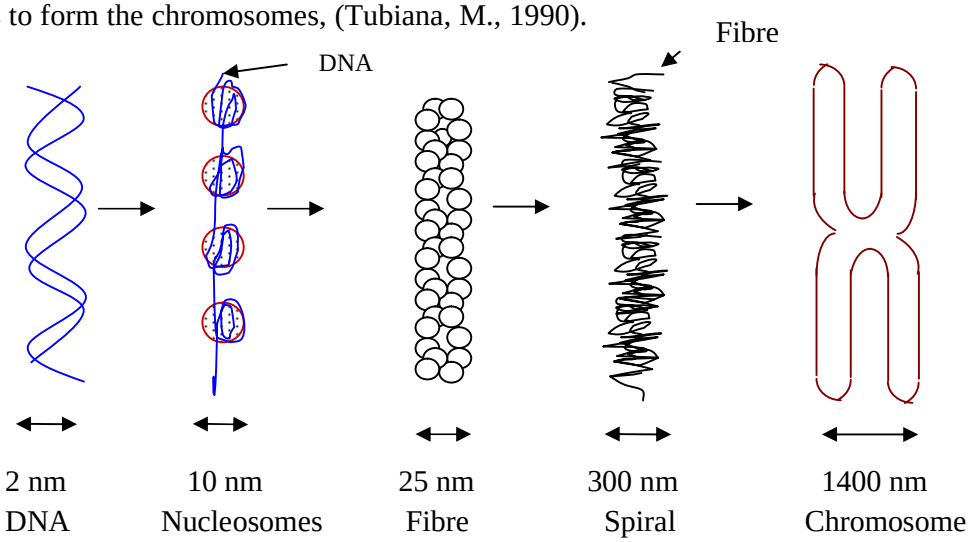

Fig. (4.4) Stages of folding and packing DNA.

Number of chromosomes in human (2n=46), (Atlas of Mammalian Chromosomes, 2006), is different from Chinese Hamster (2n=22), mouse (2n=40), etc. In human, the 22 pairs are known as autosome and the other pair (X chromosome and Y chromosome) known as sex chromosome.

4.5. Mechanism of Radiation Damage to DNA

4.5.1. Direct Cell Damage:

When radiation interacts with the DNA molecules it can cause the molecules to separate. The effect is called Direct Cellular Damage, Figure (4.5).

4.5.2. Indirect Cell Damage:

The indirect cellular damage occurs when radiation strikes the cytoplasm surrounding the nucleus, (cytoplasm is compose primarily of water and is the intercellular fluid). When radiation interacts with a water molecule, certain free radicals can be formed, (an ion radical $H_2O\cdot^+$, hydroxyl radical OH·). The free radicals are chemically reactive, and they can cause the cell to become chemically imbalanced; the result is cell damage, [(IAEA, 2005), (Hall, E., 1993)].

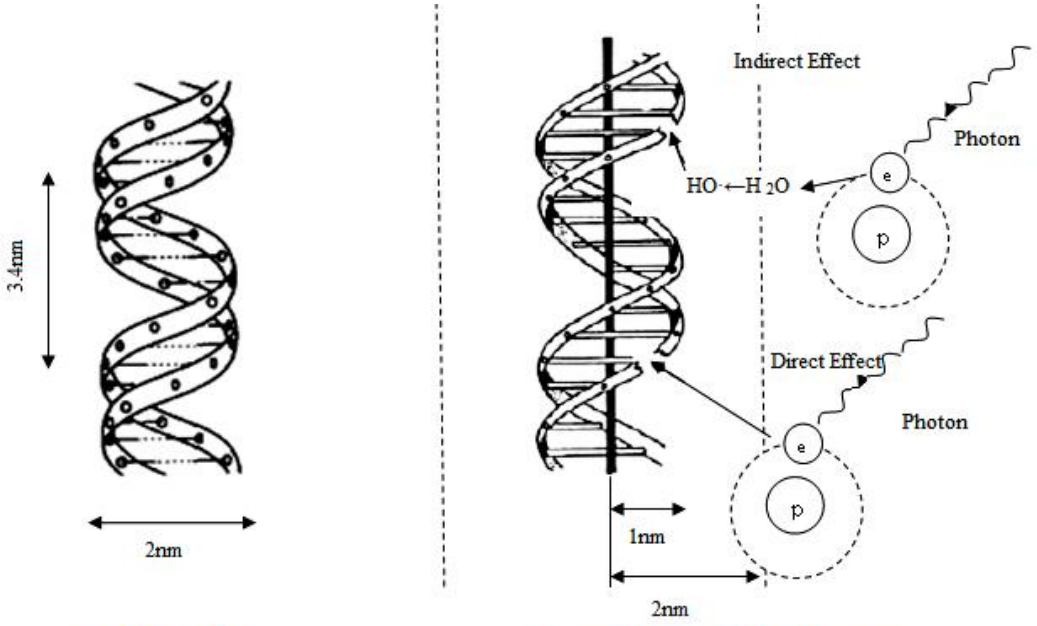

a. DNA double helix.

b. Direct and indirect effects of radiation.

Fig. (4.5) Mechanism of Radiation Damage to DNA.

As it is illustrated in Figure (4.5), the free radicals are produced in a cylinder with a diameter equal 4nm can affect the DNA, the double of DNA's diameter.

The indirect action is the dominant action in sparsely ionizing radiation, contrary to densely ionizing radiation; the direct action is the most important.

4.6. Radiation Effects on DNA:

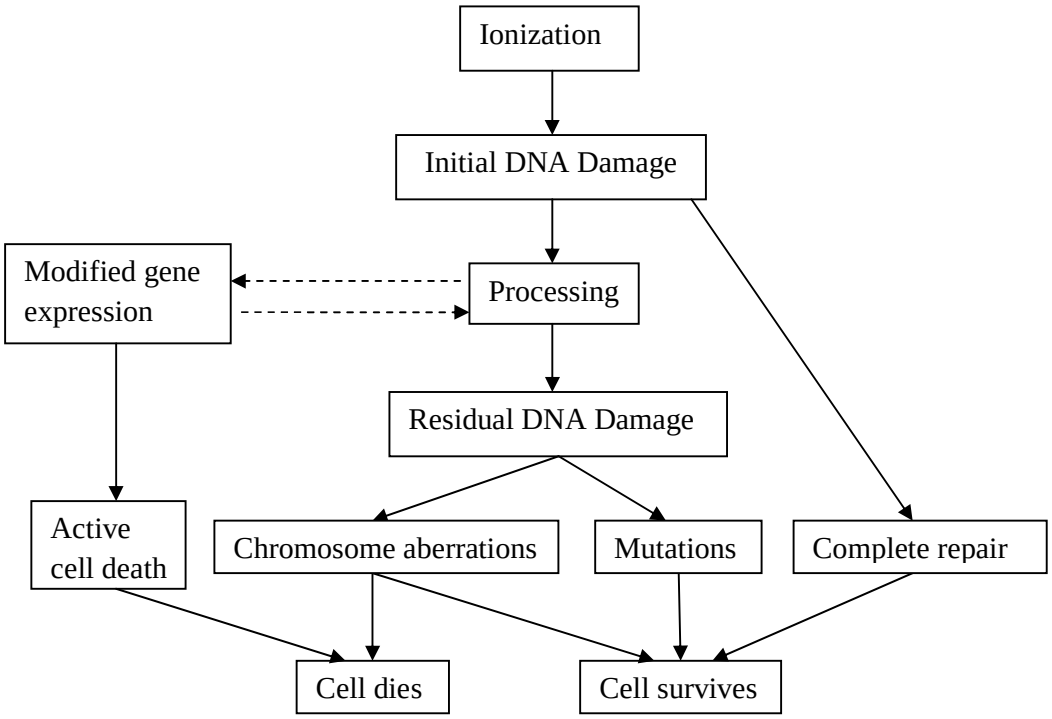

Fig. (4.6) A Summary of the processes follows exposure to ionizing radiation.

4.6.1. DNA Strands Breaks:

Interaction of radiation with DNA induces a variety of molecular damage such as single strand break (SSB), double strand break (DSB), base damage (BD), DNA-protein cross links and others, (Nikjoo, H., 2003). The most important types for strand breaks are illustrated in Figure.4.7.

DNA double-strand breaks are the critical damage for radiobiological effects; it's rejoining can be classified into two categories: correct rejoining (genomic rearrangements) and incorrect rejoining (cell lethality, mutations and the initiation of tumorigenesis), (Rothkamm, K. et al, 2008).

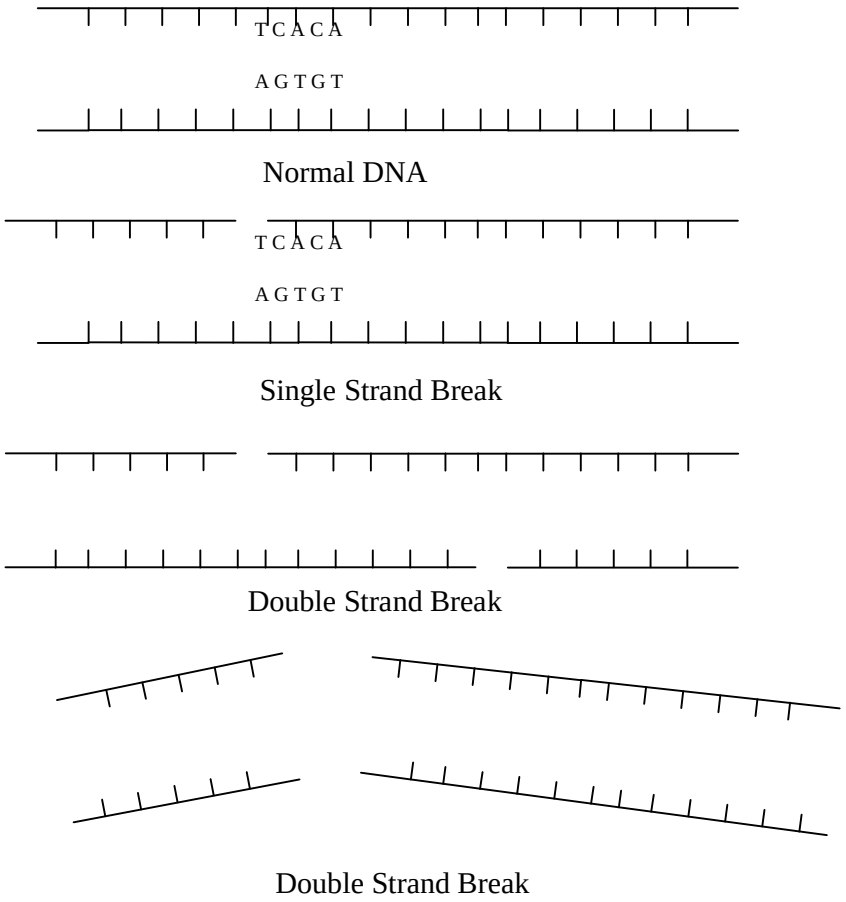

Fig. (4.7) Types of strand breaks

4.6.2. Chromosome Aberrations:

Radiation produced breaks in the chromosomes which lead to two classes of aberrations; Chromosome aberrations and chromatid aberration. Chromosome aberrations are resulted from early interaction in interphase, while the later in interphase produces the chromatid aberrations. There are many types of chromosomal aberrations and rearrangements, three of them are lethal to cell; the ring and dicentric (chromosome aberrations), and anaphase bridge (chromatid aberration), (Hall, E., 1994).

4.6.3. Somatic Effects:

Somatic effects are harm that exposed individuals suffer during their lifetime, such as radiation induced cancers (carcinogenesis), sterility, opacification of the eye lens and life shortening, (IAEA, 2005).

4.6.4. Gene Mutations:

The gene is a linear sequence of nucleotides in DNA that is needed to synthesis a protein and/or regulates cell function, (U.S. congress, 1986). Mutations are changes in the composition of DNA, generally divided according to size into:

1- Gene mutations: The structural changes in chromosomes often lead to metabolic or structural disturbances in the cell that no divisions, or only a few, will occur before cell death.

2- Chromosome mutations: affecting large portions of the chromosome, or the loss or addition of an entire chromosome.

And by their cause is divided into two categories:

1- Induced mutations, which is caused by exposure of DNA to a mutagenic agent, such as radiation, chemical agents.

2- Spontaneous mutations, in the absence of any known causative agent.

4.6.4. a. HPRT Gene:

HGPRT, (also known as HPRT or HPRT1), is the acronym for Hypoxanthine-guanine phosphor-ribosyltransferase. The human HPRT gene is found within X-Chromosome (X_q 26-27), as in figure (4.8), and has nine exons within a 45 kb expanse of genomic DNA, (Bao, C. Y., 1995).

HPRT gene produces an enzyme in the purine salvage pathway and its deficiency, causes the build up in urate metabolite. This build-up can cause kidney stones and gout. Primary symptoms of Lesch-Nyhan disease include neurological problems such as mental deficiency and self-destructive behavior.

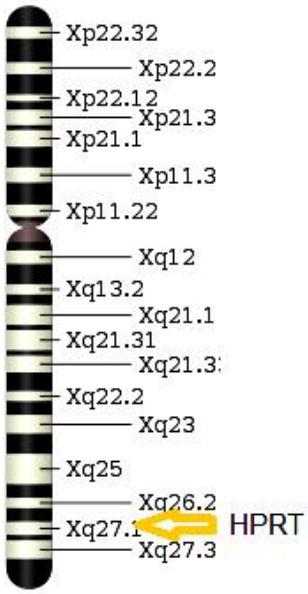

Fig. (4.8) Location of HPRT gene in X-chromosome.

4.6.4. b. HPRT Gene Importance:

The main reasons for choosing the HPRT gene as important test system in the study of mammalian cell mutagenesis are:

1- HPRT gene's location on X chromosome.

2- HPRT is a nonessential enzyme for cells growth in culture.

3- HPRT has powerful selection procedures. From (Stout, J. T., 1985).

4.6.4. c. Comparison of HPRT Gene Size and Structure:

The homology between mouse, hamster and human is>95% in coding regions and falls to ≈80% in 5' and 3' nontranslated regions, [(Stout, J. T. and Caskey, C. T., 1985), (Melton, D. W. et al, 1984)]. Seven amino acid substitutions are different between mouse and human. The HPRT gene for human, hamster and mouse covers about 45, 36 and 34 kbp, respectively.

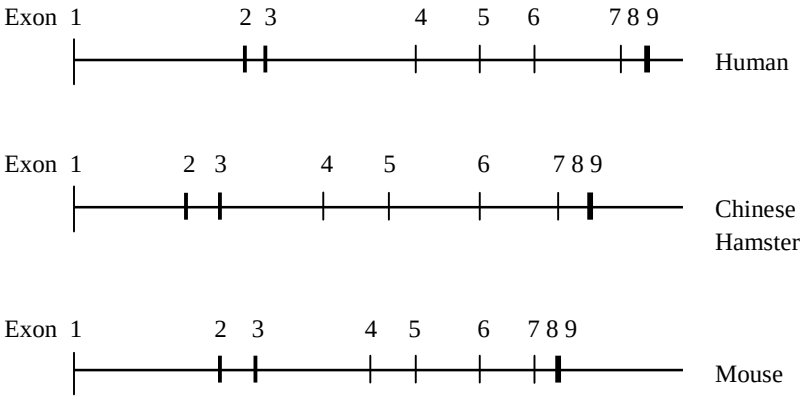

Fig.(4.9) Comparison of the organization of the human, Chinese hamster and mouse hprt gene, (Baumstrak-Khan, C., 2007).

Table (4.1) illustrates the yield of different types of radiation damage for high and low LET, (Nikjoo, H., 2003).

Table (4.1) Average yield of damage in a single mammalian cell after 1 Gy of radiation

Radiation	**Low LET**	**High LET**	**Radiation**	**Low LET**	**High LET**
Tracks in nucleus	1000	2	DNA DSB, initial	40	70
Ionisation in nucleus	100000	100000	Chromosome aberration	1	3
Ionisation in DNA	1500	1500	Dicentric	0.1	0.4
Excitation in DNA	1500	1500	HPRT mutation	10^{-6}	10^{-5}
Base Damage	10^5	10^5	Lethal lesions	0.5	2.6
DNA SSB	850	450	Cell inactivation	30%	85%

Chapter 5

Biological Parameters of Ionizing Radiation

Mathematics plays an important role in radiobiology, to relate the biological actions with the physical parameters which have been studied in chapter 3. Toward the biological data analysis and establishment of our model, this chapter illustrates the most important biological parameters and their calculations.

5.1. Models of Radiation Cell Killing

There are some models below, which are used to analyze the cell survival and radiation dose:

1. Target Theory.
2. The Linear-quadratic Model.
3. The Lethal, Potentially Lethal Damage (LPL).
4. Repair Saturation Model.

5.1.1. Cell Survival Curves

The type of radiation influences the shape of the cell survival curve. Densely ionizing radiation exhibits a cell survival curve that is almost an exponential function of dose, shown by an almost straight line on the log-linear plot.

Sparsely ionizing radiation, however, the curves show an initial slope followed by a shoulder region and then become nearly straight at higher doses.

Several mathematical methods of varying degrees of complexity have been developed to define the shape of cell survival curves, all based on the concept of the random nature of energy deposition by radiation, (Steel, G. Golden, 1997).

The linear quadratic model is now most often used to describe the cell survival curve, (IAEA, 2005) & (Hall, E. J., 2005),

$$S/S_0 = e^{-aD-bD^2} \tag{5.1}$$

Where

S/S_0 is the fraction of cells surviving at dose D.

α is a constant describing the initial (linear)slope.

β is a smaller constant describing the quadratic component of cell killing.

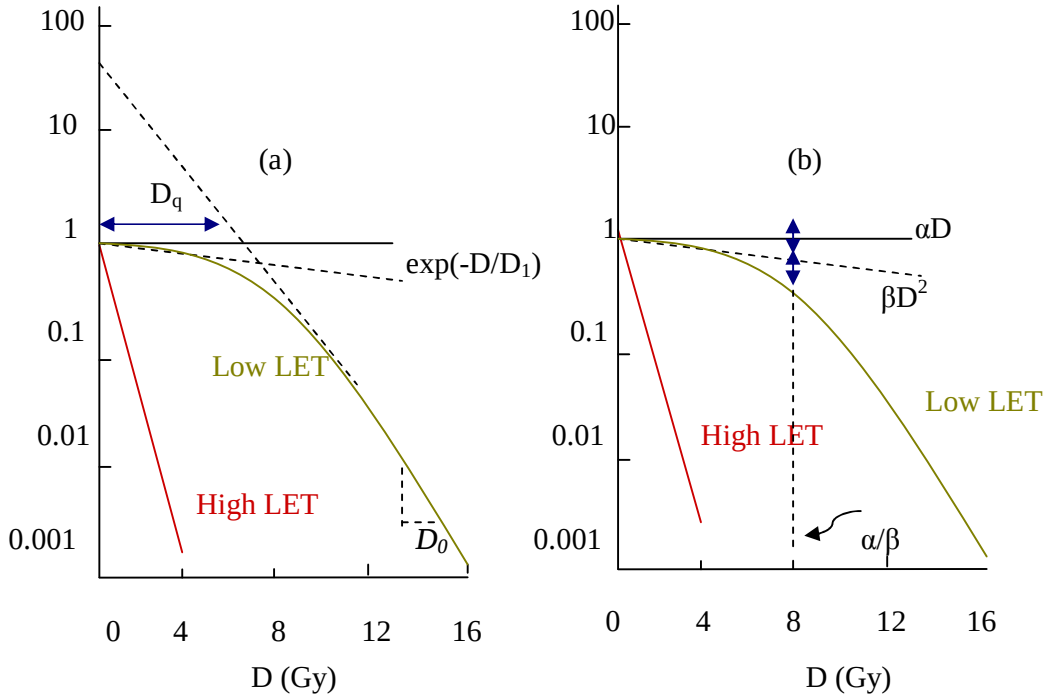

Fig . (5.1) . Typical cell survival curves for high LET (densely ionizing) radiation and low LET (sparsely ionizing) radiation. (a) The earlier multitarget single hit model; (b) the current linear quadratic model.

5.1.1.a. Calculations of Parameter α and β:

To calculate α(Gy^{-1}) and β(Gy^{-2}) equation (34) can be written in this way,

$$S/S_0 = e^{-\alpha D} \quad (5.2)$$

Taking the natural algorithm for both sides,

$$\ln(S/S_0) = -\alpha D \quad (5.3)$$

Finally

$$\left.\frac{d\ln(S/S_0)}{dD}\right|_{D=0} = -a \quad (5.4)$$

Also

$$b = -\frac{1}{2}\frac{d^2\ln(S/S_0)}{dD^2} \quad (5.5)$$

5.1.2. HPRT Mutations Curves:

The multitarget model can be used with the mutation frequency, as shown in Fig (5.2), or the linear repair kinetics model and both gave similar fit, (Cucinotta, F. A. et al, 1995).

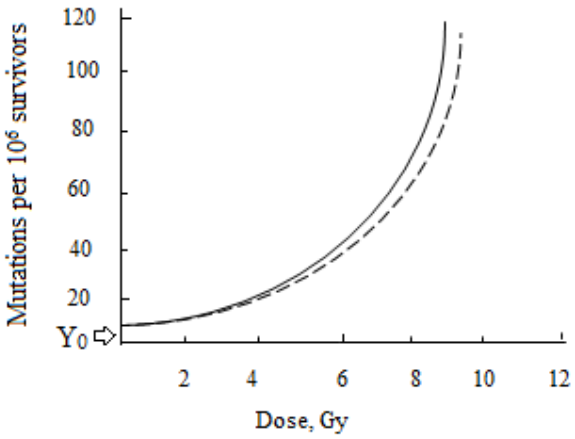

Fig. (5.2). X-ray dose-response for HPRT mutations in V79 cells; the solid line is multitarget model, and the dashed line is the linear repair kinetics model.

This curve follows the mathematical relation below,

$$Y = Y_0 + \alpha D + \beta D^2 \quad (5.6)$$

Where $\mathbf{Y_0}$ is the value of the spontaneous mutations and (α, β) as in cell survival curves.

5.1.2.a. Calculations of Parameter α and β:

To calculate $\boldsymbol{\alpha(Gy^{-1})}$ and $\boldsymbol{\beta(Gy^{-2})}$ from equation (39),

$$a = \left.\frac{dY}{dD}\right|_{D=0} \tag{5.7}$$

And

$$b = \frac{1}{2}\frac{d^2Y}{dD^2} \tag{5.8}$$

5.2. The Cross Section

5.2.1. The Geometrical Cross Section of HPRT gene and Cells in mammals:

The cell size varies among mammals and in average it is about (80μm^2), this reaches the human lymphoblasts **TK6** size (87μm^2). In contrary, the human skin fibroblasts **HSF** have greater size (220μm^2) and Chinese Hamster Lung Fibroblast **V79** (110μm^2), (Cucinotta, F. A. et al, 1995). The range of **HPRT** gene size in mammals is (34kbp-45kbp), as was mentioned in chapter (4). Stoll, U. et al. (1996), assumed that the gene in a spherical shape and calculated its size, following their steps, the average of the geometrical size of **HPRT** gene is (1.06×10^{-3} μm^2).

5.2.2. The Effective (biological) Cross Section:

The effective cross section is considered one of the most important biological parameters, as it gives the probability of the radiation interaction with the biological matter.

From (Watt, D. E., 1996), the biological cross section can be written,

$$s\left(mm^2\right) = \frac{a\left(Gy^{-1}\right).L_T\left(keV/mm\right)}{6.25} \tag{5.9}$$

Where α is the radiosensitivity parameter, L_T is the unrestricted linear energy transfer.

5.3. Mutagenicity Factor:

The ratio of inactivation and mutation induction cross section **(σ_m /σ_i)** is termed mutagenicity. This parameter indicates whether a certain ion exposure leads to more mutants per survivor than another ion.

Chapter 6

Analysis of Biological and Physical Data of HPRT Mutations

Several physical and biological parameters were mentioned in chapter 3 and chapter 5, respectively. Their methods of calculation have been used to establish the data base. In order to model the most correlation of the data, using SigmaPlot 10 programme, it is necessary to observe each biological parameter (radiosensitivity parameter, mutation cross section, inactivation cross section and mutagenicity) with the physical ones.

6.1. Densely ionizing radiation

6.1.1. Radiosensitivity parameter α_m (Gy^{-1})

The HPRT mutation radiosensitivity is derived from the mutant frequencies as a function of dose; it is one of the mutation indicators, equation (40).

Figure (6.1) illustrates that there is no relationship between parameter α_m and radiation energy E. But heavier ions like X^{132},Au^{197}, Pb^{207} and U^{238} have smaller values of parameter α_m than the lighter ions.

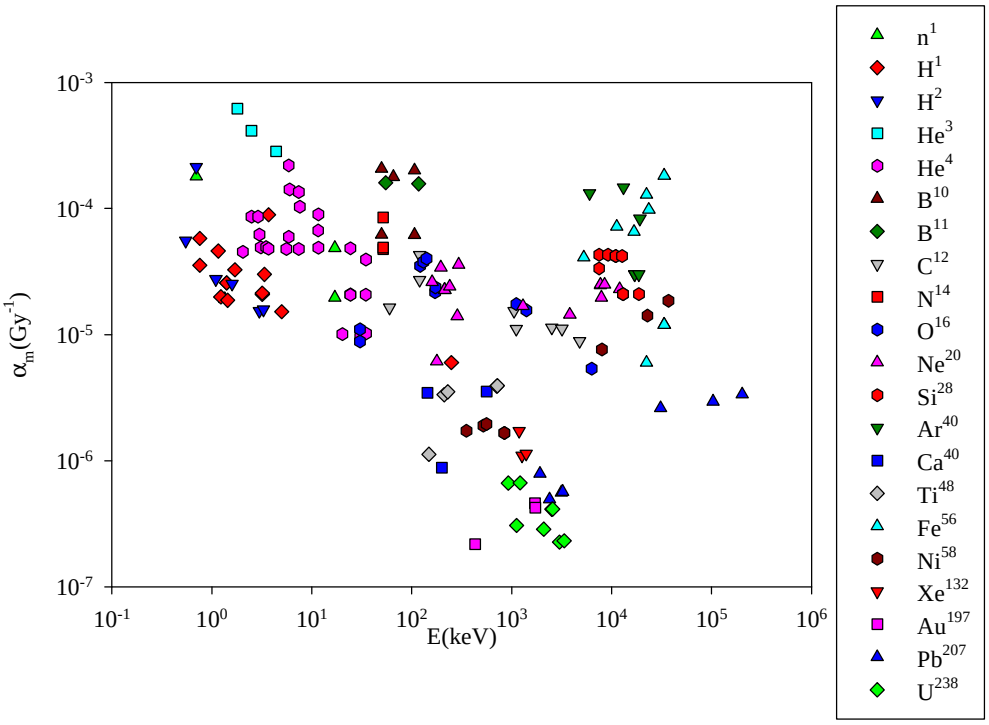

Fig. (6.1) Parameter α for mutation vs energy

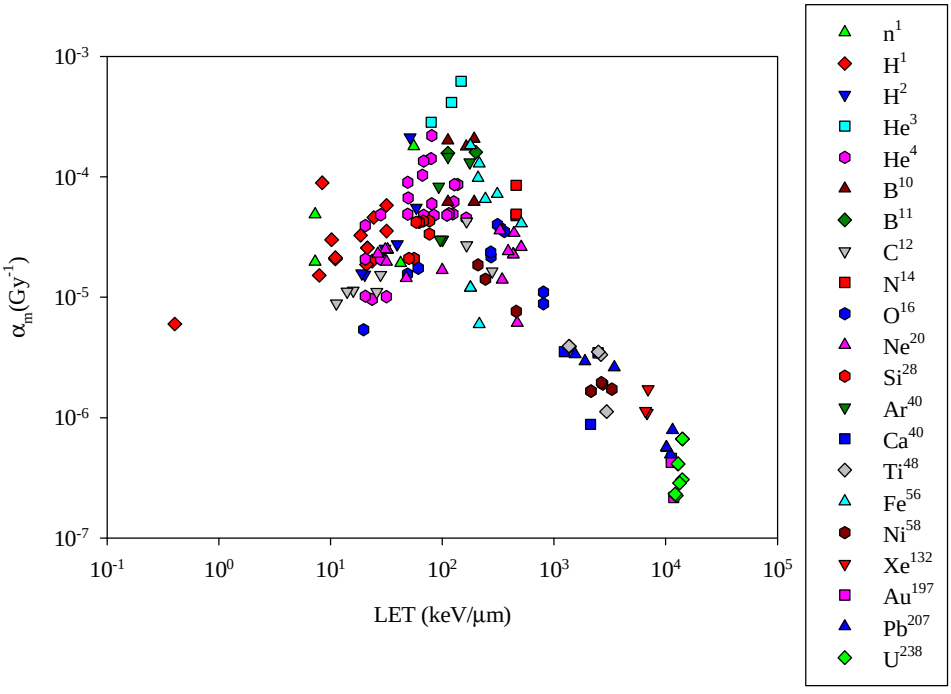

Fig. (6.2) Parameter α for mutation vs unrestricted linear energy transfer

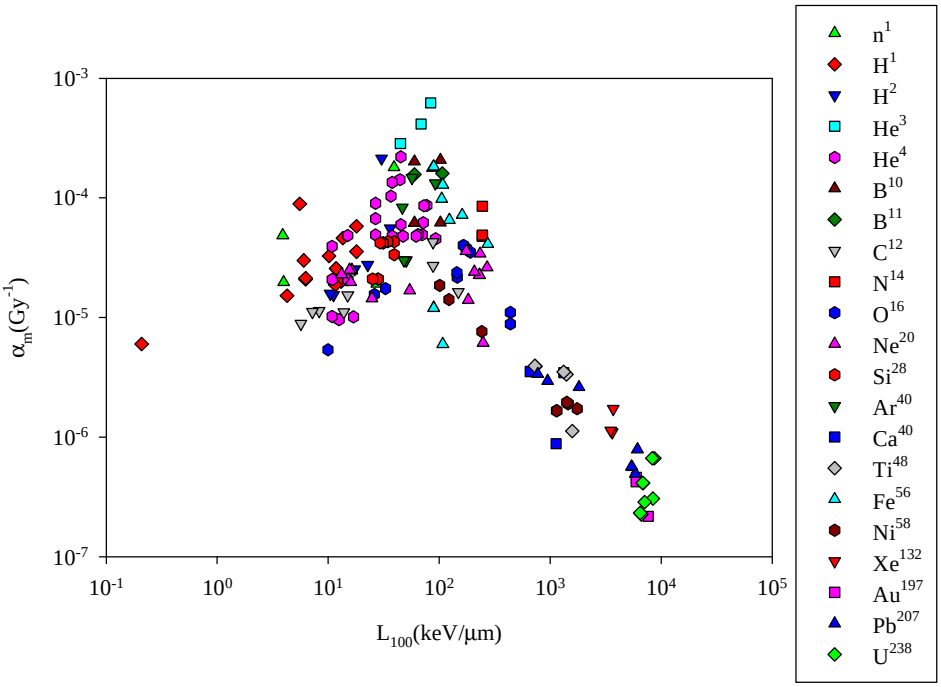

Fig. (6.3) Parameter α for mutation vs restricted linear energy transfer

The curves (6.2) and (6.3) of α_m as a function in both LET and $L_{100,}$ it is obvious that α increases to the peak up to L around 140 and 80keV, respectively. They can't be considered as a clear indication to the gene mutation, as the curves have double values.

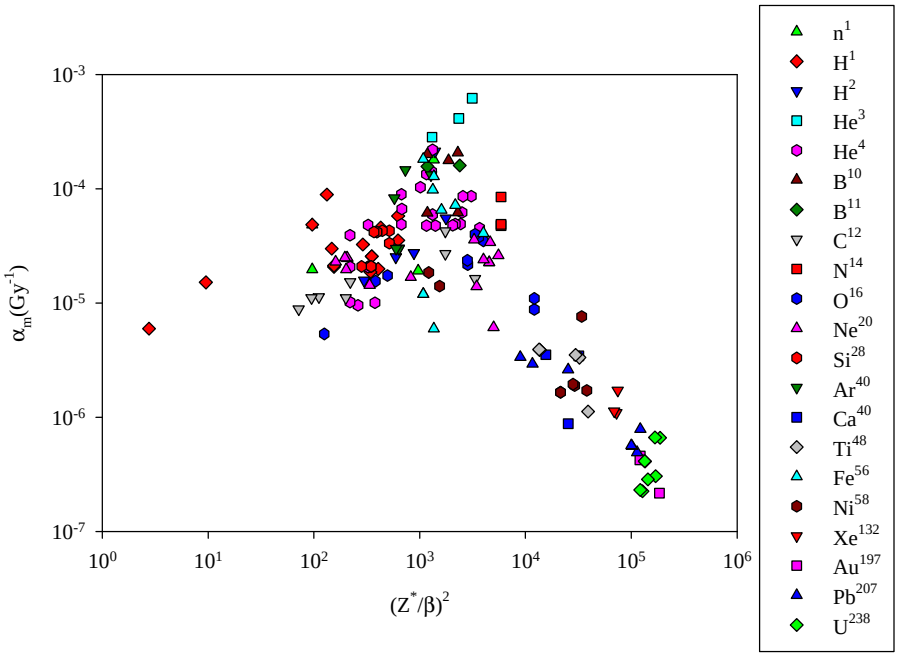

Fig. (6.4) Parameter α for mutation vs Katz's parameter

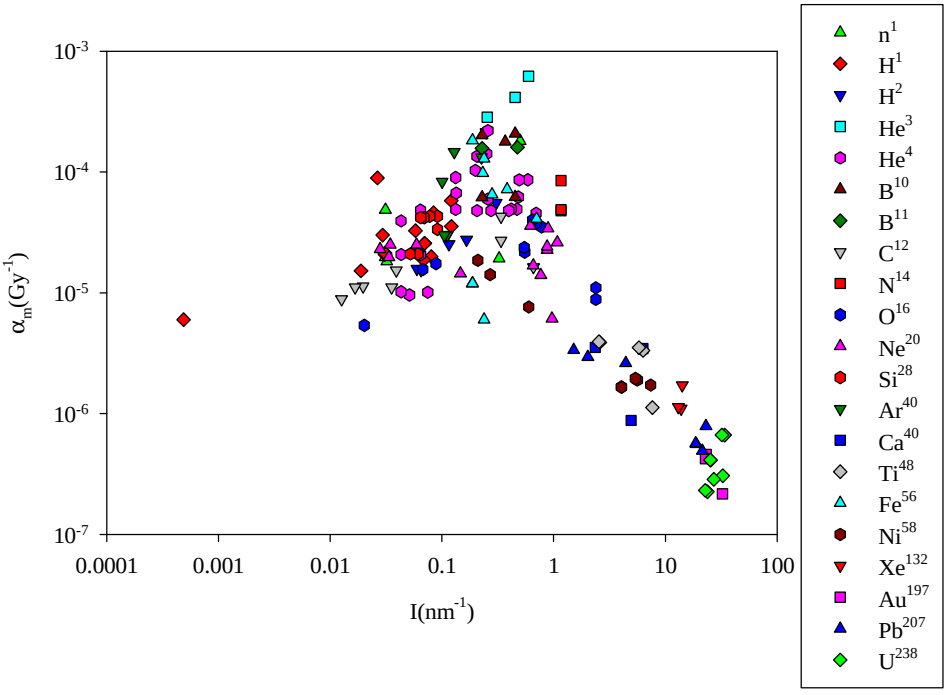

Fig. (6.5) Parameter α for mutation vs linear primary ionization I

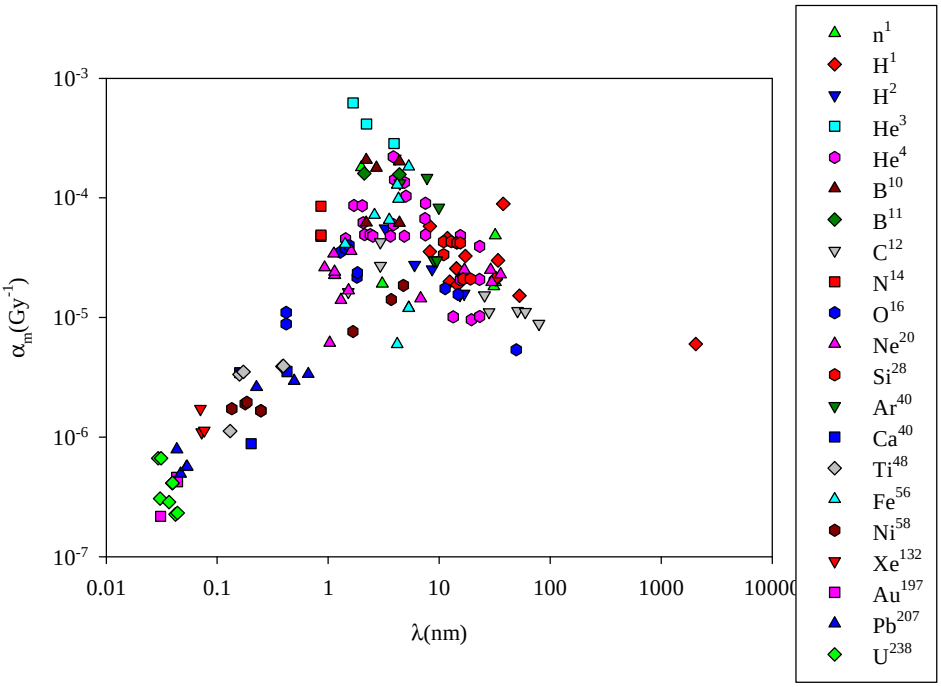

Fig. (6.6) Parameter α for mutation vs mean free path

The same observations have been found in the study of parameter α with parameter Katz, the linear primary ionization and the mean free path, figures (6.4), (6.5), (6.6).

Figures (6.7) and (6.8) show no correlation between the data.

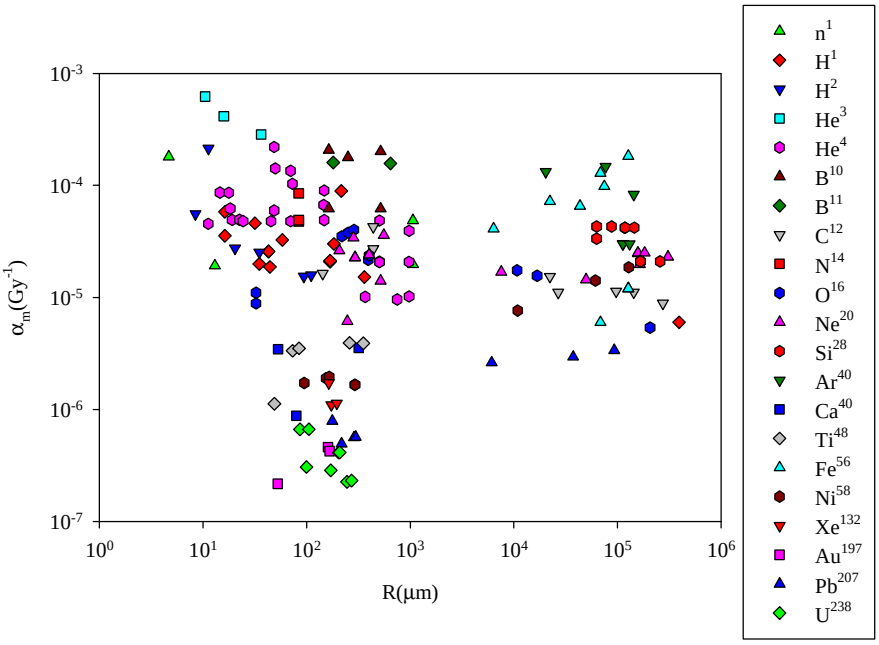

Fig. (6.7) Parameter α for mutation vs range

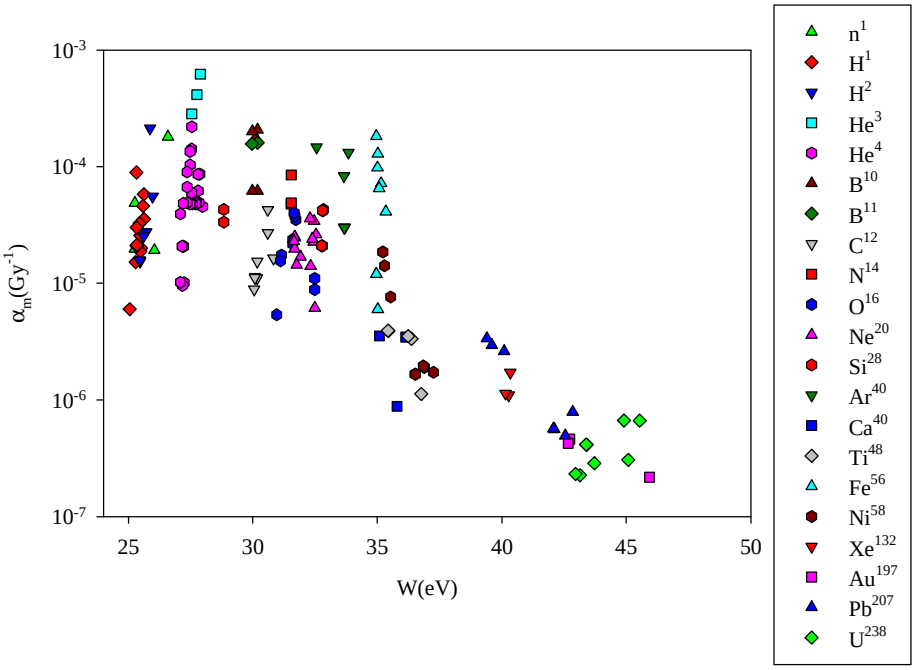

Fig. (6.8) Parameter α for mutation vs mean energy

6.1.2. Mutation cross section σ_m (μm^2):

In this part the biological parameter σ_m (μm^2) is being discussed as a function of all the physical that were mentioned in chapter 3.

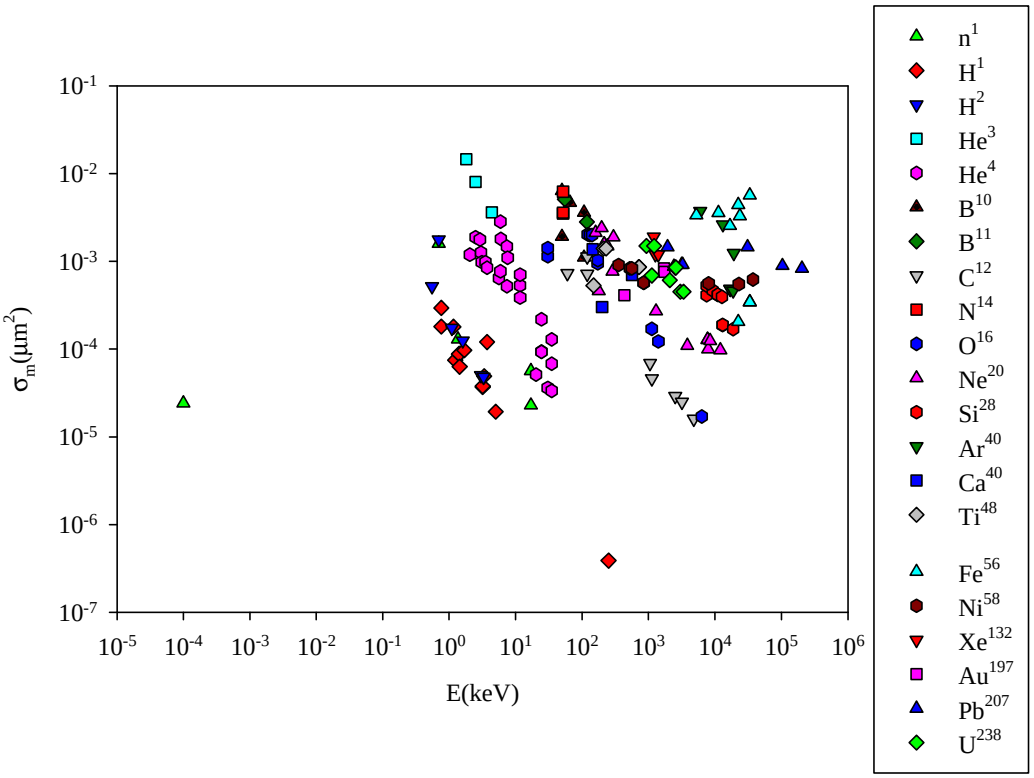

Fig. (6.9) Mutation cross section vs energy.

Figure (6.9) No special trend has been found for all ions, but a reduction in the mutation cross section with increasing the energy was noticed for many separate ions.

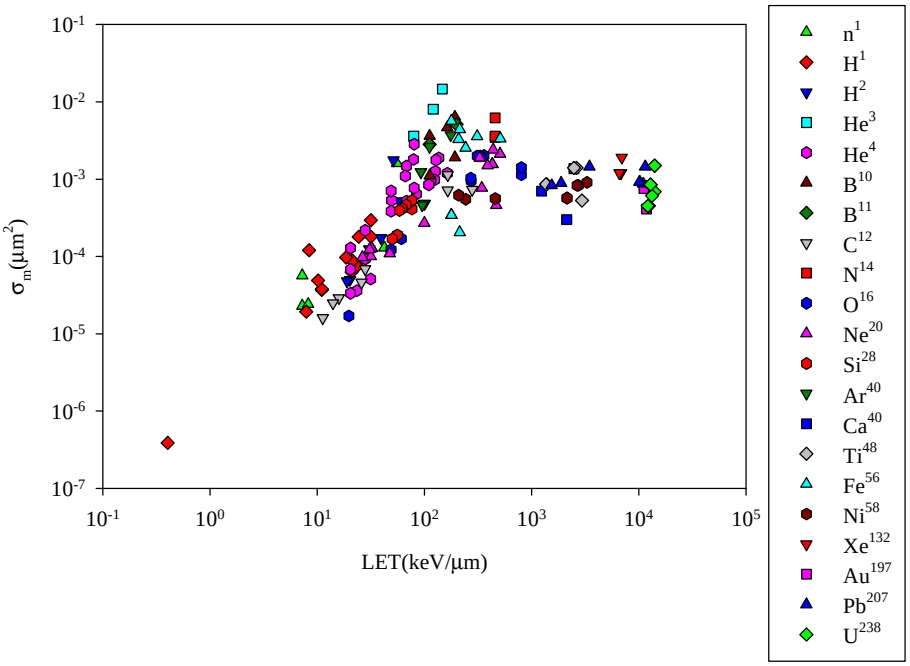

Fig. (6.10) Mutation cross section vs unrestricted linear energy transfer.

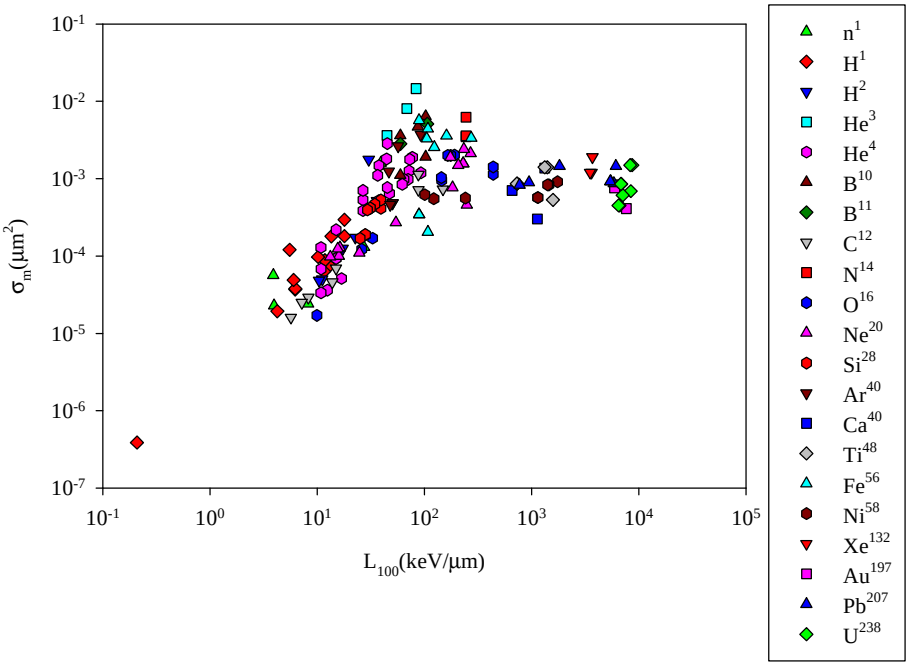

Fig. (6.11) Mutation cross section vs restricted linear energy transfer.

Figures (6.10), (6.11) shows that σ_m increase up to LET and L_{100} around 140 and 80keV/µm, respectively. With values above the mutation cross section saturates to nearly equal the gene's geometric size. Although, a relationship was found for σ_m as a function in both LET and L_{100} they still have incomplete properties to define the biological damage.

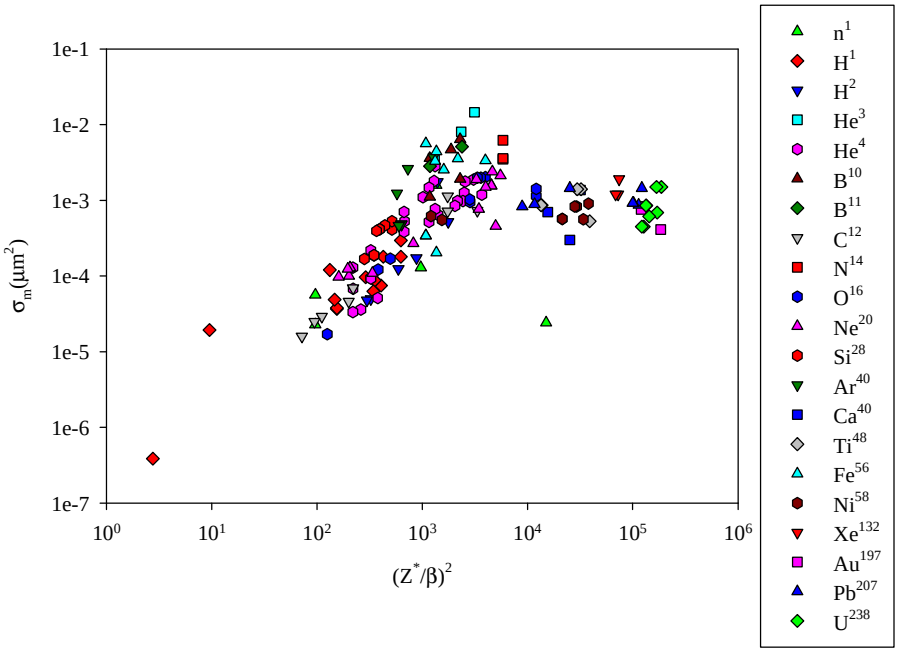

Fig. (6.12) Mutation cross section vs Katz's parameter.

The relation between the mutation cross section and Katz's parameter in figure (6.12) illustrates that there a good correlation, but this parameter also can't be considered a unifying parameter as it depends mainly on the energy. For better understanding, it is necessary to select a parameter can give a clear indication for the target and the radiation.

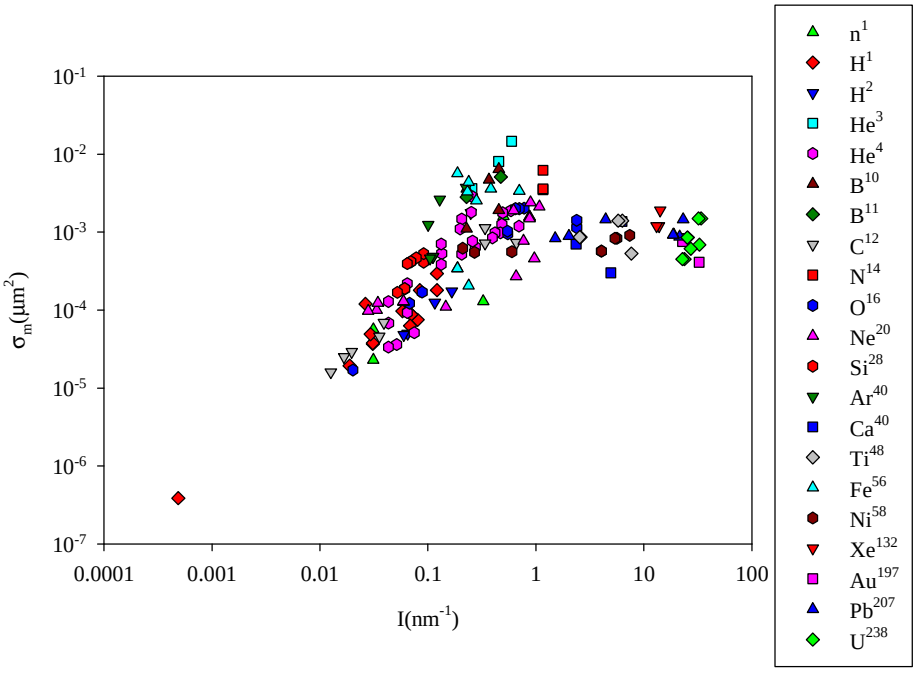

Fig. (6.13) Mutation cross section vs linear primary ionization.

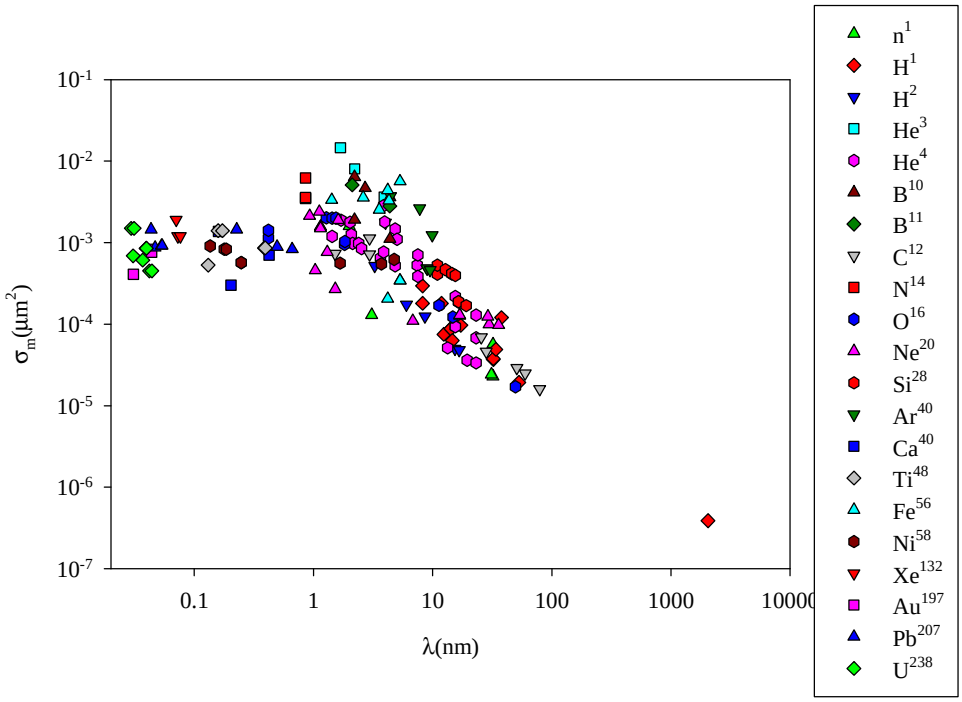

Fig. (6.14) Mutation cross section vs mean free path.

The primary ionization is the reciprocal of the mean free path, it can be considered the same parameter and the mean free path is more indicative of track structure. The main observation in figure (6.14) is that the mutation cross section has greater values for heavy ions than for light ions.

The explanation for this behavior could be the massive energy deposition for the heavy ions and the increase of effective penumbra. Light ions have lower densities of δ-rays; the effect of δ-rays reaches the maximum around the region where the cross section starts to fall.

According to cell lines, differences in the HPRT cross sections have been noticed, as mentioned in chapter 4 and 5, the HPRT gene size varies in mammals. Furthermore, this might be due to the differences in cell lines' nuclear areas, for HSF, V79 and TK6 are 220 μm^2, 110 μm^2 and 80 μm^2, respectively.

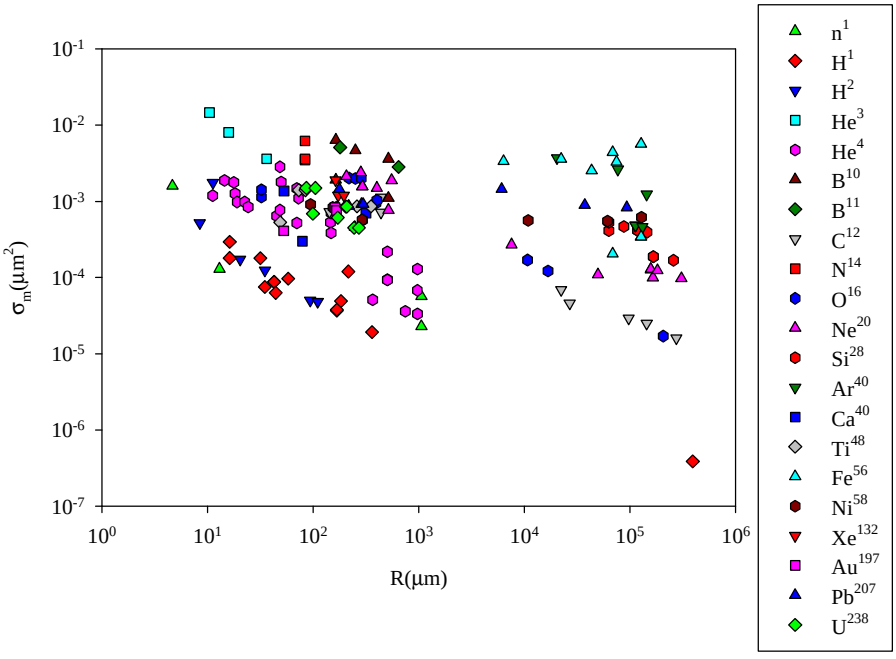

Fig. (6.15) Mutation cross section vs range.

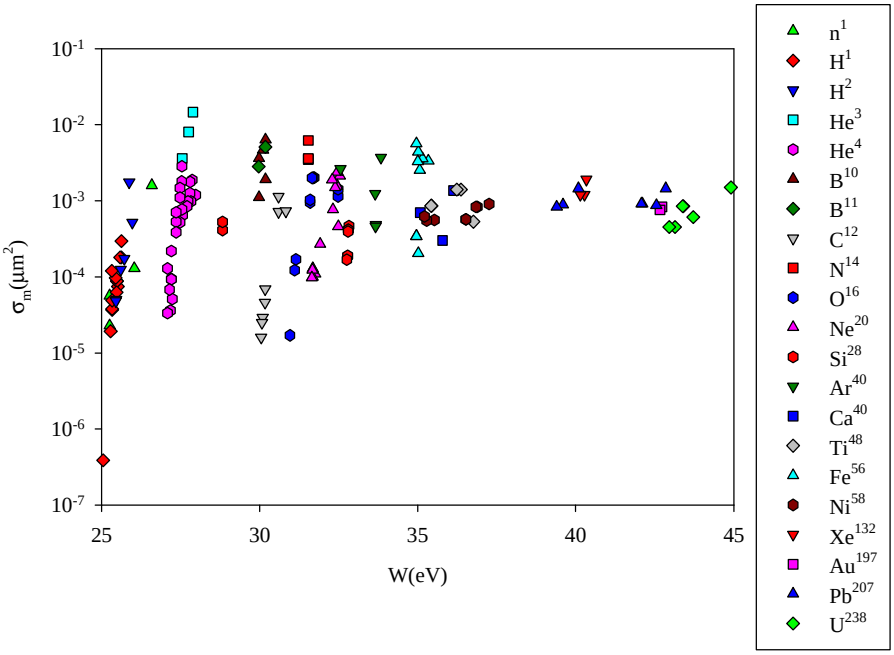

Fig. (6.16) Mutation cross section vs mean energy.

In the study of the behaviour of HPRT mutation cross section with ranges, mean energy and penumbra radius, no clear relationship were noticed with each parameter, as illustrate in figures (6.15), (6.16).

6.1.3. Inactivation cross section $\sigma_i(\mu m^2)$:

The inactivation cross section was studied by (El-Mansouri, R., 2003), in comparison with our database, there is compatibility. The heavy ions form the saturation region and the lighter form the recovery region, as figure (6.17) illustrates.

The convenient mathematical relation was found to be;

$$s(l) = \frac{s_0}{1 + \left(\frac{l}{l_0}\right)^m} \qquad (6.1)$$

Where m=1.4, σ_0=65 μm^2, λ_0=2.07nm.

The saturated cross section σ_0=65 μm^2 and the inflection point λ_0=2.07 nm are indicating the average of the geometrical size for mammalian cell (σ_g=80 μm^2) and the DNA size, respectively. Once again, DSB is responsible for the biological damage and the maximum probability of causing cell killing is due to one DSB.

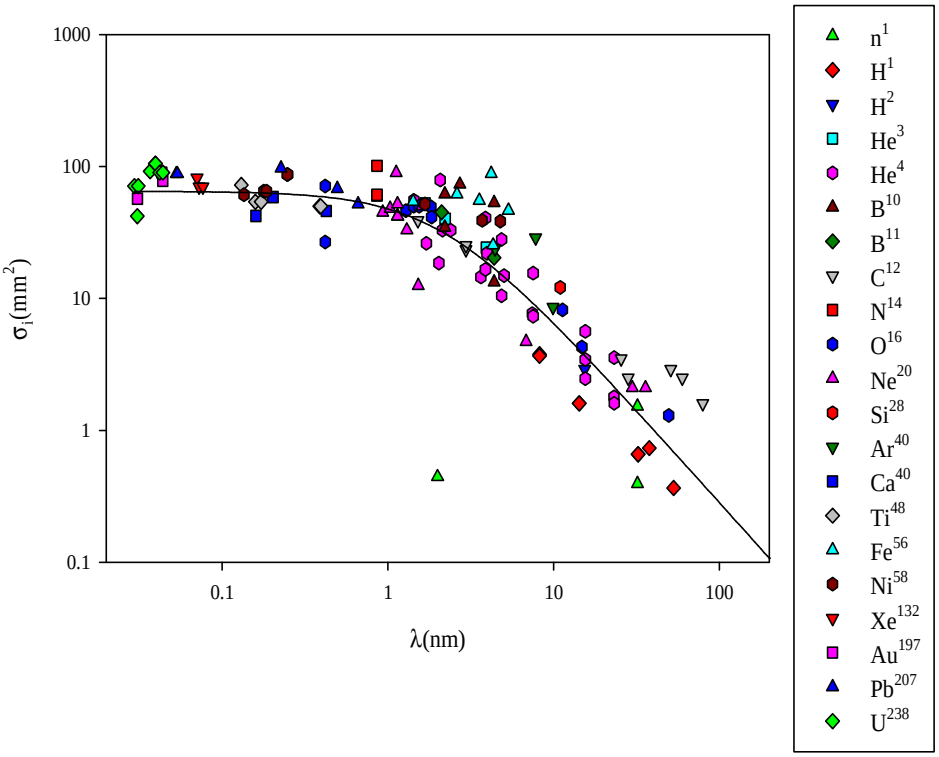

Fig. (6.17) The model between inactivation cross section and mean free path for heavy charged particles.

6.1.4. The mutagenicity factor (σ_m / σ_i):

In Fig.(6.18) the mutagenicity factor increases up to LET≈140 keV/μm, but Fig.(6.19) illustrates that the behavior of the factor with λ is the opposite, in both parameters the peak is around 4.3 nm.

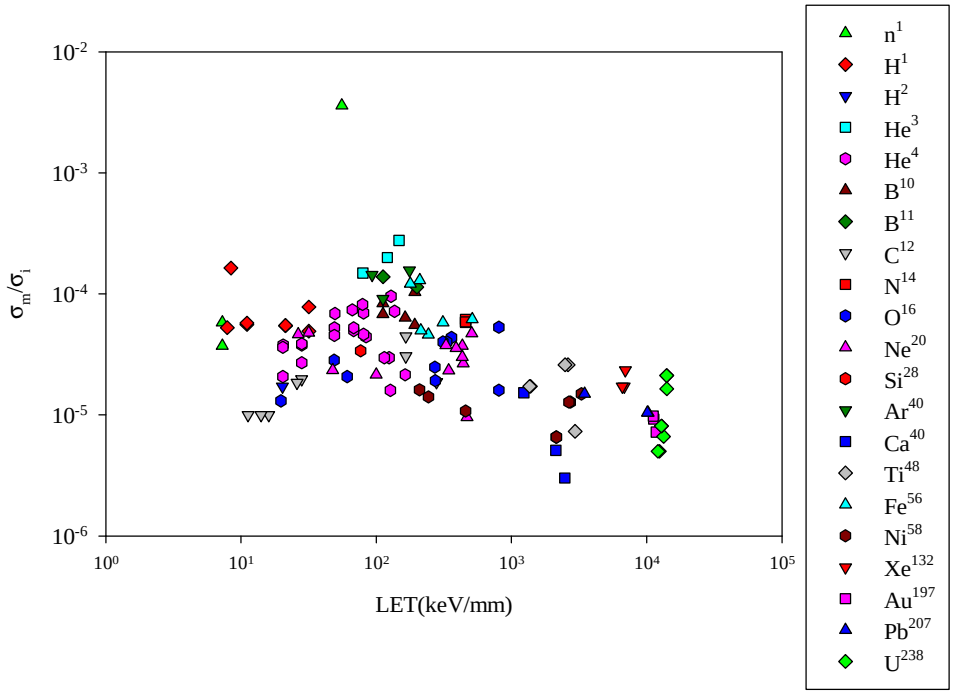

Fig. (6.18) Mutageniciy factor vs unrestricted linear energy transfer.

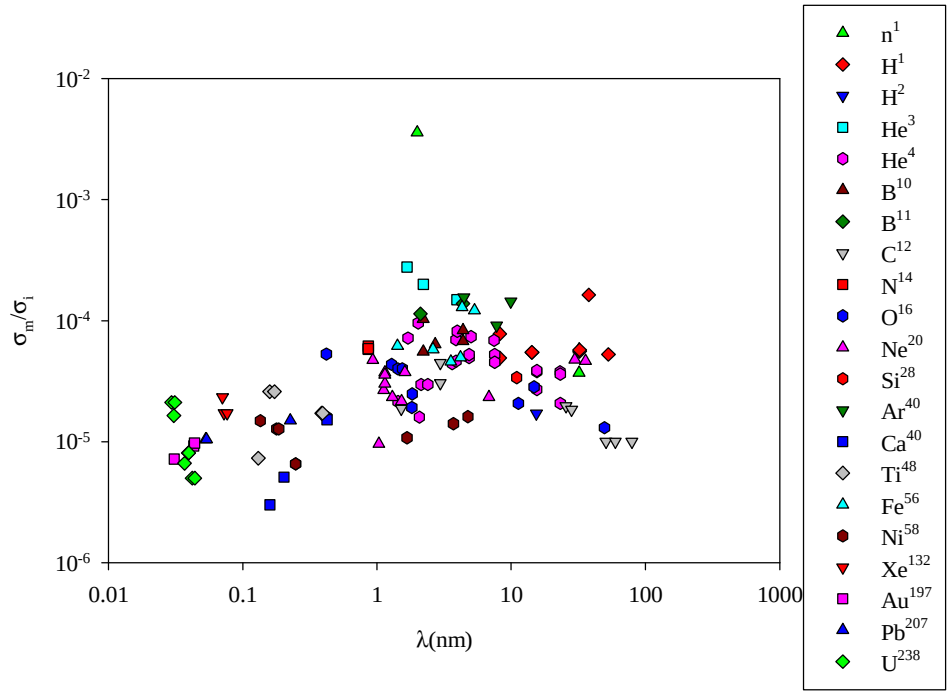

Fig. (6.19) Mutageniciy factor vs the mean free path.

6.2. Sparsely ionizing radiation:

The mutation cross section for sparsely ionizing radiation (X-ray and γ-ray), as figure (6.20) illustrating.

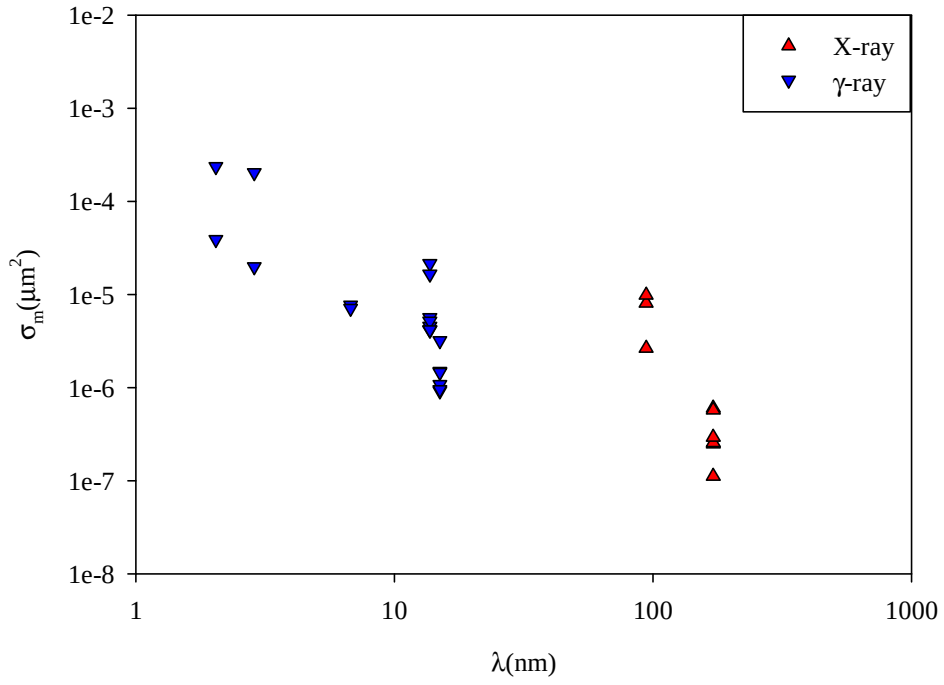

Fig. (6.20) The mutation cross section vs the mean free path for photons.

6.3. Modeling the Biological Effect for HPRT Mutations:

6.3.1. Densely Ionizing Radiation:

The best mathematical fit was found after the analysis of the mutation cross section as a function of the mean free path is:

$$s(l) = \frac{9x10^{-4}}{1+\left(\frac{l}{4}\right)^{1.4}} \qquad (6.2)$$

Where m=1.4, σ_0 =0.0009 μm^2, λ_0=4nm.

The average of HPRT geometrical cross section is about $1.06\times10^{-3}\mu m^2$, which means there is a seldom probability for repairing the gene after irradiated at the saturated region. Noticing from the curve, the reduction in the mutation cross section starts at λ=2.07nm and the inflection point at 4 nm, which interprets that there is more possibility that more than one DSB are associated in causing the HPRT mutation. When λ>4nm, the recovery in the damage become more possible.

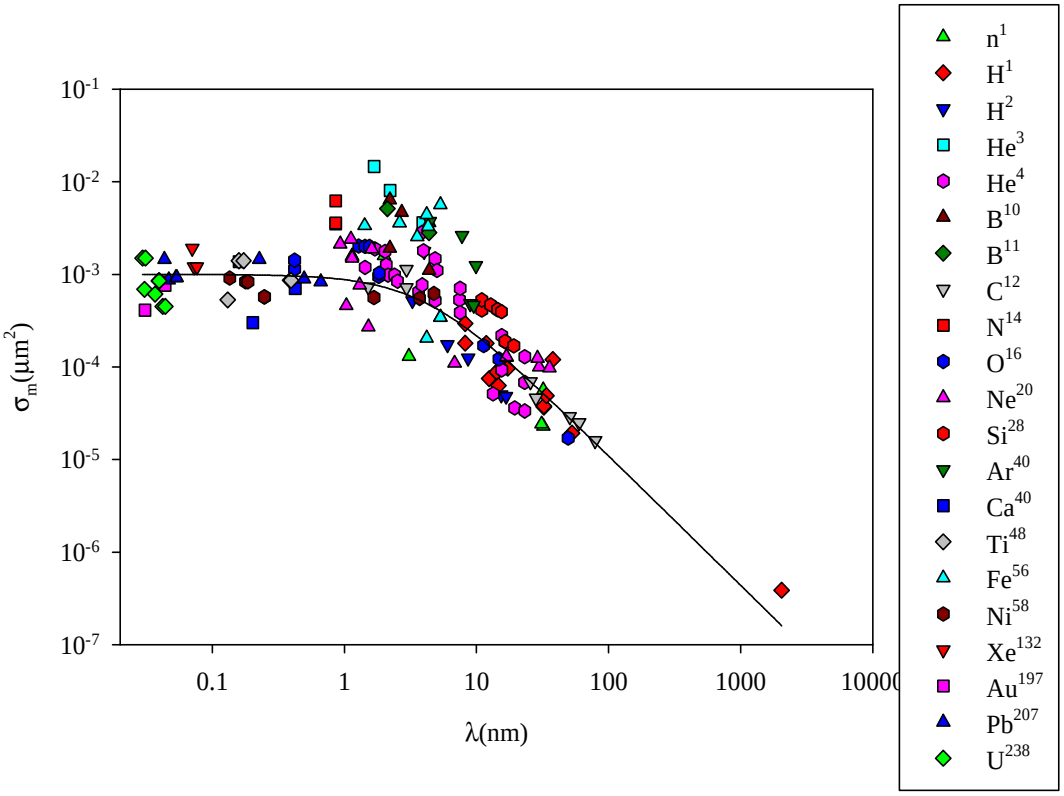

Fig. (6.21) the model between mutation cross section and the mean free path for heavy charged particles.

6.3.2 Sparsely Ionizing Radiation:

The curve between the mutation cross section and the mean free path for photons shows disappearance of the saturated region. The range of the energies of the available data id may be the reason. Another interpretation, the photons' nature of interaction, as it previously cited in chapter 4, the indirect interaction (with producing free radicals) takes place beyond the DNA size.

The correlation for the HPRT mutation cross section induced by photons follows the mathematical equation below;

$$s(l) = \frac{4x10^{-5}}{1+\left(\frac{l}{4}\right)^{1.4}} \qquad (6.3)$$

m=1.4, σ_0 =0.00004 μm^2, λ_0=4nm. With smaller cross section at the saturation and the same expected number of DSB, as in charged particles.

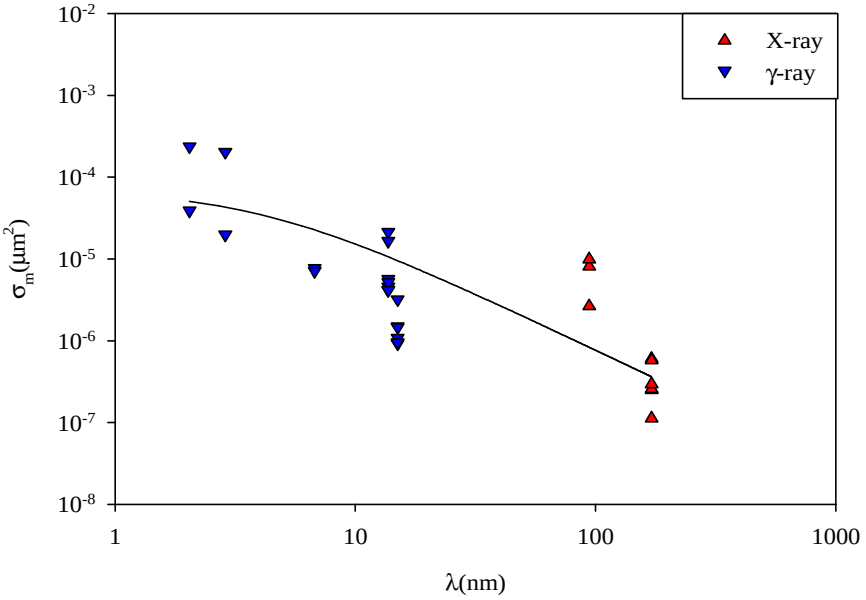

Fig. (6.22) the model between mutation cross section and the mean free path for photons.

6.3. Comparison between Densely and Sparsely Ionizing Radiation Mutation Actions:

In comparison between the action of densely and sparsely ionizing radiation Fig.(6.23), taking into account that the mutation cross section at the saturated region which reaches the average of geometrical cross section of HPRT gene in mammals ($\sigma_g \approx 1.06\times10^{-3}$ μm^2). For densely ionizing radiation σ_0 / σ_g= (1/1.17) and (1/26.3) for sparsely ionizing radiation; in other words, the probability of inducing HPRT mutation in mammalian

cells by densely ionizing radiation to sparsely ionizing radiation is about 20 times. This result is two times of the value of the yield of densely to sparsely (=10 times), which was mentioned before in chapter 4, table (4.1).

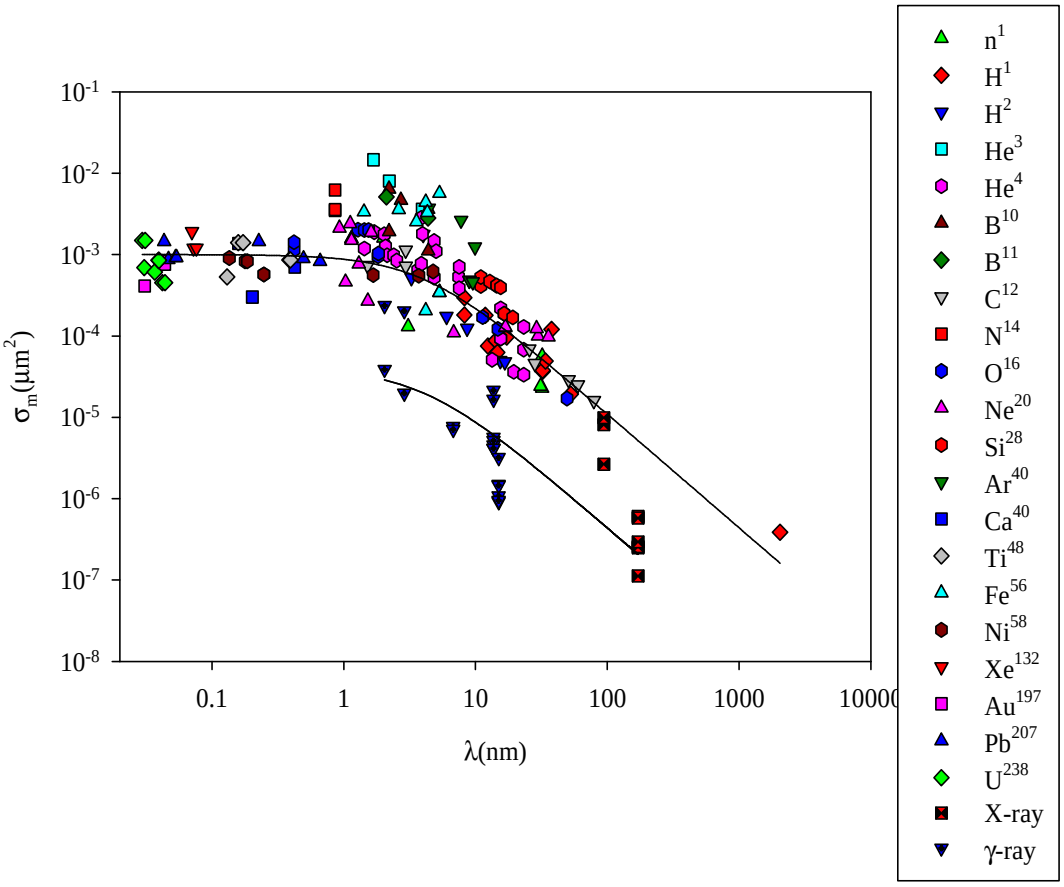

Fig. (6.23) Comparison between the HPRT mutation cross section curves induced by densely and sparsely ionizing radiation.

Conclusion

The main target in biological matter is the DNA, and its critical damage is the double strand break DSB which is considered to be a key cellular lesion by exposing to radiation, and its misrejoining. The HPRT (Hypoxanthine-guanine phosphoribosyl transferase) locus is a very useful system to study the molecular pattern of mutations, because of the ease of the selection of mutants' cells.

Judging from the literature, the mean free path was found to be the best correlation to indicate the radiation damage in the biological matter. Although, the unrestricted linear energy transfer LET, the restricted linear energy transfer L_{100} and the Katz's parameter $(Z^*/\beta)^2$ are representing a good fitting to the data. They do not interpret a clear understanding for the track structure, which determined in nanometer distances, this corresponds with (Stoll, U., 1995).

Watt and his group argued that the linear primary ionization can be considered as a good quality parameter to model the biological damage of different endpoints.

Based on the model for both densely and sparsely ionizing radiation, the inflection point λ_0=4nm, which suggests that two DSB occur within the HPRT gene and leads to the mutation. The latter is in agreement with few investigators like; (Nelson, S. L. et al, 1996), (Schmidt, P. et al, 1998) and (Ponomarev, A. L. et al, 2008) and supported the contribution of DSB misrejoining to HPRT mutation induction, (Rothkamm, K. et al, 2008).

In general, it is concluded from this research that the interaction of radiation in cells takes place within the limit of DNA, which shows a consistency with (El-Mansouri, R., 2003) and (Yousuf, A., 2006). Further investigations are needed to find the limits of exposure in terms of the mean free path for linear primary ionization, and could be used to design a biological dosimeter has a response to the biological cross section and the mean free path for linear primary ionization.

Reference

Ahluwalia, K. B., Genetics, 2nd edition. O'Brien, S. J., Menninger, J. C. and Nash, W. G. (Eds), *Chap 14: The Structure and Replication of DNA* **(116-156)**, Atlas of Mammalian Chromosomes, A John Wilet & Sons, Inc., Publication.

Alpen, E. L., *1998, Radiation Biophysics, Second Edition*, Academic Press, California, 92-96.

Attix, F. H., *1986, Introduction to radiological physics and Radiation Dosimetry*, New Yory, John Wily & Sons, Inc, 109-231.

Bao, C.-Y., Ma, A.H., Evans, H.H., Horong, M.F., Mencel, J., Hui, T. E. and Sedwick, W.D., 1995, Molecular analysis of hypoxanthine phosphoribosyltransferase gene deletions induced by α- and X-radiation in human lymphoblastoid cells, *Mutation Research*, **326,**1–15.

Barnhart, B. J. and Cox, S. H., 1979, Mutagenicity and cytotoxicity of 4.4 MeV α-particles emitted by Plutonium-238. *Radiation Research*, **80**, 542-548.

Baumstark-Khan, C., Rosendahl, I.M. and Rink, H., 2007, On the quality of mutations in mammalian cells induced by high LET radiation. *Advances in Space Research*, **40**, 474-482.

Belli, M., Cera, F., Cherbini, R., Ianzini, F., Moschini, G., Sapora, O., Simone, G., Tabochini, M. A. and Tiveron, P., 1992, RBE-LET relationship for survival and mutation induction of V79 cells irradiated with low energy protons: re-evaluation of the LET values at the LNTfacility. *International Journal of Radiation Biology*, **61,** 145-146.

Belli, M., Cera, F., Cherubini, R., Haque, M. A., Ianzini, F, Moschini, G., Sapora, O., Simone, G., Tabocchini, A. M. and Tiveron, P., 1993, Inactivation and mutation induction in V79 cells by low energy protons: re-evaluation of the results at the LNL facility. *International Journal of Radiation Biology*, **63,** 331-337.

Belli, M., Cera, F., Cherubini, R., Ianzini, F., Sapora, O., Simone, G., Tabocchini, M. and Tiveron, P., 1991, Mutation induction and RBE-LET relationship of low energy protons in V79 cells. *International Journal of Radiation biology*, **59,** 459-564.

Belli, M., Cera, F., Cherubini, R., Vecchias, M. Dalla, Haques, A. M. I., Ianzini, F., Moschini, G., Sapora, O., Simone, G., Tabocchini, M. A. and Tiverons, P., 1998, RBE-LET relationships for cell inactivation and mutation induced by low energy protons in V79 cells: further results at the LNL facility. *International Journal of Radiation Biology*, **74,** No. 4, 501-509.

Belli, M., Goodhead, D. T., Ianzini, F., Simone, G. and Tabocchini, M. A., 1992, Direct comparison of biological effectiveness of protons and alpha particles of the same LET. II. Mutation induction at the HPRT locus in V79 cells. *International Journal of Radiation Biology*, **61,** 625-629.

Blacer-Kubiczek, E. and Harrison, GH., 1991, Neoplastic transformation in C3H10T1/2 cells following exposure to 120 HZ modulated 2.45 G-HZ microwaves and phorbol ester tumour promotor. *Radiation Research*, **126**, 65-72.

Butts, J. J. and Katz, R., 1967, Theory of RBE for heavy ion bombardment of dry enzymes and viruses. *Radiation Research,* **30**, 855-871.

Chen, D., Tsuboi, K., Nguyen, T and Yang, T. C., 1994, Charged-particle mutagenesis II. Mutagenic effects of high energy charged particles in normal human fibroblasts. *Advances in Space Research*, **14**(10), 347-354.

Cherubini, R., Canova, S., Favaretto, S., Bruna, V., Battivelli, P. and Celotti, **L.**, 2002, Minisatellite and HPRT mutations in V79 cells irradiated with helium ions and gamma rays. *International Journal of radiation Biology*, **78(9)**, 791-797.

Cox, R. and Munson, W. K, 1979, "Mutation and inactivation of cultured mammalian cell exposed to beam of accelerated heavy ions. III. Human diploid fibroblasts. *International Journal of Radiation Biology*. **36**, 149-160.

Cox, R., 1994, Molecular mechanisms of radiation oncogenesis. *International Journal of Radiation Biology*. **65**, 57-64.

Cox, R., Thacker, J., Goodhead, D. T. and Munson, **R. J**, 1977, "Mutation and inactivation of cultured mammalian cells by various ionizing radiations. *Nature*(London) **267**, 425-427.

Cucinotta, F. A., Wilson, J. W., Shavers, M. R. and Katz, R., 1995, Effects of track structure and cell inactivation on the calculation of heavy ion mutation rates in mammalian cells, *International Journal of Radiation Biology*, **69**(5), 593-600.

Curry, T.S., Dowdey, J.E., and Murry, R.C.Jr., 1990. Christensen's physics of diagnostic radiology. 4th Edn. Lea and Febiger, Philadelphia. 61-69.

El-Mansouri, **R.**, 2003, *A unified approach model of radiation action on mammalian cells*. University of Garyounis, Department of Physics.

Hall, E. J., 2005, *Radiobiology for the radiologist*, Sixth Edition. Lippincott William & Wilkins, 2-35.

Harder, D., Virsk-Peuckert, R.P. and Bartels, E. R., 1994, Theory of intertrack pairwise lesion interaction. Radiation Protection Dosimetry **52**, (4-1): 13-16.

Hei, T. K., Chen, D.J., Brenner, D.J. and Hall, **E. J.**, 1988, Mutation induction by charged particles of defined linear energy transfer. *Carcinogenesis* **9**, 1233-1236.

IAEA (International Atomic Energy Agency), 1995, *Atomic and molecular data for radiotherapy and radiation research*, 641-643.

IAEA (International Atomic Energy Agency), *2005, Radiation Oncology Physics: a Handbook for teachers and Students*, 485-495.

ICRU, 1998, "Fundamental Quantities and Units for Ionizing Radiation". **Report 60.**

ICRU, 2005, "Stopping of Ions Heavier Than Helium". Report **73**. Oxford University Press.

Kagawa, Y., Shimazu, T., Gordon, A. J., Fukunishi, N., Inabe, N., Suzuki, M., Hirano, M., Hirano, T., Kato, T., Watanabe, M. and Yatagai, F., 1999, Complex HPRT deletion events after exposure of human lymphoblastoid cells to high-LET carbon and neon ion beams. *Mutagenesis*. **14**, 199-205.

Kenneth, K. S., 1988, *Introductory Nuclear Physics*. Oregon State University, John wiley & Sons Publications, chapter 7.

Kent, C. R. H., Edward, S. M. and McMillan, T.J., 1993, Mutation induction by ionizing radiation in three human bladder tumour cell lines. *International Journal of Radiation Biology*, **63(1)**, 1-5.

Kiefer, J. and Straaten, H., 1986, A model of ion track structure based on classical collision dynamics *Phys. Med. Biol*. **31**, 1201-9.

Kiefer, J., 2008, the physical basis for the biological action. *New Journal of physics*. **10**.

Kiefer, J., Schmidt, P. and Koch, S., 2001, Mutations in Mammalian induced by Heavy Changed Particles: An Indicator for Risk Assessment in Space. *Radiation Research*. **156**, 607-611.

Kiefer, J., Schreiber, A., Gutermuth, F., Koch, S. and Schmidt, P., 1999, Mutation induction by different types of radiation at the HPRT locus. *Mutation Res*earch **431**, 429-448.

Kinashi Y., Masunaga S., Takagaki M. And Ono K., 1997, Mutation effects at HPRT locus induced in Chinese hamster ovary cells by thermal neutrons with or without boron compound. *Mutation Research*, **377**, 211-215.

Kranert, T., Schneider, E. and Kiefer, J., 1988, Heavy ions irradiation induces mutations in mammalian cells. *GSI-Report*, 88-1, 228.

Kranert, T., Schneider, E. and Kiefer, J., 1990, Mutation induction in V79 Chinese hamster cells by very heavy ions. *International Journal of Radiation Biology***, 58**, 975-987.

Kranert, T., Stoll, U., Schneider, E. and Kiefer, J., 1992, Mutation induction in mammalian cells by very heavy ions. *Advances in Space Research*, **12**, issues 2-3, 111-118.

Kroneberg, A., 1991, Perspective on fast-neutron mutagenesis of human cells. *Radiation Research***, 128**, S87-S93.

Kronenberg, A. and Little, **J. B.**, 1989, Molecular characterization of thymidine kinase mutants of human cells induced by densely ionizing radiations. *Mutation Research,***211**, 215-224.

Kronenberg, A., 1994, Mutation iduction in human lymphoid cells by energetic heavy ions. *Advances in Space Research*, **14,** (10)339-346.

Kronenberg, A., Gauny, S., Criddle, K., Vannais, D., Ueno, A., Kraemer, S. and Waldren, C. A., 1995, Heavy ion mutagenesis: Linear energy transfer effects and genetic linkage. *Radiat. Environ. Biophy*. **34**, 73-78.

Kudryashov Yurii B., 2008, *Radiation Biophysics (Ionizing Radiation).* New York, Nove Science Publisher, Inc, the introduction.

Leroy, C., Rancoita, P-G., 2004, *Principles of radiation Interaction in Matter and detection*, World Scientific Publishing Co. Pte. Ltd. 34-38.

Melton, D. W., Konecki, D. S., Brennand, J. and Caskey, C. T., 1984, Structure, expression, and mutation of hypoxanthine phosphoribosyltranferase gene. *Proc. Natl. Acad. Sci.* USA **81**, 2147-2151.

Munson, R. J. , Bance, D. A., Stretch, A. and Goodhead, D. T., 1979, Mutation and inactivation of cultued mammalian cells axposed to beams of accelerated heavy ions. I. Irradiation facilities and methods. *International Journal of Radiation Biology* **36**, 127-136.

Nelson, S. L., Parks, K. K. and Grosovsky, A. J., 1996, Ionizing radiation signature mutations in human cell mutants induced by low-dose exposures. *Mutagenesis*, **11(3)**, 275-279.

Nias, **A. H. W.**, 1998, *An Introduction to Radiobiology*, Second Edition, John Wiley & Sons Ltd, 12-79.

Nikjoo, H., 2003, Radiation track and DNA damage. *Iranian Journal of Radiation Reseaech*, **1**(1), 3-16.

Podgoršak, E. B., 2006, *Radiation Physics for medical Physicists*, McGill University Health Center, 141-254.

Ponomarev, A. L., Costes, S. V. and Cucinotta, F. A., 2008, Stochastic properties of radiation-induced DSB: DSB distribution in large scale chromatin loops, the HPRT gene and within the visible volumes of DNA repair foci. *International Journal of Radiation Biology*, **84(11)**, 916-929.

Rosendahl, I.M., Baumstark-Khan, C. and Rink, H., 2005, Mutation induction in mammalian cells by accelerated heavy ions. *Advances in Space Research,* **36**, 1701-1709.

Rothkamm, K., Gunasekara, K, Warda, S. A., Krempler, A. and Lobrich, M., 2008, Radiation-induced HPRT mutations resulting from misrejoined DNA double-strand breaks. *Radiation Research*, **169**, 639-648.

Schmidt, P. and Kiefer, J., 1998, Deletion pattern analysis of alpha-particle and X-ray incuced mutations at the HPRT locus of Chinese hamster cells. *Mutation Research*, **421**, 149-161.

Scholz, M. and Kraft, **G.**, 1996, Track structure and the calculation of biological effects of heavy charged particles. *Advances in Space Research*, **18,** 5-14.

Steel, G. Gordon (editor), 1997, *Basic Clinical Radiobiology*, Oxford University Press, 53-69.

Stoll, U., Barth, B., Scheerer, N., Schneider, E. and Kiefer, J., 1996, HPRT mutations in V79 Chinese hamster cells induced by accelerated Ni, Au and Pb ions. *International Journal of Radiation Biology*. **70**, 15-22.

Stoll, U., Schmidt, A., Scneider, E. and Kiefer, J., (1995) [1], Killing and mutation of v79 Cchinese hamster cells exposed to accelerated oxygen and neon ions. *Radiation Research,* **142**, 288-294.

Stoll, U., Schneider, E., Kranert, T. and Kiefer, J., (1995) [2], Induction of **HPRT mutants** in Chinese hamster V79 cells after heavy ion exposure. *Radiat. Environ. Biophys*. **34**, 91-94.

Stout, J. T. and Caskey, C. T., 1985, HPRT: Genes Structure, expression, and mutation. *Ann. Rev. Genet*. **19**, 127-148.

Suzuki, M., Tsuruoka, C., Kanai, T., Kato, T., Yatagai, F. and Watanabe, M., 2006, Cellular and molecular effects for mutation induction in normal human cells irradiated with accelerated neon ions. *Mutation Research*, **594**, 86-92.

Suzuki, M., Watanabe, M., Kanai, T., Kase, Y., Yatagai, F., Kato, T. and Matsubara, S., 1996, LET dependence of cell death, mutation induction and chromatin damage in human cells irradiated with accelerated carbon ions. *Advances in Space Research*, **18(1/2)**, 127-136.

Thacker, J., Stretch, A. and Goodhead, D.T., 1982, The mutagenicity of α-particles from plutonium-238. *Radiation Research*, **92**, 343–352.

Tsuboi, K., Yang, T. C. and Chen, D., 1992, Changed-Particle Mutagenesis, 1. Cytotoxic and Mutagenic Effects of High-LET Charged Iron Particles on Human Skin Fibroblasts. *Radiation Research*. **129**, 171-176.

Tubiana, M., Dutreix, J. and Wambersie, A., 1990, *Introduction to radiobiology*. New York, Taylor & Francis, 15-53.

Turner, J. E., 2007, *Atoms, Radiation, and Radiation Protection*. Third edition, WILEY-VCH Verlag GmbH & Co. KGaA, Weinheim, 160-181.

US. Congress of Technology Assessment, Technologies *for Detecting* Heritable *Mutations in* Human Beings, OTA-H-298 (Washington, DC: U.S. Government Printing Office, (September 1986). Library of Congress Catalog Card Number 86-600523.

Watt, D. E., *1996, Quantities for Dosimetry of Ionizing Radiation in Liquid Water*, 3-377.

Wilson, J. W., Cucinotta, F. A. and Shinn, J. L., 1993, *Cell kinetics and track structure. In: Biological Effects and physics of Solar and Galactic Cosmic Radiation.* Edited by: C. E. Swenberg, G. Horneck and E. G. Stassinopoulos, Part A (New York: Plenum Press), 295-338.

Wu, H., Sachs, R K. and Yang, T.C., 1998, Radiation-induced total-deletion mutations in human hprt gene: a biophysical model based on random walk interphase chromatin geometry. *International Journal of Radiation biology*, **73(2)**, 149-156.

Yousuf, A., 2006, *A unified model of ionizing radiation action on chromosomes of mammalian cells*. University of Garyounis, Department of Physics.

Table (2.2) Main characteristic of photoelectric effect, Rayleigh scattering, Compton effect and pair production.

	Photoelectric Effect	**Rayleigh Scattering**	**Compton Effect**	**Pair Production**
Photon interaction	With whole atom (bound electron)	With bound electrons	With free electrons	With nuclear Coulomb field
Mode of photon interaction	Photon disappears	Photon scattered	Photon scattered	Photon disappears
Energy dependence	$1/(h\nu)^3$	$1/(h\nu)^2$	Decreases with energy	Increases with energy
Threshold energy	Shell binding energy	No	Shell binding energy	$2m_0c^2$
Particles released in absorber	Photoelectron	None	Compton (recoil) electron	Electron-positron pair
Subsequent effect	Characteristic X ray, Auger effect	None	Characteristic X ray, Auger effect	Annihilation radiation
Predominant energy region for water	<20keV	<20keV	20keV-10MeV	>10MeV

From (E. B. Podgoršak, 2006)

Appendix I. The biological and physical data base of HPRT mutations in mammalian cells induced by charged particles

No.	Ions	Energy (MeV)	Specific Energy (Mev/u)	LET (keV/μm)	L_{100} (keV/μm)	Z^{*2}/β^2	I(nm^{-1})	λ(nm)	R(μm)	W(eV)	$\alpha_i(Gy^{-1})$
1	n(fission)	7.00E-01	7.00E-01	5.56E+01	3.93E+01	1.36E+03	5.01E-01	2.00E+00	4.67E+00	2.66E+01	5.00E-02
2	n	1.35E+00	1.35E+00	4.23E+01	2.74E+01	9.70E+02	3.25E-01	3.08E+00	1.30E+01	2.60E+01	
3	n(42d-Be)	1.70E+01	1.70E+01	7.26E+00	3.97E+00	9.65E+01	3.12E-02	3.20E+01	1.06E+03	2.53E+01	3.40E-01
4	n(42d-Be)	1.70E+01	1.70E+01	7.26E+00	3.90E+00	9.65E+01	3.12E-02	3.20E+01	1.06E+03	2.53E+01	1.31E+00
5	n	1.00E-04	1.00E-04	8.26E+00	8.26E+00	1.51E+04	3.21E-02	3.11E+01	2.49E-03	6.89E+01	
6	H-1	7.60E-01	7.60E-01	3.18E+01	1.80E+01	6.26E+02	1.21E-01	8.24E+00	1.63E+01	2.56E+01	7.44E-01
7	H-1	7.60E-01	7.60E-01	3.18E+01	1.80E+01	6.26E+02	1.21E-01	8.24E+00	1.63E+01	2.56E+01	7.21E-01
8	H-1	1.16E+00	1.16E+00	2.44E+01	1.36E+01	4.27E+02	8.43E-02	1.19E+01	3.18E+01	2.56E+01	
9	H-1	1.23E+00	1.23E+00	2.36E+01	1.31E+01	4.06E+02	8.03E-02	1.25E+01	3.49E+01	2.55E+01	
10	H-1	1.41E+00	1.41E+00	2.14E+01	1.18E+01	3.53E+02	7.01E-02	1.43E+01	4.29E+01	2.55E+01	4.71E-01
11	H-1	1.41E+00	1.41E+00	2.14E+01	1.18E+01	3.53E+02	7.01E-02	1.43E+01	4.29E+01	2.55E+01	4.69E-01
12	H-1	1.44E+00	1.44E+00	2.10E+01	1.16E+01	3.44E+02	6.84E-02	1.46E+01	4.42E+01	2.55E+01	
13	H-1	1.70E+00	1.70E+00	1.86E+01	1.02E+01	2.91E+02	5.80E-02	1.72E+01	5.82E+01	2.55E+01	
14	H-1	3.20E+00	3.20E+00	1.11E+01	6.27E+00	1.55E+02	3.09E-02	3.24E+01	1.68E+02	2.53E+01	3.72E-01
15	H-1	3.20E+00	3.20E+00	1.11E+01	6.27E+00	1.55E+02	3.09E-02	3.24E+01	1.68E+02	2.53E+01	3.72E-01
16	H-1	3.36E+00	3.36E+00	1.02E+01	6.04E+00	1.47E+02	2.95E-02	3.39E+01	1.84E+02	2.53E+01	
17	H-1	3.70E+00	3.70E+00	8.43E+00	5.54E+00	1.32E+02	2.64E-02	3.79E+01	2.16E+02	2.53E+01	5.46E-01
18	H-1	5.01E+00	5.01E+00	7.93E+00	4.26E+00	9.51E+00	1.89E-02	5.30E+01	3.61E+02	2.53E+01	2.89E-01
19	H-1	2.50E+02	2.50E+02	4.04E-01	2.09E-01	2.76E+00	4.88E-04	2.05E+03	3.93E+05	2.51E+01	
20	H-2	5.50E-01	2.75E-01	5.86E+01	3.62E+01	1.77E+03	3.06E-01	3.27E+00	8.45E+00	2.60E+01	
21	H-2	7.00E-01	3.50E-01	5.15E+01	3.03E+01	1.40E+03	2.49E-01	4.02E+00	1.13E+01	2.59E+01	
22	H-2	1.10E+00	5.50E-01	3.95E+01	2.27E+01	8.81E+02	1.66E-01	6.02E+00	2.04E+01	2.57E+01	
23	H-2	1.60E+00	8.00E-01	3.07E+01	1.73E+01	5.94E+02	1.16E-01	8.64E+00	3.50E+01	2.56E+01	
24	H-2	3.00E+00	1.50E+00	2.03E+01	1.12E+01	3.26E+02	6.50E-02	1.54E+01	9.37E+01	2.55E+01	9.00E-01
25	H-2	3.30E+00	1.65E+00	1.90E+01	1.04E+01	2.99E+02	5.97E-02	1.67E+01	1.11E+02	2.55E+01	
26	He-3	1.80E+00	6.00E-01	1.47E+02	8.37E+01	3.13E+03	5.96E-01	1.68E+00	1.05E+01	2.79E+01	2.24E+00
27	He-3	2.50E+00	8.33E-01	1.21E+02	6.87E+01	2.35E+03	4.51E-01	2.22E+00	1.59E+01	2.78E+01	2.08E+00
28	He-3	4.40E+00	1.47E+00	7.96E+01	4.48E+01	1.31E+03	2.55E-01	3.93E+00	3.63E+01	2.75E+01	1.91E+00

Appendix I. The biological and physical data base of HPRT mutations in mammalian cells induced by charged particles

No.	$\alpha_m(Gy^{-1})$	$\sigma_i(\mu m^2)$	σ_m (μm^2)	σ_m/σ_i	Cell line
1	1.80E-04	4.45E-01	1.60E-03	3.60E-03	C3H10T1/2
2	1.92E-05		1.30E-04		TK6
3	1.97E-05	3.95E-01	2.29E-05	5.79E-05	V79
4	4.87E-05	1.52E+00	5.66E-05	3.71E-05	HF19
5	1.83E-05		2.42E-05		CHO
6	5.80E-05	3.78E+00	2.95E-04	7.80E-05	V79-753B
7	3.55E-05	3.66E+00	1.80E-04	4.92E-05	V79
8	4.60E-05		1.80E-04		V79-753 B
9	1.99E-05		7.50E-05		V79-4
10	2.57E-05	1.61E+00	8.78E-05	5.46E-05	V79-753B
11	2.57E-05	1.60E+00	8.78E-05	5.48E-05	V79
12	1.87E-05		6.28E-05		V79-4
13	3.26E-05		9.70E-05		V79-753 B
14	2.08E-05	6.59E-01	3.68E-05	5.59E-05	V79-753B
15	2.13E-05	6.59E-01	3.77E-05	5.73E-05	V79
16	3.00E-05	0.00E+00	4.91E-05		V79-753 B
17	8.92E-05	7.35E-01	1.20E-04	1.63E-04	HSF
18	1.52E-05	3.67E-01	1.93E-05	5.26E-05	V79
19	6.00E-06		3.88E-07		TK6
20	5.54E-05		5.19E-04		V79-753B
21	2.13E-04		1.76E-03		HSF
22	2.75E-05		1.74E-04		V79-753B
23	2.53E-05		1.24E-04		V79-753B
24	1.54E-05	2.92E+00	4.99E-05	1.71E-05	HSF
25	1.58E-05		4.80E-05		V79-753B
26	6.20E-04	5.27E+01	1.46E-02	2.77E-04	HSF
27	4.15E-04	4.02E+01	8.03E-03	2.00E-04	HSF
28	2.84E-04	2.43E+01	3.62E-03	1.49E-04	HSF

Appendix I. The biological and physical data base of HPRT mutations in mammalian cells induced by charged particles

No.	Reference
1	Blacer-Kubiczek, E. et al, 1991
2	Kronenberg, A. et al, 1991
3	Cox, R. et al, 1977.
4	Cox, R. et al, 1977.
5	Kinashi, Y. et al, 1997
6	Belli, M. et al, 1993
7	Belli, M. et al, 1998
8	Belli, M. et al, 1991
9	Belli, M. et al,1992
10	Belli, M. et al, 1993
11	Belli, M. et al, 1998
12	Belli, M. et al,1992
13	Belli, M. et al, 1991
14	Belli, M. et al, 1993
15	Belli, M. et al, 1998
16	Belli, M. et al, 1991
17	Hei, T.K. et al, 1988
18	Belli, M. et al, 1998
19	Kronenberg, A. et al, 1995
20	Belli, M. et al, 1994
21	Hei, T.K. et al, 1988
22	Belli, M. et al, 1994
23	Belli, M. et al, 1994
24	Hei, T.K. et al, 1988
25	Belli, M. et al, 1994
26	Hei, T.K. et al, 1988
27	Hei, T.K. et al, 1988
28	Hei, T.K. et al, 1988

Appendix I. The biological and physical data base of HPRT mutations in mammalian cells induced by charged particles

No.	Ions	Energy (MeV)	Specific Energy (Mev/u)	LET (keV/μm)	L_{100} (keV/μm)	Z^{*2}/β^2	I(nm^{-1})	λ(nm)	R(μm)	W(eV)	$\alpha_i(Gy^{-1})$
29	He-4	2.05E+00	5.13E-01	1.64E+02	9.29E+01	3.68E+03	6.97E-01	1.44E+00	1.12E+01	2.80E+01	2.11E+00
30	He-4	2.50E+00	6.25E-01	1.37E+02	7.75E+01	3.07E+03	5.86E-01	1.71E+00	1.46E+01	2.79E+01	1.20E+00
31	He-4	2.90E+00	7.25E-01	1.29E+02	7.29E+01	2.56E+03	4.92E-01	2.03E+00	1.78E+01	2.78E+01	9.00E-01
32	He-4	3.00E+00	7.50E-01	1.27E+02	7.19E+01	2.51E+03	4.83E-01	2.07E+00	1.83E+01	2.78E+01	
33	He-4	3.10E+00	7.75E-01	1.24E+02	7.04E+01	2.43E+03	4.68E-01	2.13E+00	1.91E+01	2.78E+01	
34	He-4	3.50E+00	8.75E-01	1.15E+02	6.48E+01	2.17E+03	4.18E-01	2.39E+00	2.25E+01	2.77E+01	1.66E+00
35	He-4	3.70E+00	9.25E-01	1.10E+02	6.22E+01	2.05E+03	3.96E-01	2.53E+00	2.43E+01	2.77E+01	
36	He-4	5.60E+00	1.40E+00	8.42E+01	4.73E+01	1.41E+03	2.75E-01	3.64E+00	4.52E+01	2.76E+01	1.08E+00
37	He-4	5.90E+00	1.48E+00	8.05E+01	4.52E+01	1.32E+03	2.58E-01	3.88E+00	4.86E+01	2.75E+01	1.29E+00
38	He-4	5.90E+00	1.48E+00	8.05E+01	4.52E+01	1.32E+03	2.58E-01	3.88E+00	4.86E+01	2.75E+01	3.16E+00
39	He-4	6.00E+00	1.50E+00	7.93E+01	4.44E+01	1.29E+03	2.52E-01	3.97E+00	4.98E+01	2.75E+01	1.73E+00
40	He-4	7.40E+00	1.85E+00	6.81E+01	3.78E+01	1.16E+03	2.06E-01	4.86E+00	7.00E+01	2.75E+01	9.61E-01
41	He-4	7.40E+00	1.85E+00	6.81E+01	3.78E+01	1.16E+03	2.06E-01	4.86E+00	7.00E+01	2.75E+01	2.57E+00
42	He-4	7.60E+00	1.90E+00	6.65E+01	3.68E+01	1.01E+03	1.99E-01	5.02E+00	7.29E+01	2.75E+01	1.40E+00
43	He-4	1.16E+01	2.90E+00	4.95E+01	2.68E+01	6.78E+02	1.34E-01	7.45E+00	1.46E+02	2.74E+01	9.72E-01
44	He-4	1.17E+01	2.93E+00	4.91E+01	2.68E+01	6.71E+02	1.33E-01	7.52E+00	1.48E+02	2.74E+01	9.33E-01
45	He-4	1.17E+01	2.93E+00	4.91E+01	2.68E+01	6.71E+02	1.33E-01	7.52E+00	1.48E+02	2.74E+01	1.98E+00
46	He 4	2.03E+01	5.08E+00	3.16E+01	1.69E+01	3.78E+02	7.48E-02	1.34E+01	3.67E+02	2.72E+01	
47	He-4	2.44E+01	6.10E+00	2.81E+01	1.50E+01	3.26E+02	6.44E-02	1.55E+01	5.04E+02	2.72E+01	5.49E-01
48	He-4	2.44E+01	6.10E+00	2.81E+01	1.50E+01	3.26E+02	6.44E-02	1.55E+01	5.04E+02	2.72E+01	1.25E+00
49	He-4	2.44E+01	6.10E+00	2.81E+01	1.50E+01	3.26E+02	6.44E-02	1.55E+01	5.04E+02	2.72E+01	7.67E-01
50	He 4	3.05E+01	7.63E+00	2.36E+01	1.25E+01	2.62E+02	5.13E-02	1.95E+01	7.47E+02	2.72E+01	
51	He-4	3.48E+01	8.70E+00	2.05E+01	1.09E+01	2.20E+02	4.32E-02	2.31E+01	9.70E+02	2.72E+01	5.49E-01
52	He-4	3.49E+01	8.73E+00	2.04E+01	1.09E+01	2.19E+02	4.31E-02	2.32E+01	9.75E+02	2.71E+01	4.91E-01
53	He-4	3.49E+01	8.73E+00	2.04E+01	1.09E+01	2.19E+02	4.31E-02	2.32E+01	9.75E+02	2.71E+01	1.09E+00
54	B-10	4.98E+01	4.98E+00	1.93E+02	1.03E+02	2.29E+03	4.53E-01	2.21E+00	1.64E+02	3.02E+01	1.12E+00
55	B-10	4.98E+01	4.98E+00	1.93E+02	1.03E+02	2.29E+03	4.53E-01	2.21E+00	1.64E+02	3.02E+01	2.00E+00
55	B-10	6.56E+01	6.56E+00	1.64E+02	8.74E+01	1.87E+03	3.68E-01	2.72E+00	2.51E+02	3.01E+01	2.79E+00

Appendix I. The biological and physical data base of HPRT mutations in mammalian cells induced by charged particles

No.	$\alpha_m(Gy^{-1})$	$\sigma_i(\mu m^2)$	σ_m (μm^2)	σ_m/σ_i	Cell line
29	4.54E-05	5.54E+01	1.19E-03	2.15E-05	V79
30	8.62E-05	2.63E+01	1.89E-03	7.18E-05	V79-4
31	8.60E-05	1.86E+01	1.77E-03	9.56E-05	V79
32	6.20E-05	7.90E+01	1.26E-03	1.59E-05	V79
33	4.92E-05	3.30E+01	9.80E-04	2.97E-05	V79
34	4.94E-05	3.30E+01	9.80E-04	2.97E-05	V79
35	4.79E-05		8.44E-04		CHO
36	4.78E-05	1.46E+01	6.44E-04	4.42E-05	V79
37	5.97E-05	1.66E+01	7.69E-04	4.63E-05	V79
38	2.20E-04	4.07E+01	2.83E-03	6.96E-05	HF19 strain
39	1.42E-04	2.20E+01	1.80E-03	8.18E-05	V79
40	4.78E-05	1.05E+01	5.21E-04	4.97E-05	V79
41	1.35E-04	2.80E+01	1.47E-03	5.25E-05	HF19 strain
42	1.03E-04	1.49E+01	1.10E-03	7.38E-05	V79
43	6.69E-05	7.70E+00	5.30E-04	6.88E-05	V79
44	4.90E-05	7.33E+00	3.85E-04	5.25E-05	V79
45	8.99E-05	1.56E+01	7.07E-04	4.54E-05	HF19 strain
46	1.01E-05		5.11E-05		V79-4
47	2.08E-05	2.47E+00	9.36E-05	3.79E-05	V79
48	4.85E-05	5.64E+00	2.18E-04	3.87E-05	HF19 strain
49	2.07E-05	3.45E+00	9.30E-05	2.70E-05	V79
50	9.60E-06		3.62E-05		V79-4
51	2.07E-05	1.80E+00	6.80E-05	3.78E-05	V79
52	1.02E-05	1.61E+00	3.34E-05	2.08E-05	V79
53	3.94E-05	3.57E+00	1.29E-04	3.61E-05	HF19 strain
54	6.21E-05	3.45E+01	1.92E-03	5.54E-05	V79
55	2.07E-04	6.17E+01	6.39E-03	1.04E-04	HF19 strain
55	1.78E-04	7.32E+01	4.67E-03	6.38E-05	HF19 strain

Appendix I. The biological and physical data base of HPRT mutations in mammalian cells induced by charged particles

No.	Reference
29	Kranert, T. et al, 1992
30	Thacker, J. et al, 1982
31	Cherubini, R. et al, 2002
32	Kranert, T. et al, 1988
33	Kiefer, J. et al (2001)
34	Schmidt, P. et al, 1998
35	Barnhart, B. et al, 1979
36	Cherubini, R. et al, 2002
37	Munson, R. et al, 1979
38	Cox, R. et al,1979
39	Kranert, T. et al, 1990
40	Munson, R. et al, 1979
41	Cox, R. et al,1979
42	Kranert, T. et al, 1990
43	Kranert, T. et al, 1990
44	Munson, R. et al, 1979
45	Cox, R. et al,1979
46	Belli, M. et al,1992
47	Munson, R. et al, 1979
48	Cox, R. et al,1979
49	Kranert, T. et al, 1990
50	Belli, M. et al,1992
51	Kranert, T. et al, 1990
52	Munson, R. et al, 1979
53	Cox, R. et al,1979
54	Munson, R. et al, 1979
55	Cox, R. et al,1979
55	Cox, R. et al,1979

Appendix I. The biological and physical data base of HPRT mutations in mammalian cells induced by charged particles

No.	Ions	Energy (MeV)	Specific Energy (Mev/u)	LET (keV/μm)	L_{100} (keV/μm)	Z^{*2}/β^2	I(nm^{-1})	λ(nm)	R(μm)	W(eV)	$\alpha_i(Gy^{-1})$
56	B-10	1.07E+02	1.07E+01	1.12E+02	5.99E+01	1.18E+03	2.28E-01	4.38E+00	5.17E+02	3.00E+01	2.96E+00
57	B-10	1.07E+02	1.07E+01	1.12E+02	5.99E+01	1.18E+03	2.28E-01	4.38E+00	5.17E+02	3.00E+01	7.40E-01
58	B-11	5.50E+01	5.00E+00	2.00E+02	1.07E+02	2.40E+03	4.74E-01	2.11E+00	1.80E+02	3.02E+01	1.41E+00
59	B-11	1.18E+02	1.07E+01	1.12E+02	5.98E+01	1.18E+03	2.29E-01	4.38E+00	6.44E+02	3.00E+01	1.13E+00
60	C-12	1.20E+02	1.00E+01	1.66E+02	8.81E+01	1.75E+03	3.38E-01	2.96E+00	4.40E+02	3.06E+01	8.87E-01
61	C-12	6.00E+01	5.00E+00	2.79E+02	1.49E+02	3.34E+03	6.60E-01	1.52E+00	1.43E+02	3.08E+01	8.73E-01
62	C-12	1.20E+02	1.00E+01	1.66E+02	8.81E+01	1.75E+03	3.38E-01	2.96E+00	4.40E+02	3.06E+01	9.55E-01
63	C-12	1.06E+03	8.80E+01	2.81E+01	1.51E+01	2.20E+02	3.90E-02	2.56E+01	2.23E+04	3.02E+01	7.79E-01
64	C-12	1.12E+03	9.30E+01	2.59E+01	1.38E+01	2.00E+02	3.55E-02	2.82E+01	2.69E+04	3.02E+01	6.03E-01
65	C-12	2.52E+03	2.10E+02	1.60E+01	8.29E+00	1.11E+02	1.97E-02	5.08E+01	9.72E+04	3.01E+01	1.13E+00
66	C-12	3.18E+03	2.65E+02	1.41E+01	7.21E+00	9.47E+01	1.67E-02	5.98E+01	1.44E+05	3.01E+01	1.11E+00
67	C-12	4.80E+03	4.00E+02	1.13E+01	5.70E+00	7.18E+01	1.26E-02	7.92E+01	2.75E+05	3.01E+01	8.87E-01
68	N-14	5.18E+01	3.70E+00	4.57E+02	2.45E+02	5.87E+03	1.16E+00	8.61E-01	8.38E+01	3.15E+01	8.21E-01
69	N-14	5.18E+01	3.70E+00	4.57E+02	2.45E+02	5.87E+03	1.16E+00	8.61E-01	8.38E+01	3.15E+01	1.38E+00
70	N-14	5.18E+01	3.70E+00	4.57E+02	2.45E+02	5.87E+03	1.16E+00	8.61E-01	8.38E+01	3.15E+01	8.34E-01
71	O-16	3.04E+01	1.90E+00	8.06E+02	4.39E+02	1.21E+04	2.38E+00	4.19E-01	3.24E+01	3.25E+01	5.52E-01
72	O-16	3.04E+01	1.90E+00	8.06E+02	4.39E+02	1.21E+04	2.38E+00	4.19E-01	3.24E+01	3.25E+01	2.08E-01
73	O-16	1.22E+02	7.60E+00	3.60E+02	1.92E+02	3.99E+03	7.79E-01	1.28E+00	2.19E+02	3.17E+01	8.06E-01
74	O-16	1.31E+02	8.20E+00	3.31E+02	1.76E+02	3.60E+03	6.99E-01	1.43E+00	2.51E+02	3.17E+01	9.44E-01
75	O-16	1.41E+02	8.80E+00	3.12E+02	1.66E+02	3.34E+03	6.47E-01	1.54E+00	2.86E+02	3.17E+01	1.00E+00
76	O-16	1.71E+02	1.07E+01	2.73E+02	1.46E+02	2.85E+03	5.50E-01	1.82E+00	3.92E+02	3.16E+01	1.13E+00
77	O-16	1.73E+02	1.08E+01	2.72E+02	1.45E+02	2.83E+03	5.45E-01	1.83E+00	4.01E+02	3.16E+01	9.55E-01
78	O-16	1.12E+03	6.97E+01	6.10E+01	3.29E+01	4.98E+02	8.83E-02	1.13E+01	1.07E+04	3.12E+01	8.41E-01
79	O-16	1.41E+03	8.80E+01	4.88E+01	2.62E+01	3.82E+02	6.75E-02	1.48E+01	1.68E+04	3.11E+01	5.50E-01
80	O-16	6.34E+03	3.96E+02	1.98E+01	9.98E+00	1.25E+02	2.02E-02	4.95E+01	2.06E+05	3.10E+01	4.11E-01
81	Ne-20	1.60E+02	8.00E+00	5.09E+02	2.71E+02	5.54E+03	1.08E+00	9.29E-01	2.06E+02	3.25E+01	5.53E-01
82	Ne-20	1.78E+02	8.90E+00	4.68E+02	2.49E+02	5.00E+03	9.68E-01	1.03E+00	2.48E+02	3.25E+01	6.40E-01
83	Ne-20	1.96E+02	9.80E+00	4.40E+02	2.34E+02	4.63E+03	8.92E-01	1.12E+00	2.83E+02	3.25E+01	1.28E+00

Appendix I. The biological and physical data base of HPRT mutations in mammalian cells induced by charged particles

No.	α_m(Gy^{-1})	σ_i(μm^2)	σ_m (μm^2)	σ_m/σ_i	Cell line
56	2.01E-04	5.32E+01	3.61E-03	6.79E-05	HF19 strain
57	6.18E-05	1.33E+01	1.11E-03	8.35E-05	V79
58	1.60E-04	4.50E+01	5.12E-03	1.14E-04	V79
59	1.57E-04	2.04E+01	2.82E-03	1.38E-04	V79
60	2.71E-05	2.35E+01	7.17E-04	3.05E-05	V79
61	1.63E-05	3.90E+01	7.30E-04	1.87E-05	V79
62	4.27E-05	2.53E+01	1.13E-03	4.47E-05	V79
63	1.54E-05	3.50E+00	6.90E-05	1.97E-05	V79
64	1.11E-05	2.50E+00	4.60E-05	1.84E-05	V79
65	1.13E-05	2.90E+00	2.90E-05	1.00E-05	V79
66	1.11E-05	2.50E+00	2.50E-05	1.00E-05	V79
67	8.87E-06	1.60E+00	1.60E-05	1.00E-05	V79
68	4.77E-05	6.01E+01	3.49E-03	5.81E-05	V79
69	8.50E-05	1.01E+02	6.22E-03	6.16E-05	HF19 strain
70	4.89E-05	6.10E+01	3.58E-03	5.87E-05	V79
71	8.84E-06	7.12E+01	1.14E-03	1.60E-05	V79
72	1.10E-05	2.68E+01	1.42E-03	5.30E-05	V79
73	3.51E-05	4.64E+01	2.02E-03	4.35E-05	V79
74	3.78E-05	5.00E+01	2.00E-03	4.00E-05	V79
75	4.01E-05	5.00E+01	2.00E-03	4.00E-05	V79
76	2.17E-05	4.95E+01	9.50E-04	1.92E-05	V79
77	2.37E-05	4.15E+01	1.03E-03	2.48E-05	V79
78	1.74E-05	8.20E+00	1.70E-04	2.07E-05	V79
79	1.56E-05	4.30E+00	1.22E-04	2.84E-05	V79
80	5.37E-06	1.30E+00	1.70E-05	1.31E-05	V79
81	2.62E-05	4.50E+01	2.13E-03	4.73E-05	V79
82	6.14E-06	4.80E+01	4.60E-04	9.58E-06	V79
83	3.41E-05	9.00E+01	2.40E-03	2.67E-05	V79

Appendix I. The biological and physical data base of HPRT mutations in mammalian cells induced by charged particles

No.	Reference
56	Cox, R. et al,1979
57	Munson, R. et al, 1979
58	Kranert, T. et al, 1990
59	Kranert, T. et al, 1990
60	Kiefer, J. et al (2001)
61	Kiefer, J. et al (2001)
62	Kiefer, J. et al (2001)
63	Kiefer, J. et al (2001)
64	Kiefer, J. et al (2001)
65	Kiefer, J. et al (2001)
66	Kiefer, J. et al (2001)
67	Kiefer, J. et al (2001)
68	Munson, R. et al, 1979
69	Cox, R. et al,1979
70	Kranert, T. et al, 1990
71	Stoll, U. et al (1995) & Kiefer, J. et al (2001)
72	Rosendahl, I.M. et al (2005)
73	Rosendahl, I.M. et al (2005)
74	Kranert, T. et al, 1990
75	Stoll, U. et al (1995) & Kiefer, J. et al (2001)
76	Stoll, U. et al (1995) & Kiefer, J. et al (2001)
77	Rosendahl, I.M. et al (2005)
78	Rosendahl, I.M. et al (2005)
79	Stoll, U. et al (1995) & Kiefer, J. et al (2001)
80	Stoll, U. et al (1995) & Kiefer, J. et al (2001)
81	Stoll, U. et al (1995) & Kiefer, J. et al (2001)
82	Kranert, T. et al, 1990
83	Kranert, T. et al, 1992

Appendix I. The biological and physical data base of HPRT mutations in mammalian cells induced by charged particles

No.	Ions	Energy (MeV)	Specific Energy (Mev/u)	LET (keV/μm)	L_{100} (keV/μm)	Z^{*2}/β^2	I(nm^{-1})	λ(nm)	R(μm)	W(eV)	$\alpha_i(Gy^{-1})$
84	Ne-20	2.14E+02	1.07E+01	4.32E+02	2.30E+02	4.54E+03	8.74E-01	1.14E+00	2.92E+02	3.25E+01	6.07E-01
85	Ne-20	2.14E+02	1.07E+01	4.32E+02	2.30E+02	4.54E+03	8.74E-01	1.14E+00	2.92E+02	3.25E+01	7.52E-01
86	Ne-20	2.40E+02	1.20E+01	3.89E+02	2.07E+02	4.01E+03	8.74E-01	1.14E+00	4.02E+02	3.24E+01	6.75E-01
87	Ne-20	2.86E+02	1.43E+01	3.44E+02	1.83E+02	3.45E+03	7.68E-01	1.30E+00	5.17E+02	3.23E+01	6.00E-01
88	Ne-20	2.96E+02	1.48E+01	3.28E+02	1.75E+02	3.27E+03	6.20E-01	1.61E+00	5.55E+02	3.23E+01	9.55E-01
89	Ne-20	1.30E+03	6.50E+01	1.00E+02	5.42E+01	8.25E+02	6.57E-01	1.52E+00	7.57E+03	3.19E+01	7.80E-01
90	Ne-20	3.82E+03	1.91E+02	4.76E+01	2.48E+01	3.36E+02	1.47E-01	6.83E+00	4.96E+04	3.18E+01	6.17E-01
91	Ne-20	7.75E+03	3.88E+02	3.22E+01	1.63E+01	2.07E+02	5.93E-02	1.69E+01	1.57E+05	3.17E+01	
92	Ne-20	7.75E+03	3.88E+02	3.22E+01	1.63E+01	2.07E+02	5.93E-02	1.69E+01	1.57E+05	3.17E+01	
93	Ne-20	7.90E+03	3.95E+02	3.17E+01	1.60E+01	2.02E+02	3.35E-02	2.98E+01	1.65E+05	3.17E+01	4.14E-01
94	Ne-20	8.50E+03	4.25E+02	3.10E+01	1.56E+01	1.96E+02	3.44E-02	2.91E+01	1.82E+05	3.17E+01	
95	Ne-20	1.21E+04	6.03E+02	2.65E+01	1.33E+01	1.61E+02	2.79E-02	3.58E+01	3.07E+05	3.17E+01	4.95E-01
96	Si-28	7.50E+03	2.68E+02	7.68E+01	3.94E+01	5.18E+02	9.12E-02	1.10E+01	6.28E+04	2.88E+01	9.90E-01
97	Si-28	7.50E+03	2.68E+02	7.68E+01	3.94E+01	5.18E+02	9.12E-02	1.10E+01	6.28E+04	2.88E+01	
98	Si-28	9.24E+03	3.30E+02	6.79E+01	3.45E+01	4.43E+02	7.80E-02	1.28E+01	8.75E+04	3.28E+01	
99	Si-28	1.10E+04	3.93E+02	6.20E+01	3.13E+01	3.94E+02	6.93E-02	1.44E+01	1.18E+05	3.28E+01	
100	Si-28	1.10E+04	3.93E+02	6.20E+01	3.13E+01	3.94E+02	6.93E-02	1.44E+01	1.18E+05	3.28E+01	
101	Si-28	1.28E+04	4.56E+02	5.87E+01	2.95E+01	3.69E+02	6.45E-02	1.55E+01	1.45E+05	3.28E+01	
102	Si-28	1.30E+04	4.64E+02	5.61E+01	2.82E+01	3.48E+02	6.08E-02	1.65E+01	1.66E+05	3.28E+01	
103	Si-28	1.30E+04	4.64E+02	5.61E+01	2.82E+01	3.48E+02	6.08E-02	1.65E+01	1.66E+05	3.28E+01	
104	Si-28	1.88E+04	6.70E+02	5.03E+01	2.51E+01	2.83E+02	5.22E-02	1.92E+01	2.57E+05	3.28E+01	
105	Ar-40	6.00E+03	1.50E+02	1.76E+02	9.25E+01	1.28E+03	2.26E-01	4.43E+00	2.03E+04	3.38E+01	8.45E-01
106	Ar-40	1.32E+04	3.30E+02	1.12E+02	5.70E+01	7.32E+02	1.29E-01	7.78E+00	7.68E+04	3.26E+01	1.61E+00
107	Ar-40	1.70E+04	4.25E+02	1.00E+02	5.06E+01	6.35E+02	1.11E-01	8.98E+00	1.12E+05	3.37E+01	
108	Ar-40	1.70E+04	4.25E+02	1.00E+02	5.06E+01	6.35E+02	1.11E-01	8.98E+00	1.12E+05	3.37E+01	
109	Ar-40	1.88E+04	4.70E+02	9.59E+01	4.82E+01	6.00E+02	1.05E-01	9.52E+00	1.31E+05	3.37E+01	
110	Ar-40	1.92E+04	4.80E+02	9.30E+01	4.67E+01	5.77E+02	1.01E-01	9.93E+00	1.44E+05	3.37E+01	5.77E-01
111	Ca-40	1.44E+02	3.60E+00	2.48E+03	1.33E+03	3.20E+04	6.27E+00	1.59E-01	5.31E+01	3.61E+01	1.06E-01

Appendix I. The biological and physical data base of HPRT mutations in mammalian cells induced by charged particles

No.	$\alpha_m(Gy^{-1})$	$\sigma_i(\mu m^2)$	σ_m (μm^2)	σ_m/σ_i	Cell line
84	2.27E-05	4.20E+01	1.57E-03	3.74E-05	V79
85	2.27E-05	5.20E+01	1.57E-03	3.02E-05	V79
86	2.41E-05	4.20E+01	1.50E-03	3.57E-05	V79
87	1.40E-05	3.30E+01	7.70E-04	2.33E-05	V79
88	3.60E-05	5.02E+01	1.89E-03	3.76E-05	V79
89	1.69E-05	1.25E+01	2.70E-04	2.16E-05	V79
90	1.44E-05	4.70E+00	1.10E-04	2.34E-05	V79
91	2.47E-05		1.27E-04		TK6
92	2.50E-05		1.29E-04		TK6
93	1.97E-05	2.10E+00	1.00E-04	4.76E-05	V79
94	2.50E-05		1.24E-04		TK6
95	2.30E-05	2.10E+00	9.75E-05	4.64E-05	HSF
96	3.35E-05	1.22E+01	4.12E-04	3.38E-05	TK6
97	4.30E-05		5.28E-04		TK6
98	4.30E-05		4.67E-04		TK6
99	4.19E-05		4.16E-04		TK6
100	4.20E-05		4.17E-04		TK6
101	4.20E-05		3.94E-04		TK6
102	2.09E-05		1.88E-04		TK6
103	2.10E-05		1.89E-04		TK6
104	2.10E-05		1.69E-04		TK6
105	1.32E-04	2.38E+01	3.72E-03	1.56E-04	HSF
106	1.47E-04	2.89E+01	2.63E-03	9.10E-05	HSFs
107	3.01E-05		4.83E-04		TK6
108	3.00E-05		4.81E-04		TK6
109	3.00E-05		4.60E-04		TK6
110	8.30E-05	8.59E+00	1.23E-03	1.44E-04	HSF
111	3.45E-06	4.22E+01	1.37E-03	3.00E-06	V79

Appendix I. The biological and physical data base of HPRT mutations in mammalian cells induced by charged particles

No.	Reference
84	Kranert, T. et al, 1990
85	Stoll, U. et al (1995) & Kiefer, J. et al (2001)
86	Stoll, U. et al (1995) & Kiefer, J. et al (2001)
87	Stoll, U. et al (1995) & Kiefer, J. et al (2001)
88	Kranert, T. et al, 1992
89	Stoll, U. et al (1995) & Kiefer, J. et al (2001)
90	Stoll, U. et al (1995) & Kiefer, J. et al (2001)
91	Kronenberg, A. et al, 1991
92	Kronenberg, A. et al, 1994
93	Stoll, U. et al (1995) & Kiefer, J. et al (2001)
94	Kronenberg, A. et al, 1995
95	Chen, D., 1994
96	Kronenberg, A. et al, 1991
97	Kronenberg, A. et al, 1994
98	Kronenberg, A. et al, 1995
99	Kronenberg, A. et al, 1991
100	Kronenberg, A. et al, 1994
101	Kronenberg, A. et al, 1989 &Kronenberg, A. et al, 1995
102	Kronenberg, A. et al, 1991
103	Kronenberg, A. et al, 1994
104	Kronenberg, A. et al, 1995
105	Chen, D. et al, 1994
106	Tsuboi, K et al.,1992
107	Kronenberg, A. et al, 1991
108	Kronenberg, A. et al, 1994
109	Kronenberg, A. et al, 1989 &Kronenberg, A. et al, 1995
110	Chen, D. et al, 1994
111	Rosendahl, I.M. et al (2005)

Appendix I. The biological and physical data base of HPRT mutations in mammalian cells induced by charged particles

No.	Ions	Energy (MeV)	Specific Energy (Mev/u)	LET (keV/μm)	L_{100} (keV/μm)	Z^{*2}/β^2	I(nm^{-1})	λ(nm)	R(μm)	W(eV)	$\alpha_i(Gy^{-1})$
112	Ca-40	2.00E+02	5.00E+00	2.13E+03	1.14E+03	2.53E+04	4.94E+00	2.03E-01	7.92E+01	3.58E+01	1.73E-01
113	Ca-40	5.64E+02	1.41E+01	1.24E+03	6.60E+02	1.56E+04	2.35E+00	4.25E-01	3.17E+02	3.51E+01	2.32E-01
114	Ti-48	1.49E+02	3.10E+00	2.95E+03	1.59E+03	3.91E+04	7.66E+00	1.31E-01	4.87E+01	3.68E+01	1.54E-01
115	Ti-48	2.11E+02	4.40E+00	2.62E+03	1.40E+03	3.23E+04	6.31E+00	1.59E-01	7.33E+01	3.64E+01	1.29E-01
116	Ti-48	2.30E+02	4.80E+00	2.49E+03	1.33E+03	2.97E+04	5.80E+00	1.72E-01	8.46E+01	3.62E+01	1.36E-01
117	Ti-48	7.10E+02	1.48E+01	1.38E+03	7.38E+02	1.37E+04	2.58E+00	3.87E-01	3.53E+02	3.54E+01	2.26E-01
118	Ti-48	7.20E+02	1.50E+01	1.37E+03	7.29E+02	1.35E+04	2.54E+00	3.94E-01	2.60E+02	3.54E+01	2.29E-01
119	Fe-56	5.26E+03	9.40E+01	5.12E+02	2.74E+02	3.99E+03	7.03E-01	1.42E+00	6.36E+03	3.53E+01	6.64E-01
120	Fe-56	1.13E+04	2.01E+02	3.11E+02	1.61E+02	2.17E+03	3.82E-01	2.62E+00	2.23E+04	3.52E+01	1.06E-01
121	Fe-56	1.68E+04	3.00E+02	2.43E+02	1.24E+02	1.60E+03	2.81E-01	3.56E+00	4.34E+04	3.51E+01	1.42E+00
122	Fe-56	2.24E+04	4.00E+02	2.14E+02	1.08E+02	1.36E+03	2.38E-01	4.19E+00	6.85E+04	3.50E+01	2.59E+00
123	Fe-56	2.24E+04	4.00E+02	2.14E+02	1.08E+02	1.36E+03	2.38E-01	4.19E+00	6.85E+04	3.50E+01	
124	Fe-56	2.36E+04	4.22E+02	2.10E+02	1.06E+02	1.33E+03	2.32E-01	4.31E+00	7.46E+04	3.50E+01	7.56E-01
125	Fe-56	3.36E+04	6.00E+02	1.79E+02	8.94E+01	1.08E+03	1.88E-01	5.33E+00	1.27E+05	3.50E+01	1.50E+00
126	Fe-56	3.36E+04	6.00E+02	1.79E+02	8.94E+01	1.08E+03	1.88E-01	5.33E+00	1.27E+05	3.50E+01	
127	Fe-56	3.36E+04	6.00E+02	1.79E+02	8.94E+01	1.08E+03	1.88E-01	5.33E+00	1.27E+05	3.50E+01	
128	Ni-58	3.54E+02	6.10E+00	3.29E+03	1.75E+03	3.81E+04	7.38E+00	1.35E-01	9.48E+01	3.73E+01	1.16E-01
129	Ni-58	5.22E+02	9.00E+00	2.73E+03	1.45E+03	2.92E+04	5.60E+00	1.79E-01	1.54E+02	3.69E+01	1.49E-01
130	Ni-58	8.47E+02	1.46E+01	2.14E+03	1.14E+03	2.14E+04	4.03E+00	2.48E-01	2.93E+02	3.65E+01	2.54E-01
131	Ni-58	5.61E+02	9.66E+00	2.66E+03	1.41E+03	2.82E+04	5.39E+00	1.85E-01	1.65E+02	3.68E+01	1.53E-01
132	Ni-58	8.44E+02	1.45E+01	2.15E+03	1.15E+03	2.14E+04	4.04E+00	2.48E-01	2.92E+02	3.65E+01	2.53E-01
133	Ni-58	8.02E+03	1.38E+02	4.59E+02	2.42E+02	3.40E+04	5.97E-01	1.67E+00	1.09E+04	3.55E+01	7.08E-01
134	Ni-58	2.28E+04	3.94E+02	2.43E+02	1.23E+02	1.54E+03	2.70E-01	3.71E+00	6.12E+04	3.53E+01	1.00E+00
135	Ni-58	3.72E+04	6.41E+02	2.09E+02	1.01E+02	1.22E+03	2.10E-01	4.77E+00	1.28E+05	3.52E+01	1.15E+00
136	Xe-132	1.19E+03	9.03E+00	6.95E+03	3.70E+03	7.44E+04	1.42E+01	7.06E-02	1.63E+02	4.03E+01	7.38E-02
137	Xe-132	1.27E+03	9.63E+00	6.83E+03	3.63E+03	7.25E+04	1.38E+01	7.26E-02	1.73E+02	4.03E+01	6.41E-02
138	Xe-132	1.40E+03	1.06E+01	6.60E+03	3.52E+03	6.90E+04	1.31E+01	7.65E-02	1.96E+02	4.02E+01	6.63E-02
139	Au-197	4.33E+02	2.20E+00	1.18E+04	7.66E+03	1.84E+05	3.24E+01	3.09E-02	5.26E+01	4.59E+01	3.02E-02

Appendix I. The biological and physical data base of HPRT mutations in mammalian cells induced by charged particles

No.	$\alpha_m(Gy^{-1})$	$\sigma_i(\mu m^2)$	σ_m (μm^2)	σ_m/σ_i	Cell line
112	8.80E-07	5.88E+01	3.00E-04	5.10E-06	V79
113	3.54E-06	4.60E+01	7.00E-04	1.52E-05	V79
114	1.12E-06	7.25E+01	5.30E-04	7.31E-06	V79
115	3.33E-06	5.40E+01	1.40E-03	2.59E-05	V79
116	3.52E-06	5.40E+01	1.40E-03	2.59E-05	V79
117	3.89E-06	5.00E+01	8.60E-04	1.72E-05	V79
118	3.93E-06	5.00E+01	8.60E-04	1.72E-05	V79
119	4.10E-05	5.43E+01	3.36E-03	6.18E-05	HSF
120	7.20E-05	6.17E+01	3.58E-03	5.81E-05	HSF
121	6.53E-05	5.52E+01	2.54E-03	4.60E-05	HSFs
122	1.29E-04	8.85E+01	4.41E-03	4.98E-05	HSFs
123	6.00E-06		2.05E-04		TK6
124	9.80E-05	2.53E+01	3.28E-03	1.30E-04	HSF
125	1.82E-04	4.65E+01	5.65E-03	1.22E-04	HSFs
126	1.20E-05		3.43E-04		TK6
127	1.20E-05		3.43E-04		TK6
128	1.73E-06	6.10E+01	9.10E-04	1.49E-05	V79
129	1.90E-06	6.50E+01	8.30E-04	1.28E-05	V79
130	1.66E-06	8.70E+01	5.70E-04	6.55E-06	V79
131	1.95E-06	6.50E+01	8.30E-04	1.28E-05	V79
132	1.66E-06	8.70E+01	5.70E-04	6.55E-06	V79
133	7.62E-06	5.20E+01	5.60E-04	1.08E-05	V79
134	1.41E-05	3.90E+01	5.50E-04	1.41E-05	V79
135	1.86E-05	3.85E+01	6.20E-04	1.61E-05	V79
136	1.72E-06	8.20E+01	1.91E-03	2.33E-05	V79
137	1.10E-06	7.00E+01	1.20E-03	1.71E-05	V79
138	1.14E-06	7.00E+01	1.20E-03	1.71E-05	V79
139	2.17E-07	5.70E+01	4.10E-04	7.19E-06	V79

Appendix I. The biological and physical data base of HPRT mutations in mammalian cells induced by charged particles

No.	Reference
112	Kiefer, J. et al (2001)
113	Stoll, U. et al (1995) & Kiefer, J. et al (2001)
114	Kiefer, J. et al (2001)
115	Kranert, T. et al.,1990
116	Stoll, U. et al (1995) & Kiefer, J. et al (2001)
117	Kranert, T. et al.,1990
118	Stoll, U. et al (1995) & Kiefer, J. et al (2001)
119	Chen, D. et al, 1994
120	Chen, D. et al, 1994
121	Tsuboi, K et al.,1992
122	Tsuboi, K et al.,1992
123	Kronenberg, A. et al, 1995
124	Chen, D. et al, 1994
125	Tsuboi, K et al.,1992
126	Kronenberg, A. et al, 1995
127	Kronenberg, A., 1994
128	Stoll, U. et al (1995) & Kiefer, J. et al (2001)
129	Kranert, T. et al.,1990
130	Kranert, T. et al.,1990
131	Stoll, U. et al (1995) & Kiefer, J. et al (2001)
132	Stoll, U. et al (1995) & Kiefer, J. et al (2001)
133	Stoll, U. et al (1995) & Kiefer, J. et al (2001)
134	Stoll, U. et al (1995) & Kiefer, J. et al (2001)
135	Stoll, U. et al (1995) & Kiefer, J. et al (2001)
136	Kiefer, J. et al (2001)
137	Stoll, U. et al (1995) & Kiefer, J. et al (2001)
138	Kranert, T. et al.,1990
139	Stoll, U. et al (1995) & Stoll, U. et al (1996) &Kiefer, J. et al (2001)

Appendix I. The biological and physical data base of HPRT mutations in mammalian cells induced by charged particles

No.	Ions	Energy (MeV)	Specific Energy (Mev/u)	LET (keV/μm)	L_{100} (keV/μm)	Z^{*2}/β^2	I(nm^{-1})	λ(nm)	R(μm)	W(eV)	$\alpha_i(Gy^{-1})$
140	Au-197	1.71E+03	8.70E+00	1.13E+04	5.99E+03	1.22E+05	2.31E+01	4.32E-02	1.61E+02	4.27E+01	4.99E-02
141	Au-197	1.73E+03	8.80E+00	1.12E+04	5.96E+03	1.20E+05	2.28E+01	4.38E-02	1.66E+02	4.27E+01	4.35E-02
142	Pb-207	1.93E+03	9.30E+00	1.15E+04	6.11E+03	1.22E+05	2.31E+01	4.34E-02	1.77E+02	4.29E+01	
143	Pb-207	2.40E+03	1.16E+01	1.10E+04	5.87E+03	1.14E+05	2.14E+01	4.68E-02	2.18E+02	4.26E+01	
144	Pb-207	3.15E+03	1.52E+01	1.02E+04	5.47E+03	1.02E+05	1.89E+01	5.29E-02	2.88E+02	4.21E+01	5.37E-02
145	Pb-207	3.24E+03	1.57E+01	1.01E+04	5.42E+03	1.00E+05	1.86E+01	5.37E-02	2.98E+02	4.21E+01	5.43E-02
146	Pb-207	3.11E+04	1.50E+02	3.47E+03	1.82E+03	2.53E+04	4.42E+00	2.26E-01	6.10E+03	4.01E+01	1.75E-01
147	Pb-207	1.04E+05	5.00E+02	1.89E+03	9.48E+02	1.17E+04	2.02E+00	4.95E-01	3.73E+04	3.96E+01	2.25E-01
148	Pb-207	2.03E+05	9.80E+02	1.54E+03	7.74E+02	8.94E+03	1.51E+00	6.62E-01	9.32E+04	3.94E+01	2.11E-01
149	U-238	9.28E+02	3.90E+00	1.41E+04	8.67E+03	1.87E+05	3.39E+01	2.95E-02	8.62E+01	4.55E+01	3.15E-02
150	U-238	1.12E+03	4.70E+00	1.41E+04	8.42E+03	1.70E+05	3.26E+01	3.07E-02	9.97E+01	4.51E+01	1.86E-02
151	U-238	1.21E+03	5.10E+00	1.41E+04	8.32E+03	1.68E+05	3.21E+01	3.12E-02	1.05E+02	4.49E+01	3.15E-02
152	U-238	2.09E+03	8.80E+00	1.33E+04	7.09E+03	1.43E+05	2.71E+01	3.69E-02	1.71E+02	4.37E+01	4.32E-02
153	U-238	2.52E+03	1.06E+01	1.29E+04	6.87E+03	1.35E+05	2.54E+01	3.94E-02	2.04E+02	4.34E+01	5.09E-02
154	U-238	2.57E+03	1.08E+01	1.28E+04	6.85E+03	1.34E+05	2.52E+01	3.96E-02	2.08E+02	4.34E+01	5.11E-02
155	U-238	3.02E+03	1.27E+01	1.24E+04	6.64E+03	1.27E+05	2.38E+01	4.20E-02	2.45E+02	4.31E+01	4.52E-02
156	U-238	3.36E+03	1.41E+01	1.21E+04	6.48E+03	1.22E+05	2.28E+01	4.39E-02	2.72E+02	4.30E+01	4.64E-02

Appendix I. The biological and physical data base of HPRT mutations in mammalian cells induced by charged particles

No.	$\alpha_m(Gy^{-1})$	$\sigma_i(\mu m^2)$	σ_m (μm^2)	σ_m/σ_i	Cell line
140	4.61E-07	9.00E+01	8.30E-04	9.22E-06	V79
141	4.24E-07	7.79E+01	7.60E-04	9.76E-06	V79
142	7.89E-07		1.45E-03		V79
143	4.94E-07		8.70E-04		V79
144	5.62E-07	8.80E+01	9.20E-04	1.05E-05	V79
145	5.67E-07	8.80E+01	9.20E-04	1.05E-05	V79
146	2.61E-06	9.70E+01	1.45E-03	1.49E-05	V79
147	2.94E-06	6.80E+01	8.90E-04		V79
148	3.36E-06	5.20E+01	8.30E-04		V79
149	6.65E-07	7.10E+01	1.50E-03	2.11E-05	V79
150	3.06E-07	4.20E+01	6.90E-04	1.64E-05	V79
151	6.66E-07	7.10E+01	1.50E-03	2.11E-05	V79
152	2.86E-07	9.21E+01	6.10E-04	6.62E-06	V79
153	4.12E-07	1.05E+02	8.50E-04	8.10E-06	V79
154	4.14E-07	1.05E+02	8.50E-04	8.10E-06	V79
155	2.26E-07	9.00E+01	4.50E-04	5.00E-06	V79
156	2.32E-07	9.00E+01	4.50E-04	5.00E-06	V79

Appendix I. The biological and physical data base of HPRT mutations in mammalian cells induced by charged particles

No.	Reference
140	Stoll, U. et al (1995) & Stoll, U. et al (1996) &Kiefer, J. et al (2001)
141	Rosendahl, I.M. et al (2005)
142	Kiefer, J. et al (2001)
143	Stoll, U. et al (1995) & Stoll, U. et al (1996) &Kiefer, J. et al (2001)
144	Stoll, U. et al (1995) & Stoll, U. et al (1996) &Kiefer, J. et al (2001)
145	Kranert, T. et al.,1990
146	Stoll, U. et al (1995) & Stoll, U. et al (1996) &Kiefer, J. et al (2001)
147	Stoll, U. et al (1995) & Stoll, U. et al (1996) &Kiefer, J. et al (2001)
148	Stoll, U. et al (1995) & Stoll, U. et al (1996) &Kiefer, J. et al (2001)
149	Stoll, U. et al (1995) & Kiefer, J. et al (2001)
150	Kranert, T. et al, 1988
151	Kranert, T. et al.,1990
152	Rosendahl, I.M. et al (2005)
153	Kranert, T. et al.,1990
154	Stoll, U. et al (1995) & Kiefer, J. et al (2001)
155	Stoll, U. et al (1995) & Kiefer, J. et al (2001)
156	Kranert, T. et al.,1990

Appendix II. The biological and physical data base of HPRT mutations in mammalian cells induced by photons

No.	Ions	Source	Energy (MeV)	LET (keV/μm)	L_{100} (keV/μm)	I(nm^{-1})	λ(nm)	α_m(Gy^{-1})	σ_m (μm^2)	Cell line	Reference
1	g	Cs-137	0.1588	0.753	0.505	0.0106	94.150	6.70E-05	8.07E-06	HSF	Hei, T.K., 1988
2	g	Cs-137	0.1588	0.753	0.505	0.0106	94.150	8.20E-05	9.88E-06	HE	Suzuki, M. et al,1996
3	g	Cs-137	0.1588	0.753	0.505	0.0106	94.150	2.20E-05	2.65E-06	HSF	Suzuki, M. et al, 2006
4	g	Co-60	0.3553	0.444	0.284	0.0058	171.200	8.50E-06	6.04E-07	CHO	Kinashi, Y. et al, 1997
5	g	Co-60	0.3553	0.444	0.284	0.0058	171.200	3.50E-06	2.49E-07	V79	Thacker, J.,1979
6	g	Co-60	0.3553	0.444	0.284	0.0058	171.200	1.58E-06	1.12E-07	V79	Kent, C. R. H., 1993
7	g	Co-60	0.3553	0.444	0.284	0.0058	171.200	8.14E-06	5.78E-07	V79	Kent, C. R. H., 1993
8	g	Co-60	0.3553	0.444	0.284	0.0058	171.200	3.61E-06	2.56E-07	V79	Kent, C. R. H., 1993
9	g	Co-60	0.3553	0.444	0.284	0.0058	171.200	4.14E-06	2.94E-07	V79	Cherubini, R. et al, 2002
10	Ck x-rays	1.5 KVp	0.00013	22.08	22.06	0.4900	2.041	1.10E-05	3.89E-05	V79	Goodhead, D.T.,1979
11	Ck x-rays	1.5 KVp	0.00013	22.08	22.06	0.4900	2.041	6.70E-05	2.37E-04	HF19	Goodhead, D.T.,1979
12	Alk x-rays	3 KVp	0.00053	16.74	15.06	0.3476	2.877	7.40E-06	1.98E-05	V79	Cox, R., 1977.
13	Alk x-rays	3 KVp	0.00053	16.74	15.06	0.3476	2.877	7.59E-05	2.03E-04	HF19	Cox, R., 1977.
14	x-rays	100 KVp	0.00734	8.035	6.681	0.1477	6.772	6.00E-08	7.71E-08	TK6	Kronenberg, A., 1991
15	x-rays	100 KVp	0.00734	8.035	6.681	0.1477	6.772	5.50E-06	7.07E-06	TK6	Kronenberg, A., 1991
16	x-rays	250 KVp	0.01582	4.309	3.325	0.0729	13.710	3.10E-05	2.14E-05	HF19 strain	Cox, R.,1979
17	x-rays	250 KVp	0.01582	4.309	3.325	0.0729	13.710	6.00E-06	4.14E-06	V79-753 B	Belli, M., 1991
18	x-rays	250 KVp	0.01582	4.309	3.325	0.0729	13.710	6.60E-06	4.55E-06	V79-4	Thacker, J., 1982
19	x-rays	250 KVp	0.01582	4.309	3.325	0.0729	13.710	8.20E-06	5.65E-06	TK6	Bao, C.-Y. et al, 1995
20	x-ray	250 KVp	0.01582	4.309	3.325	0.0729	13.710	2.40E-05	1.65E-05	HF10	Wu, H. et al, 1998
21	x-ray	250 KVp	0.01582	4.309	3.325	0.0729	13.710	7.50E-06	5.17E-06	HF12	Wu, H. et al, 1998
22	x-rays	250 KVp	0.01582	4.309	3.325	0.0729	13.710	6.03E-06	4.16E-06	V79	Belli, M., 1998
23	x-rays	300 KVp	0.01911	3.965	3.043	0.0667	15.000	1.70E-06	1.08E-06	V79	Stoll, U. et al, 1995
24	x-rays	300 KVp	0.01911	3.965	3.043	0.0667	15.000	1.45E-06	9.20E-07	V79	Kranert, T. et al,1990
25	x-rays	300 KVp	0.01911	3.965	3.043	0.0667	15.000	5.03E-06	3.19E-06	V79	Rosendahl, I.M. et al, 2005
26	x-rays	300 KVp	0.01911	3.965	3.043	0.0667	15.000	2.36E-06	1.50E-06	V79	Schmidt, P. et al, 1998
27	x-rays	300 KVp	0.01911	3.965	3.043	0.0667	15.000	2.30E-06	1.46E-06	V79	Kiefer, J. et al, 2001
28	x-rays	300 KVp	0.01911	3.965	3.043	0.0667	15.000	1.50E-06	9.52E-07	V79	Kiefer, J. et al, 1999